LIQUEFACT

Assessment and mitigation of Liquefaction potential across Europe: a holistic approach to protect structures/infrastructure for improved resilience to earthquake-induced Liquefaction disasters.

H2020-DRA-2015

GA no. 700748

DELIVERABLE D3.1

State of the art review of numerical modelling strategies to simulate liquefaction-induced structural damage and of uncertain/random factors on the behaviour of liquefiable soils

Author(s):	António Viana da Fonseca, Maxim Millen, Fernando Gómez-Martinez, Xavier Romão, Julieth Quintero, Fausto Gómez, Pedro Costa, Sara Rios, Mirko Kosič, Matjaž Dolšek, Janko Logar, Sadik Oztoprak, Ilknur Bozbey, Kubilay Kelesoglu, Ferhat Ozcep, Alessandro Flora, Alessandro Rasulo, Giuseppe Modoni and Paolo Croce.
Responsible Partner:	University of Porto (UPorto)
Version:	1.0
Date:	20/10/2017
Distribution Level (CO, PU)	

LIQUEFACT
Deliverable D3.1
State of the art review of numerical modelling strategies to simulate liquefaction-induced
structural damage and of uncertain/random factors on the behaviour of liquefiable soils
v. 1.0

This project has received funding
from the European Union's
Horizon 2020 research and
innovation programme under
grant agreement No. 700748

DOCUMENT REVISION HISTORY

Date	Version	Editor	Comments	Status
31/10/2017	1		First Draft	Draft

LIST OF PARTNERS

Participant	Name	Country
UPORTO	Universidade do Porto	Portugal
Istan-Uni	Istanbul Universitesi	Turkey
ULJ	Univerza V Ljubljani	Slovenia
UNINA	Universita degli Studi di Napoli Federico II	Italy
NORSAR	Stiftelsen Norsar	Norway
ARU	Anglia Ruskin University Higher Education Corporation	United Kingdom
UNIPV	Università degli Studi di Pavia	Italy
UNICAS	Universita degli Studi di Cassino e del Lazio Meridionale	Italy

GLOSSARY

Term	Description
Acceleration (Floor Acceleration)	At a floor level, the acceleration of the centre of mass relative to a fixed point in space (see FEMA P-58 (2012))
Acceleration Spike	A strong high frequency pulse of shaking
Adjacent Buildings	Buildings that are close to the site being considered
Angularity	The shape of the soil particles
Assessment	A survey of a real or potential disaster to estimate the actual or expected damages and to make recommendations for prevention, preparedness and response (see World Meteorological Organization (2006))

LIQUEFACT
Deliverable D3.1
State of the art review of numerical modelling strategies to simulate liquefaction-induced
structural damage and of uncertain/random factors on the behaviour of liquefiable soils
v. 1.0

Bearing Capacity Failure	The loss of foundation support due the vertical demand of the structure exceeding the soil capacity
Bedrock	Any solid, naturally occurring, hard consolidated material located either at the surface or underlying soil. Rocks have a shear-wave velocity of at least 500 m/s at small (0.0001 per cent) levels of strain (see GEM-ASV Guidelines (D'Ayala et al. 2015))
Bond-Slip	Deformation of a concrete member where the concrete slips along the reinforcing bar
Building Aspect Ratio	The ratio of the building height to foundation width
Building Code	A set of ordinances or regulations and associated standards intended to control aspects of the design, construction, materials, alteration and occupancy of structures that are necessary to ensure human safety and welfare, including resistance to collapse and damage (see UNISDR (2009))
Collapse Fragility	A mathematical relationship that defines the probability of incurring structural collapse as a function of ground motion intensity (see FEMA P-58 (2012))
Collapse Mode(S)	One or more ways in which a building would be expected to collapse, ranging from partial to complete collapse. Possible collapse modes include single-story collapse, multi-story collapse, or total collapse (see FEMA P-58 (2012))
Computational Time Step	The increment of time that a numerical analysis considers during a time history analysis
Consequences	The losses resulting from earthquake damage in terms of potential casualties, repair and replacement costs, repair time, and unsafe placarding (see FEMA P-58 (2012))
Critical State	The conditions of the soil at large shear strain when subject to further strain no volume change occurs
Critical State Compatible	soil constitutive models that are consistent or based on the critical state soil mechanics framework
Crust	A layer of soil on the surface, typically it maintains it strength during shaking
Cyclic Resistance Ratio (CRR)	The equivalent level of cyclic stress required to trigger liquefaction for a given number of cycles or magnitude
Cyclic Stress Ratio (CSR)	The equivalent cyclic stress applied to a layer of soil based on the peak ground surface acceleration , earthquake magnitude and total vertical stress, normalised by the vertical effective stress
Damping	A velocity dependent force, used in numerical simulations to represent physical energy loss for non-strain dependent phenomena and to improve numerical stability
Demand	A parameter that is predictive of component or building damage states, including peak floor (or ground) acceleration, peak component deformation, peak (or residual) story drift, peak floor (or ground) velocity, or peak component force (or stress) (see FEMA P-58 (2012))
Deposition	The process that formed the soil profile (e.g. deposited by airborne soil particles)

LIQUEFACT
Deliverable D3.1
State of the art review of numerical modelling strategies to simulate liquefaction-induced
structural damage and of uncertain/random factors on the behaviour of liquefiable soils
v. 1.0

Design Spectra	Spectra used in earthquake-resistant design which correlate with design earthquake ground motion values. A design spectrum is typically a spectrum having a broad frequency content. The design spectrum can be either site-independent or site-dependent. The site-dependent spectrum tends to be less broad band as it depends also on (narrow band) local site conditions (see GEM-ASV Guidelines (D'Ayala et al. 2015))
Deterministic Approach	A method to evaluate a situation that does not consider uncertainty
Differential Settlement	The difference in vertical displacement of pad footings
Direct Damages	Property damage, injuries and loss of life that occur as a direct result of a natural disaster (see World Meteorological Organization (2006))
Directivity Effects	The consideration of the direction of fault rupture in the intensity and length of shaking, typically of concern is forward directivity effects where the shaking that occurs in line with the direct of rupture is strong and short due to the seismic waves superimposing
Deviatoric Stress	The difference in the applied normal stress to a soil element
Drainage	The flow of water through a soil body
Duration	The length of time that significant shaking occurs
Dynamic Settlement	Settlement that occurs during shaking
Ejecta	The manifestation of sand boils at the surface due to excess pore pressure build up below the surface
Empirical-Based Approach	A method to evaluate a situation that is based on relationships that have been derived from previous occurrences
Epicentre	The point of the surface of the earth above where fault rupture started
Equivalent Linear	A modelling technique where a nonlinear system is represented by a linear system using suitable stiffness and damping assumptions
Equivalent Viscous Damping	Damping that is used to represent hysteretic energy loss
Fabric	The soil characteristics such as grain orientation and cementation, typically they are considered independently to stress and void ratio independent characteristics
Failure Mechanism	The development of a deformation mode that continues to deform under constant applied load
Fixed Base	The assessment of a structure when considering the foundation and soil to be rigid
Flexural Demand	The moment demand on a structural member
Flexure-Critical Elements	elements where performance is expected to be governed by flexure-related conditions
Flow Rule	An equation to determine the direction of plastic deformation of a soil element inside a soil constitutive model
Flow-Like Behaviour	where the static shear stress caused by a free face or downward slope can result in large strains and contractive soil behaviour, eventually leading to a dramatic loss of soil shear strength
Foundation Flexibility	The ability of the foundation to deform

LIQUEFACT
Deliverable D3.1
State of the art review of numerical modelling strategies to simulate liquefaction-induced
structural damage and of uncertain/random factors on the behaviour of liquefiable soils
v. 1.0

Foundation Rotation	The rotation of the foundation about one of its horizontal axes (synonymous with foundation tilt)
Foundation Tilting	The difference in vertical displacement of the outer most edges of the foundation divided by the horizontal distance between them
Foundation Uplift	The detachment of one edge of the foundation due to an applied overturning moment
Fragility (Component Fragility Curve/Function	A probability-valued function of an engineering demand parameter (EDP), that represents the probability of violating (exceeding) a given limit-state or damage-state of the component, given the value of EDP that it has been subjected to. Essentially, it is the cumulative distribution function (CDF) of the EDP-capacity value for the limit-state and it is thus often characterized by either a normal or (more often) a lognormal distribution, together with the associated central value and dispersion of EDP-capacity (see GEM-ASV Guidelines (D'Ayala et al. 2015))
Framework	A structure to explain the underlying phenomena that influence a situation
Free-Field	A site soil where the pore pressure and soil stress are not influenced by the presence of buildings
Free-Field Settlement	The vertical displacement of the ground surface of a free field soil deposit
Fully Coupled Effective Stress Soil Modelling	A numerical simulation that accounts for soil contraction and dilation through the change in pore water pressure and accounts for the flow of water through the changes in water pressure
Fundamental Site Period	The lowest frequency of natural vibration of the soil profile (synonymous with characteristic site period)
Fundamental Structural Period	The lowest frequency of natural vibration of the structure
Global Settlement	The average settlement of the foundation
Grain Size Distribution	The composition of a soil in terms of the size of the soil particles
Ground Improvement	A liquefaction mitigation technique where the soil profile is modified
Ground Motion	The shaking on the surface, typically measured as acceleration with time
Hydraulic Gradient	The difference in pore water pressure
In Situ Test	A test that is performed on soil while it is in the deposit (e.g. CPT or SPT)
Indirect Damages	Economic losses resulting from the multiplier or ripple effect in the economy caused by damage to infrastructure resulting from a natural disaster. Damage done to lifelines such as the energy distribution network, transportation facilities, water-supply systems and waste-management systems, can result in indirect economic losses greater than the direct economic damage to these systems and a long-term drain on the regional or national economy (see World Meteorological Organization (2006))
Inertial Interaction	The generation of inertial effects in the structure that will give rise to additional soil-structure interaction forces. The difference in inertia causes the heavy structure to lag behind the soil and push against it and eventually oscillates out-of-phase to the soil
Inertial Seismic Forces	The apparent force (mass x acceleration) of the structure during shaking
Initial Stress	The level of stress prior to seismic shaking

LIQUEFACT
Deliverable D3.1
State of the art review of numerical modelling strategies to simulate liquefaction-induced
structural damage and of uncertain/random factors on the behaviour of liquefiable soils
v. 1.0

Intensity Measure (IM)	Particularly for use within this document, IM will refer to a scalar quantity that characterizes a ground motion accelerogram and linearly scales with any scale factor applied to the record. While non-linear IMs and vector IMs have been proposed in the literature and often come with important advantages, they will be excluded from the present guidelines due to the difficulties in computing the associated hazard (see GEM-ASV Guidelines (D'Ayala et al. 2015))
Kinematic Interaction	the change in ground-motion due to the difference in stiffness between the soil and foundation/structure
Lateral Spreading	The movement of a large mass of soil down-hilll or towards a free-face
Liquefiable Soil	Soil that is susceptible to liquefaction (independent of seismic demand)
Liquefied Soil	Soil that is in a state of liquefaction
Loss Of Functionality	The use of a building is impaired
Low Strain Stiffness	The stiffness of a soil element under very little shear strain, synonymous with initial shear stiffness
Low-Pass Filter	A signal processing tool that removes high frequency content that is above a certain cut-off frequency
Lumped/Concentrated Plasticity	models that concentrate inelastic deformations at the end of elements
Magnitude	A quantity characteristic of the total energy released by an earthquake, as contrasted to intensity that describes its effects at a particular place.
Mat Foundation	A foundation that has contact with the soil over the whole building footprint
Mean Confining Stress	The average applied normal stresses to a soil element
Mitigation Technique	A method to reduce the occurrence of something or its impact
Monte Carlo Simulation	In Monte Carlo simulation, probability distributions are proposed for the uncertain variables for the problem (system) being studied. Random values of each of the uncertain variables are generated according to their respective probability distributions and the model describing the system is executed. By repeating the random generation of the variable values and model execution steps many times the statistics and an empirical probability distribution of system output can be determined (see World Meteorological Organization (2006))
Near-Field Effects	The specific aspects of ground shaking that are only seen when very close (i.e. within 20km) of the fault rupture, (e.g. velocity pulses, high vertical acceleration)
Non-structural Component	A building component that is not part of the structural system (see FEMA P-58 (2012))
Numerical Stability	Numerical algorithms that do not cumulatively magnify errors
Out-Of-Plane Deformation	When an element deforms perpendicular to the direction of loading
Over-Turning Moment	The moment demand applied to a foundation or building around a horizontal axis
Overburden Pressure	The vertical stress due to the weight of the material above it
P-Delta	The moment demand created by a weight being horizontally displacement
Pad Footing	A single element that supports the structure as part of a pad foundation

LIQUEFACT
Deliverable D3.1
State of the art review of numerical modelling strategies to simulate liquefaction-induced
structural damage and of uncertain/random factors on the behaviour of liquefiable soils
v. 1.0

Pad Foundation	A foundation that is made of of individual pad footings that are typically placed under load bearing structural elements
Peak Acceleration	The value of the absolutely highest acceleration in a certain frequency range taken from strong-motion recordings.
Peak Interstorey Drift	The maximum difference in horizontal displacements between two consecutive storeys
Performance	The probable damage and resulting consequences as a result of earthquake shaking or other hazards (see FEMA P-58 (2012))
Permanent Deformation	A permanent change in shape of a body, (e.g. the remaining distortion of a building after an earthquake)
Permanent Ground Deformation	The deformation of the ground (vertical and horizontal movement) measured after the ground movement has ceased
Permeability	The ability of the soil to allow pore water flow
Phase Transformation Line	The soil state where the soil starts to dilate instead of contract under increasing shear stress
Physics-Based Approach	A method to evaluate a situation that is based on theories of physics and reasoning
Pore Pressure Dissipation	The reduction in pore pressure through pore water flow
Pore Pressure Ratio	The ratio of the excess pore pressure to the initial effective vertical stress
Presence Of Buildings	The pore pressure and soil stresses are influenced by adjacent buildings
Probabilistic Approach	A method to evaluate a situation that considers uncertainty through probabilities of occurrence
Punching-Shear Mechanism	The loss of foundation support due to the soil shearing through a strong layer compressing a softer layer below, such that a full Prandtl failure mechanism does not occur
Push Over Analysis	A simulation technique where a horizontal force is applied to a structure to represent an equivalent inertial seismic demand
Relative Density	The difference between the maximum soil void ratio and the current void ratio, divided by the difference between the maximum and minimum void ratios, typically presented as a percentage.
Repair Cost	The cost, in present dollars, necessary to restore a building to its pre-earthquake condition, or in the case of total loss, to replace the building with a new structure of similar construction (see FEMA P-58 (2012))
Residual Drift	The difference in permanent displacement between the center of mass of two adjacent floors as a result of earthquake shaking (see FEMA P-58 (2012))
Response Spectrum	The peak response of a series of simple harmonic oscillators having different natural periods when subjected mathematically to a particular earthquake ground motion. The response spectrum shows in graphical form the variations of the peak spectral acceleration, velocity and displacement of the oscillators as a function of vibration period and damping (see World Meteorological Organization (2006))

LIQUEFACT
Deliverable D3.1
State of the art review of numerical modelling strategies to simulate liquefaction-induced
structural damage and of uncertain/random factors on the behaviour of liquefiable soils
v. 1.0

Return Period	For ground shaking, return period denotes the average period of time — or recurrence interval — between events causing ground shaking that exceeds a particular level at a site; the reciprocal of annual probability of exceedance.
Rigid-Body Tilting	Foundation tilting when no deformations occur within the foundation
Risk	The combination of the probability of an event and its negative consequences (see UNISDR (2009))
Seismicity	The distribution of earthquake in space and time (see IDNDR- DHA (1992))
Shallow Foundation	A foundation that is supported by directly bearing on the soil, instead of deep foundations that use piles
Shear-Critical Elements	Elements where performance is expected to be governed by shear-related conditions
Shear-Induced Settlement	Settlement that is caused by a displacement of soil skeleton
Simplified Approach/Procedure	A method to evaluate a situation that can be performed without the aid of a computer
Site Response Analysis	The performance of a soil profile under seismic shaking
Soil Failure	A general term used to describe large soil deformation
Soil Heterogeneity	Spatial variation in soil properties
Soil Shear Stiffness	The increase in shear stiffness for a given increase in shear strain
Soil Skeleton	The soil without the consideration of what is in the pores
Soil Strength	The shear stress capacity of the soil, typically using some yield criterion (e.g. Mohr-Coulomb), or defined as the point where increasing deformation occurs with no increase in load. However, liquefied soils do not conform to traditional yield criterion concepts and instead the strength should be defined in terms of level of strain and effective confining stress
Soil-Foundation-Structure Interaction	A subclass of soil-structure interaction, where the structure is on a foundation that is in contact with the soil (e.g. a building)
Soil-Structure Interaction	The stresses, deformations, displacements and forces that are caused by the presence of a structure in contact with soil
Static Bearing Pressure	The pressure applied by the foundation and structure to the soil
Stiffness Contrast	A difference in stiffness between two adjacent soil layers
Story Drift	The instantaneous difference in lateral displacement between the centre of mass of two adjacent floors (see FEMA P-58 (2012))
Strain-Hardening	The increase in stiffness of a soil from an increase in effective confining stress caused by the soil dilating under large strain
Strong Shaking	The part of seismic excitation that is significant for assessing performance
Structural Displacement Ductility	The inelastic displacement of the structure divided by the yielding displacement
Structural System	A collection of structural components acting together in resisting gravity forces, seismic forces, or both (see FEMA P-58 (2012))
Superstructure Energy Dissipation	The release of energy from the superstructure usually through inelastic deformation

LIQUEFACT
Deliverable D3.1
State of the art review of numerical modelling strategies to simulate liquefaction-induced
structural damage and of uncertain/random factors on the behaviour of liquefiable soils
v. 1.0

Susceptibility	Susceptibility of soils to liquefaction is the tendency of certain geomaterials to undergo a severe loss of shear strength due to the pore water pressure build-up caused by earthquake ground shaking.
Time History Analysis	The simulation of a system subjected to a seismic motion, synonymous with time series analysis
Total Replacement Cost	The cost to replace an entire building (core, shell, and tenant improvements) as it exists in its pre-earthquake condition, including costs associated with demolition of the damaged building and clearing the site of debris (see FEMA P-58 (2012))
Transient Deformation	A temporary change in shape of a body, (e.g. the distortion of a building during an earthquake)
Uncertainty	A general term that is used within this document to describe the variability in determining any EDP, cost, or loss value. The typical sources considered are the ground motion variability, the damage state capacity and associated cost variability, and the errors due to modelling assumptions or imperfect analysis methods (see GEM-ASV Guidelines (D'Ayala et al. 2015))
Void Ratio	The ratio of the volume of voids to the volume of solids in a soil
Volumetric-Induced Settlement	Settlement that is caused by a reduction in the volume of the soil skeleton
Vulnerability	The characteristics and circumstances (physical, social, economic and environmental) of a community, system or asset that make it susceptible to the damaging effects of a hazard (see UNISDR (2009))
Water Table Depth	The distance from the ground surface to the level of the ground water
Yield Drift	The value of drift at which a structure reaches its effective yield strength (see FEMA P-58 (2012))

NOTATION AND SYMBOLS

Acronym	Description
a_{max}	Peak ground surface acceleration
AC	Asbestos cement
B	Building width
BEM	Boundary Element Method
B_f	Width of the foundation element
c	Foundation aspect ratio correction

CAV_{dp}	Standardised cumulative absolute velocity
C_D	Correction factor for the depth of embedment
CI	Cast iron
CPT	Cone Penetration Test
CRR	Cyclic resistance ratio
$CRR_{M7.5}$	Cyclic resistance ratio for a magnitude of 7.5
CSR	Cyclic stress ratio
$CSR_{M7.5}$	Cyclic stress ratio for a magnitude of 7.5
CTL	Cumulative thickness of liquefying layers
D_R	Relative density
DS	Damage state
e	Void ratio
e_C	Void ratio at critical state
e_{IC}	Void ratio of the soil at its loosest state consolidated isotopically to the initial confining stress
EILD	Earthquake-induced liquefaction disasters
e_{QSS}	Void ratio at quasi steady state conditions
FLAC	Fast Lagrangian Analysis of Continua numerical modelling software
FOSM	First Order Second Moment
FS	Factor of safety
FS_{deg}	Degraded static factor of safety
FS_v	Bearing capacity factor of safety under purely vertical load
g	Acceleration of gravity
GMPGV	Geometric mean peak ground velocity
H	Height of the deposit

H_C	Thickness of superficial crust
H_e	Effective height
H_{eff}	Effective height of the equivalent single degree of freedom structure
H_L	Thickness of the liquefiable layer
IDA	Incremental Dynamic Analysis
IM	Earthquake intensity measure
I_s	State Index
K_α	Corrected term for influence of static shear stress
K_σ	Corrected term for overburden pressure
K_{eff}	Effective stiffness
L	Liquefaction
LBS	Index of equivalent liquefaction-induced shear strain on the free-field
LiDAR	Airborne Light Detection and Ranging
LPI	Liquefaction Potential Index
LSN	Liquefaction Severity Number
m	Natural vibration modes
MDOF	Multi degree of freedom
m_e	Equivalent mass
MFS	Method Fundamental Solution
m_i	Mass distribution
MPVC	Modified polyvinyl chloride
$M_{p\Delta}$	P-delta moment
MSF	Magnitude scaling factor
$m_{SS,eff}$	Effective mass of the structure

LIQUEFACT
Deliverable D3.1
State of the art review of numerical modelling strategies to simulate liquefaction-induced
structural damage and of uncertain/random factors on the behaviour of liquefiable soils
v. 1.0

M_W	Earthquake Magnitude
N	Axial load applied to the foundation
$(N_1)_{60}$	N value corrected to effective vertical stress of 1 atmosphere and 60% of the freefall energy reaching the sampler
$(N_1)_{60CS}$	Equivalent clean sand number of corrected N value
n	Number of storeys
N_{LR}	"Strength index" of liquefiable soils
N_S	Number of excitation cycles
N_{SPT}	Number of blows to advance the SPT sampler 30 cm.
P'	Mean effective stress
PDMY	Pressure Depend Multi Yield material constitutive model
PEER	Pacific Earthquake Engineering Research
PGA	Peak ground acceleration
PGD	Permanent ground deformations
PGS	Transient ground strain
PGV	Peak ground velocity
PL	Probability of liquefaction
PVC	Polyvinyl chloride
q	Deviatoric stress
q_f	Static bearing pressure
q_c	Tip resistance in cone penetration test
q_{c1Ncs}	Equivalent clean sand normalized cone tip resistance
RC	Reinforced concrete
RR	Repair rate
r_d	Corrected term for reduced shaking amplitude at depth

LIQUEFACT
Deliverable D3.1
State of the art review of numerical modelling strategies to simulate liquefaction-induced
structural damage and of uncertain/random factors on the behaviour of liquefiable soils
v. 1.0

r_u	Pore pressure ratio
S	Settlement
S_0	Basic settlement value depending on the seismic intensity
S_{V1D}	One-dimensional consolidation settlement
$S_a(T)$	Acceleration response spectrum
SDOF	Single degree of freedom
S_e	Ejecta-induced settlement
SFS	Soil foundation structure
SFSI	Soil foundation structure interaction
S_{max}	Maximum footing settlement
SPT	Standard Penetration Test
S_S	Dynamic settlement
SSI	Soil Structure Interaction
S_v	volumetric-induced settlement
T	Fundamental period
T_S	Period of excitation cycles
T_{soil}	Soil fundamental period
u	Pore pressure
V_b	Design base shear
V_S	Shear wave velocity
V_{S1}	Normalized shear wave velocity
z	Depth
Z_L	Liquefied thickness
$Z_{L,m}$	Equivalent liquefied thickness in homogeneous, infinite free field

α	Initial (static) shear stress ratio
α_k	Damage median value
β	Angular distortion
β_k	Damage standard deviation value
Δ_e	equivalent SDOF displacement
Δ_i	Displaced shape of the structure-foundation-soil system
Δ_u	Excess pore pressure
ε_v	Volumetric consolidation strains
ε_h	Horizontal strain
ε_{lim}	Limiting tensile strain
η	Displacement reduction factor
ξ_{sys}	Equivalent viscous damping
λ	Excitation wave length
Θ_1 and Θ_2	Unutmaz and Cetin (2012) model parameters
Θ_f	Foundation tilt
σ_v	Total vertical stress
σ_v'	Effective vertical stress
σ	Normal stress
τ_b	Shear stress of building's inertia forces
τ_{soil}	Shear stress of soil column mass
ϕ_{deg}	Equivalent degraded friction angle of the liquefiable layer
ψ	State parameter
γ	Shear strain
τ	Shear stress

LIQUEFACT
Deliverable D3.1
State of the art review of numerical modelling strategies to simulate liquefaction-induced
structural damage and of uncertain/random factors on the behaviour of liquefiable soils
v. 1.0

This project has received funding from the European Union's Horizon 2020 research and innovation programme under grant agreement No. 700748

CONTENTS

LIQUEFACT
Deliverable D3.1
State of the art review of numerical modelling strategies to simulate liquefaction-induced
structural damage and of uncertain/random factors on the behaviour of liquefiable soils
v. 1.0

LIQUEFACT
Deliverable D3.1
State of the art review of numerical modelling strategies to simulate liquefaction-induced
structural damage and of uncertain/random factors on the behaviour of liquefiable soils
v. 1.0

LIST OF FIGURES AND TABLES

FIGURES

LIQUEFACT
Deliverable D3.1
State of the art review of numerical modelling strategies to simulate liquefaction-induced
structural damage and of uncertain/random factors on the behaviour of liquefiable soils
v. 1.0

TABLES

LIQUEFACT
Deliverable D3.1
State of the art review of numerical modelling strategies to simulate liquefaction-induced
structural damage and of uncertain/random factors on the behaviour of liquefiable soils
v. 1.0

EXECUTIVE SUMMARY

Earthquake-induced liquefaction can cause significant damages in buildings and loss of human lives. Although important technical achievements in liquefaction mitigation have been accomplished in the last decades in the field of earthquake geotechnical engineering, significant damage still occurs in seismic areas around the world. In particular, the problem of estimating liquefaction-induced damage to critical infrastructures is still not properly addressed due to its vast complexity. The main issues that hinder a simple answer to this problem are: the uncertainties associated to soil behaviour, and the need to consider the soil-structure interaction to obtain the overall behaviour. Although numerical simulations are a valuable help in these complex problems it is important to identify the main phenomena responsible for building damage to simplify the models, saving computation time, while keeping them accurate. This report covers the most influential mechanisms in this problem, including the initiation of liquefaction in the free-field, the influence of the building on the initiation of liquefaction, the dynamic response of the soil, the dynamic response of the structure, the structural damage mechanisms as well as the quantification of loss. A modulated approach based on the major mechanisms is a vital part of the adopted research approach to understanding the complex interacting behaviour between the soil, water, foundation and structure.

SCOPE AND PURPOSE

Physics-based simulation of liquefaction-induced structural damage requires the analysis of interacting behaviour between the response of the soil and the response of the structure. Due to the complexity of such phenomenon and significant uncertainty involved, the simulation of liquefaction-induced structural damage is extremely difficult and computationally demanding. For this reason, the problem is often treated in a probabilistic manner. In fact, one of the objectives of the WP3 is to focus on the development of an efficient probabilistic numerical procedure for the simulation of liquefaction-induced damage and fragility analysis of critical structures and infrastructures. The goal is to develop a procedure that will provide proper balance between the computational effort and the expected accuracy.

This report is the first deliverable of WP3 and focuses on the major mechanisms that contribute to the seismic performance of buildings resting on liquefiable soils. The aim is to review existing procedures for simulation of liquefaction-induced structural damage, including the assessment of the current techniques available to capture these mechanisms with numerical simulations, as numerical approaches are a cornerstone to liquefaction-related research. Based on this report a methodology will be defined to address the final WP3 goal.

This report first covers case history examples to highlight the critical aspects of structural damage; case history data also provides a useful benchmark for the validation of analytical procedures as they implicitly account for the influencing factors of infrastructure performance from micro-level soil behaviour through to societal demands. The second section covers the phenomena of liquefaction, how it develops in the free-field and different techniques for numerical modelling its occurrence and effects. The third section focuses on the modification to the development of liquefaction due to the presence of buildings, and covers the mechanisms and techniques to estimate permanent deformations. Permanent deformations are typically used as a measure of the performance of a building, and the extreme weakening of the soil due to liquefaction often results in considerable settlement and tilting of the foundation. The fourth section covers the dynamic response of buildings. Shaking is a major cause of seismic building damage and the occurrence of liquefaction dramatically affects the level of shaking and the dynamic response of the building. The response and performance of embankments and pipelines is investigated in section five, covering the major contributors to damage and recent work to quantify the damage. The final section covers the general techniques used for performance-based engineering and the quantification of infrastructure vulnerability through fragility curves.

The contents of this report should be considered a work in progress which will be amended and modified throughout the duration of the LIQUEFACT project, to reflect emerging issues identified by project partners; issues identified by the external stakeholders; and advice received from the expert advisory groups.

Although the report is publically available it is principally an internal working document intended for the LIQUEFACT project partners and researchers.

1. INTRODUCTION

1.1   FIELD EVIDENCE

Field reconnaissance data is an essential part of liquefaction research, not only does it provide a laboratory of data that can be used for the back calculation of empirical relations (e.g. cyclic resistance ratio CRR), but field investigations can highlight unforeseen issues and responses that were not predicted by simplified models. Field investigation discoveries force researchers to re-evaluate the current tools available to account for the complex system response of the soil, the buildings and the community.

It is well known that earthquake-induced liquefaction can cause significant damages in buildings and loss of human lives. Although important technical achievements in liquefaction mitigation have been accomplished in the last decades in the field of earthquake geotechnical engineering, significant damage still occurs in seismic areas around the world.

On June 16, 1964, an earthquake registered as $M_W7.5$ hit the cities of Niigata and Yamagata in Japan. The greatest damage was concentrated in Niigata and other small towns near the Sea of Japan. The epicentre was on the continental shelf of the northwest coast of Honshu, approximately 50 km north of Niigata (Diaz, 2016). During the Niigata earthquake, approximately 340 reinforced concrete buildings in the city of Niigata were damaged as result of extensive liquefaction of the sandy ground (Yoshimi and Tokimatsu, 1977). About one-third of the affected buildings suffered some kind of damage to the superstructure, while the rest of the buildings settled, tilted or overturned without presenting any damage on the superstructure (Ohsaki, 1966). **Figure 1.1a** shows one of the most famous cases of liquefaction in the world, the buildings in Kawagishi-cho in Niigata, in which several buildings tilted over yet did not exhibit significant structural damage. The photo on the right shows the soil that emerged to the surface, a clear indication of liquefaction in the area.

| (a) | (b) |

Figure 1.1: (a) Tilt and settlement of some buildings in Kawagishi-cho (Diaz, 2016); (b) Evidence of liquefaction outside the Higashi Police Station (Diaz, 2016)

LIQUEFACT
Deliverable D3.1
State of the art review of numerical modelling strategies to simulate liquefaction-induced
structural damage and of uncertain/random factors on the behaviour of liquefiable soils
v. 1.0

According to analytical studies performed by Yoshimi and Kuwabara (1973), about one minute after the earthquake significant pore water pressure dissipation in the lower part of the liquefied sand had not yet occurred, at which time the buildings probably settled (Yoshimi and Tokimatsu, 1977).

On 16th July 1990, a great earthquake registered as $M_W7.8$ hit the island of Luzon in Philippines, located 110 km north of Manila, the capital of the country (Diaz, 2016). During the earthquake, widespread soil liquefaction in the alluvial plain along the southern coast of the Lingayen Gulf was observed. Numerous damages occurred due to liquefaction, such as settlement and tilt of the buildings, collapse of bridges and lateral spreading along the river, mainly in Dagupan City. Ground failure such as sand boils and cracks were also observed throughout the city (Adachi et al., 1992). **Figure 1.2** presents cases of severe liquefaction in the city of Dagupan. The photo on the left shows a three-storey building that suffered large differential settlements; on the right the photo shows the collapsed Magsaysay Bridge as a result of the lateral displacement of the ground. This bridge crosses the River Pantal and was the main communication route of the city with its surroundings (Diaz, 2016).

(a) (b)

Figure 1.2: (a) Tilted building in Dagupan, Philippines (Diaz, 2016); (b) Magsaysay bridge collapsed by lateral displacement of soil (Bird and Bommer, 2004)

At the end of the 20th century, in Adapazari, Turkey, more than 1200 buildings collapsed or were damaged, hundreds of structures settled and tilted due to liquefaction and ground softening, during the August 17, 1999 Kocaeli Earthquake registered as $M_W7.4$ (Sancio et al., 2002). The soils that led to severe building damage were generally low plasticity silts. Data from the ground surveys indicated that 20% of reinforced concrete buildings and 56% of timber/brick buildings were severely damaged or destroyed. The Sakarya station recorded a peak horizontal (east-west) ground acceleration, velocity and displacement of 0.41g, 81 cm/s and 220 cm respectively (Bray et al., 2001). **Figure 1.3** shows a building with non-uniform downward movement of 10-15 cm at the SE corner and 150 cm at the NW corner. Bulging and cracking of the pavement is evident as a consequence of downward movement of building.

Figure 1.3: A 5-storey high building affected by liquefaction in Adapazari, Turkey (Bray et al., 2001)

Another devastating earthquake (M_W8.8) occurred on February 27, 2010, in the south-central part of Chile, specifically in the vicinity of the coast of Maule. After the main shock, a long series of aftershocks continued striking the region (Diaz, 2016). The earthquake caused a tsunami that hit the coast of the country, destroying nearby localities and increasing the number of victims and damages. Liquefaction was present in most of the territory affected by the earthquake. The river sediments along the Chilean coast and the long duration of the earthquake shaking significantly contributed to the extensive triggering of liquefaction; Valparaiso, Viña del Mar, Arauco, Concepción and Lebu were some of the cities where this phenomenon occurred. On the other hand, in the vicinity of the epicentre, the observed liquefaction was minimal (GEER Association, 2010). Significant damages were reported in road infrastructure, railroads system, ports, buildings, agriculture facilities, irrigation channels, tailing dams, among others (Verdugo and Gonzalez, 2015). The photos presented in **Figure 1.4** show typical cases of post-liquefaction settlements.

A recent earthquake, registered as M_w6.3 on February 22, 2011, occurred in Christchurch, New Zealand being the most damaging in the history of the country. The earthquake epicentre was near Lyttelton, about 10 km southeast of downtown Christchurch, at a depth of 5.9 km. The earthquake shaking caused serious damage to thousands of residential and commercial buildings, as well as a large part of the city's service infrastructures, roads and bridges in the Christchurch and Kaiapoi areas. A particular feature of this earthquake was the large area covered by liquefaction (**Figure 1.5a**). Large eruptions of saturated sand occurred covering practically all the streets in some suburbs (Diaz, 2016). Liquefaction was more severe in the eastern residential areas of the Central Business District (CBD). Several multi-storey buildings were damaged. A majority of the 4,000 buildings within the CBD were demolished, including most of the city's high-rise buildings. The seismic performance of modern multi-storey buildings and buried utilities in the CBD were most significantly affected by soil liquefaction (Bray et al., 2017a).

(a)   (b)

Figure 1.4: Post-liquefaction settlements. (a) Costanera route in Concepción (Verdugo and Gonzalez, 2015); (b) Railways near to Concepción City (Verdugo and Gonzalez, 2015)

(a)   (b)

Figure 1.5: (a) Liquefaction in a residential area of Christchurch (Diaz, 2016); (b) House with 40 cm of settlement in Kaiapoi (GEER Association, 2011)

The suburbs most affected by liquefaction were located over alluvial deposits of loose sand and silt. In the first five to six metres of depth, completely loose soils were found (GEER Association, 2011). **Figure 1.5b** shows a house located in the northern region of Kaiapoi with a settlement of approximately 40 cm, where the surface in this site was completely covered with expelled material (Diaz, 2016).

Most recently (2016), in Kumamoto, Japan, the two major seismic events on 14th and 16th April (M$_W$6.5 and M$_W$7.3), induced catastrophic damage to infrastructures and buildings in the source region as well as in the Kumamoto plain. Soil liquefaction and related damage also occurred mainly during the second one. **Figure 1.6** show typical damage to a wooden house and a reinforced concrete 3-storey building (Tokimatsu et al., 2017).

(a)	(b)

Figure 1.6: (a) Liquefaction-induced tilt of a 2-storey wooden house in Karikusa town; (b) Liquefaction-induced settlement of a 3-storey reinforced concrete building in Karikusa town (Tokimatsu et al., 2017)

The peak ground accelerations recorded in the Kumamoto plain were 4.24 m/s^2 and 8.51 m/s^2 for the first and second events, respectively. Despite the very strong earthquake shaking, the area of soil liquefaction was limited to a particular zone, registered as an artificially reclaimed river channel, where concentrated liquefaction-induced settlement and tilting of buildings was observed. In the southern part of the liquefied zone, all old wooden houses with unreinforced weak foundations also suffered unacceptable deformations of their superstructures (Tokimatsu et al., 2017). In any case, the Kumamoto earthquake is an interesting case to be investigated in order to understand how the buildings, mainly supported on spread foundations, behaved under very strong shaking.

The events summarised above highlight the extensive damage that can occur due to liquefaction and have provided useful insights to understanding the behaviour of infrastructure in liquefiable soil deposits. Many of the cases are located on old river deposits as these flat fertile sites tend to provide immediate benefits for the building of cities, however, the loose sandy saturated soil deposits tend to be highly susceptible to liquefaction. Historical decisions predating our appreciation of the consequences of liquefaction have resulted in many large cities being exposed to the risk of liquefaction. The understanding of liquefaction must go beyond just predicting its occurrence, as liquefaction risk already exists and as communities grow there will be further pressure to build infrastructure on these fertile yet liquefaction susceptible lands.

1.1.1 RECONNAISSANCE DATA

Historical data of past earthquakes is important to develop and validate methods for the assessment of liquefaction and of its consequences. Field case histories have been compiled over time and geotechnical engineers have created diverse databases with information such as whether liquefaction was triggered, site conditions, site geotechnical characterization, peak ground acceleration (PGA) values, duration of the earthquake, identification of critical layers, field examples of the consequences of liquefaction, etc.

At least since 1971, case histories collections have been published for liquefaction triggering, mainly to support the development and updating of CRR curves. Seed and Idriss (1971) gathered 35 cases from 12

LIQUEFACT
Deliverable D3.1
State of the art review of numerical modelling strategies to simulate liquefaction-induced
structural damage and of uncertain/random factors on the behaviour of liquefiable soils
v. 1.0

earthquakes in Chile, Japan, and the United States. That database included 23 cases where liquefaction was triggered and 12 cases where liquefaction was not observed (NASEM, 2016).

Other liquefaction triggering databases have been compiled, varying in their levels of information. **Table 1.1** summarizes the collection of case histories used to create five liquefaction triggering curves, commonly accepted in engineering practice. The table is divided in the three in situ test methods used to characterize soil resistance, reporting the number of data points for cases where liquefaction was triggered, cases where no liquefaction occurred and borderline cases (yes/no liquefaction) in each database. This table includes the depths to the centre of the layer with the lowest factor of safety against triggering, the effective overburden pressure associated with the critical layer, the fines content, the normalized value of the in situ parameter (($N_1)_{60cs}$, q_{c1Ncs}, V_{S1}), the cyclic stress ratio and the earthquake magnitude for each database (NASEM, 2016).

Table 1.1: Summary of recently compiled liquefaction triggering case history databases for level-ground conditions (NASEM, 2016)

Parameter	SPT		CPT		V_s
	Cetin et al., 2004	**Boulanger and Idriss 2014**	**Moss et al., 2006**	**Boulanger and Idriss 2014**	**Kayen et al., 2013**
Liquefaction triggered	109	133	139	180	287
No liquefaction triggered	88	118	44	71	124
Yes/No liquefaction	3	3	0	2	4
Critical depth (m)	1.1-20.5	1.8-14.3	1.4-14.0	1.4-11.8	1.1-18.5
Effective overburden stress σ'_{v0} (kPa)	8.1-198.7	20.3-170.9	14.1-145.0	19.0-147.0	11.0-176.1
Fines content (% by weight)	0-92	0-92	-	0-85	-
($N1)_{60cs}$, q_{c1Ncs} (atm), or V_{S1} (m/s)	2.2-66.1[a]	4.6-63.7	11.2-252.0	16.1-311.9	81.7-362.9
Cyclic stress ratio $CSR_{M7.5}$	0.05-0.66	0.04-0.69	0.08-0.55[b]	0.06-0.65	0.02-0.73[b]
Earthquake magnitude M_W	5.9-8.0	5.9-8.3	5.9-8.0	5.9-9.0	5.9-9.0

[a]($N_1)_{60}$ values; [b]CSR values

An appropriate liquefaction triggering database should supply information about the nature of the earthquake, properties of the soil layers most susceptible to liquefaction and information about their behaviour when subjected to ground motion. In particular, the observations should contain in situ properties before the earthquake and earthquake-induced ground motions measurements at the site. However, soil profile properties are generally determined only after the earthquake, that is when the soils have already been disturbed by the earthquake shaking, and the seismic loading is estimated for the site instead of being directly recorded. Information about the extent of subsurface liquefaction or excess pore water pressure distribution is also usually not provided in the databases, only referring surface

LIQUEFACT
Deliverable D3.1
State of the art review of numerical modelling strategies to simulate liquefaction-induced
structural damage and of uncertain/random factors on the behaviour of liquefiable soils
v. 1.0

manifestations. On the other hand, estimating differential ground movements on a regional scale involves great uncertainty mainly because of the lack of sufficient geotechnical data; a borehole at each corner of a building would allow a reasonable estimation of the variability in the settlements, even though retaining some uncertainties (Bird et al., 2006). Due to this, considerable judgment is required to use case history data for development, calibration or validation of liquefaction analyses and different interpretations of the same field information may rise (NASEM, 2016).

The quality of the information in these databases is expected to improve, given the growing number and level of detail of recent field case histories. For instance, Unutmaz and Cetin (2012) thoroughly documented the seismic performance of numerous 3-to-6 storey buildings after 1999 Kocaeli and Duzce earthquakes (in Turkey), mapping foundation settlements relative to available elevation references, such as peripheral concrete pavements, drainage pipes and ditches, and entrance stairs, located in the immediate vicinity of the buildings. From this data, a simple yet accurate procedure for the assessment of post-cyclic displacement response of mat foundations was developed (Unutmaz and Cetin, 2012).

2. LIQUEFIABLE SOIL BEHAVIOUR

2.1   PHENOMENA

2.1.1   OVERVIEW

Soil liquefaction is a phenomenon in which the strength and stiffness of saturated, loose, frictional soils are significantly reduced by pore pressure build-up, often caused by earthquake shaking. Liquefaction phenomena are categorized into two groups: (*i*) flow liquefaction and (*ii*) cyclic mobility. Both are triggered by the pore water pressure increase, but under static and cyclic load conditions, respectively. Ramos (2011) described the flow liquefaction process as the collapse of the structure of the sand during undrained shearing. Cyclic mobility is achieved at large excess pore water pressure build-up close to the initial vertical effective stress, however, some level of shear stiffness is recovered during cyclic loading as soil dilation and contraction causes a cyclic decrease and increase in pore pressure.

The development of liquefaction on flat ground in free-field conditions occurs due to cyclic shear stress (τ) and strain (γ) generated by the seismic shear waves (**Figure 2.1a**). The soil particles rearrange under shear strain and the soil tries to contract; however, the pore water cannot easily escape under the rapid seismic load (**Figure 2.1b**). The pore water compresses under each cycle and increases in pressure, thus decreasing the mean effective stress (p') (**Figure 2.1c**). The reduction in effective stress causes a reduction in the low strain stiffness, which consequently leads to increased strain and increased pore pressure build up (**Figure 2.1d**).
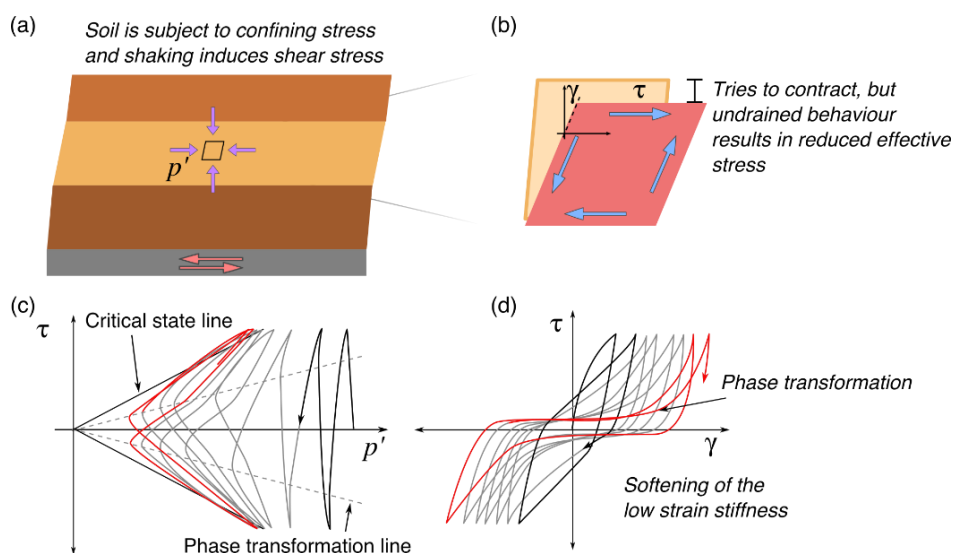

Figure 2.1. Liquefaction behaviour in the free-field

Figure 2.1 also illustrates some other important aspects of the behaviour of liquefiable soils. In **Figure 2.1c** there are two boundary lines, the critical state line and the phase transformation line. The critical state line

in τ-p' space denotes the stress ratio of the soil at large shear strain where no further volume change occurs under shear strain. The phase transformation line denotes the stress ratio where the soil changes from contractive to dilative under shear strain. This dilative behaviour is seen in **Figure 2.1c** when the shear stress exceeds this boundary, and the effective stress starts to increase. As the loading continues the behaviour stabilises and forms a butterfly shape (shown in red). Therefore, in a single cycle of loading the pore pressure increases and decreases twice. This dilative behaviour has very important consequences for the performance of structures in terms of the strength of the soil, the propagation of shear waves and the flow of pore water, as explained throughout this report.

In liquefaction analyses, the build-up of pore pressure is often described as excess pore pressure and expressed as a pore pressure ratio (r_u), which is defined as the ratio of the excess pore pressure to the initial vertical effective stress. Furthermore, r_u indicates the proximity of triggering of soil liquefaction. Prior to cyclic loading r_u value is 0, while at the triggering of liquefaction, it is near to 1.

One of the most important aspects of assessing the performance of structures on liquefiable soil deposits, is to determine whether the soil is in fact liquefiable. Kramer (1996) defines liquefaction susceptibility through the following criteria:

- Historical criterion: addresses the seismic activity of the zone and involves seismic factors like magnitude, acceleration and duration.
- Geological criterion: involves the origin, formation, fabric, structure of soils. Furthermore, in this criterion is included the permeability and cohesion of material, which may affect the pore pressure dissipation and effective stress reduction.
- Compositional criterion: focuses on the grain size distribution and the shape of the soil particles.
- State criterion: relates the degree of saturation, initial stress conditions and the relative density of the soil.

The above criteria are useful for classifying the expected behaviour of a soil during a seismic event, and there is a wealth of research on the influence of various soil properties on the liquefaction susceptibility (e.g. Boulanger and Idriss, 2014). This report is focused on the performance of buildings on liquefiable deposits, and therefore it does not address those properties, instead it assumes a soil to be either liquefiable or not. The key soil behaviour for the performance of buildings is the tendency to contract or dilate, thus increasing or decreasing the excess pore water pressure.

As seen in **Figure 2.1**, the dilative or contractive behaviour of soil is dependent on the stress state, but it is also dependent on the soil properties and density. While loose soils, have a greater tendency for contraction, dense soils have a tendency to dilate under large shear strain. The difference between these types of soil can be explained by examining the soil under monotonic loading using the framework of critical state soil mechanics.

2.1.2   UNDRAINED MONOTONIC LOADING

Figure 2.2 depicts the behaviour of four soil specimens under a direct shear load, conceptually developed based on the experimental tests presented by Verdugo and Ishihara (1996). **Figure 2.2a** shows the

LIQUEFACT
Deliverable D3.1
State of the art review of numerical modelling strategies to simulate liquefaction-induced
structural damage and of uncertain/random factors on the behaviour of liquefiable soils
v. 1.0

behaviour in *e-p'* (void ratio versus mean effective stress) space, the other plots depict the deviatoric stress, q = 2·τ, the shear strain (γ) and the pore pressure ratio (r_u).
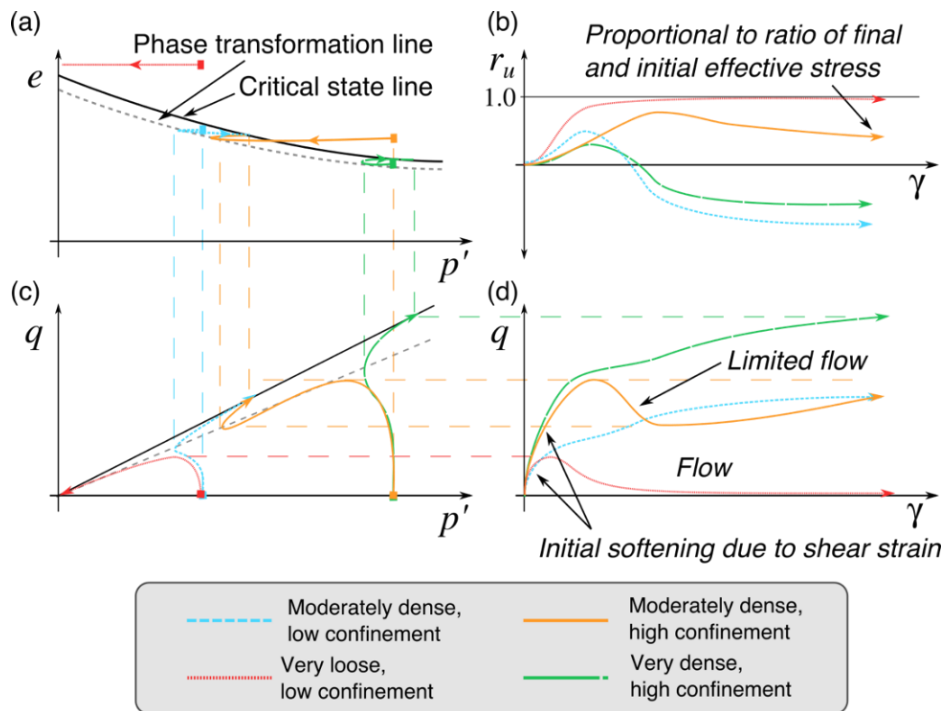
Figure 2.2: Monotonic undrained behaviour of sand

Following the behaviour of the 'Moderately dense – high confinement' specimen (orange line), in **Figure 2.2a** it can be seen that it starts at a state above the critical state line and contracts until it reaches the phase transformation line, at which point it dilates back to the critical state line. Tracing this behaviour down to **Figure 2.2c**, it can be seen that the deviatoric stress initially increases to a maximum value, and then the build-up in pore pressure results in a softening and decrease in strength, until it crosses the phase transformation line, where it dilates and increases in strength to reach the critical state. In *q-γ* space (**Figure 2.2d**), the behaviour shows the increase in load with a softening of the response, the softening at low strain is related to the shear strain (and also occurs for drained behaviour), this can be seen by **Figure 2.2b** where there is almost no pore pressure build up in the initial part of the loading, it is also reflected in **Figure 2.2c**, where the loading is almost vertical in the *q-p'* space, denoting that there was minimal change in pore pressure. The softening at larger strains for the 'Moderately dense - high confinement' specimen in **Figure 2.2d** is due to the build-up of pore pressure and eventually limited flow can be observed, before the soil state reaches the phase transformation line and hardens; the final excess pore pressure ratio being less than 1.0.

The behaviour of this soil specimen can be contrasted with the 'Moderately dense – low confinement' specimen (blue line). In **Figure 2.2a** it can be seen that the state is below the critical state line but above the phase transformation line. The soil initial contracts just like the first soil, and then dilates to the same point on the critical state line. The behaviour of this soil in the *q-p'* and *q-γ* space is slightly different though, it

does not reach a maximum stress state until the end of loading and does not show the limited flow behaviour of the first specimen. Finally, it can be seen in **Figure 2.2d** that overall the soil dilated and the pore pressure decreased below its initial value.

The behaviour of the 'very dense – high confinement' specimen (green line), is almost identical to the second specimen, however, the behaviour is all at higher stresses. This apparent similarity in behaviour provides the basis for critical state mechanics, where it can be seen that both soils are initially contractive and then dilative and do not exhibit flow. The stress state and density of the soil are intrinsically linked. The final specimen, 'very loose – low confinement' specimen (red line), is an extreme case where the soil state is well above the critical state line (**Figure 2.2a**). In this case the soil contracts but only reaches the critical state line at very low mean effective stress, where the soil essentially loses all of its shear strength and stiffness. This behaviour is call 'flow'.

2.1.3   STATE PARAMETERS

To quantify the relationship between stress and density, Been and Jefferies (1985) defined the state parameter (ψ) based on critical state soil mechanics (**Figure 2.3**). ψ is a useful reference point for understanding liquefiable soil behaviour during undrained monotonic loading, where dramatic differences can be observed through the change of initial density and confining stress.
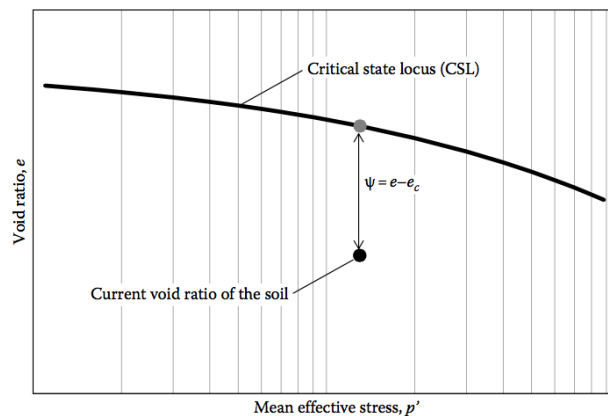
Figure 2.3. Definition of state parameter (Jefferies and Been, 2015)

The state parameter (ψ) is simply the void ratio difference between the current state of the soil and the critical state at the same mean effective stress (Jefferies and Been, 2015). ψ can be represented mathematically as in **Equation (1)**:

$$\psi = e - e_c \tag{1}$$

where e is void ratio and e_c is the void ratio under steady-state (critical state) conditions, which measures the vertical distance between the initial state of a soil and its critical-final state. The advantage of this

LIQUEFACT
Deliverable D3.1
State of the art review of numerical modelling strategies to simulate liquefaction-induced
structural damage and of uncertain/random factors on the behaviour of liquefiable soils
v. 1.0

parameter is that it quantifies the influence of the void ratio and the stress level in the evaluation of sands behaviour (Andrade, 2009).

Another boundary condition that is often used in soil state mechanics is the quasi steady state (Yoshimine and Ishihara, 1998). This state exists when the soil deforms at constant volume during phase transformation and occurs for some loading conditions depending on the initial stress and density of the specimen (Alarcon-Guzman et al., 1988). Ishihara (1993) argues that the quasi steady state is a more appropriate reference point for soil behaviour as it is obtained at moderate to large strains (5-20%) compared to the critical state which is often only reached at strains of 20-30%. To quantify the behaviour against the quasi steady state, the State Index (I_S) parameter was defined (**Equation (2)**).

$$I_S = \frac{e_{IC} - e_0}{e_{IC} - e_{QSS}} \tag{2}$$

where e_0 is the initial void ratio, e_{IC} represents the void ratio of the soil at its loosest state consolidated isotopically to the initial confining stress and e_{QSS} the void ratio at quasi steady state conditions (QSS).

The critical state mechanics framework provides the basis for the majority of advanced soil constitutive models, thorough the use of the state parameter or state index. The relationship between density and confining stress allows the behaviour of the soil to be described over a wide range of stress and density states using the same set of model parameters. The critical state framework also provides a useful tool for understanding the macro-behaviour of the soil in the presence of a building, as a building provides both additional shear and confining stress compared to free-field conditions.

The major difference between the use of the quasi steady line and the critical state line is that the critical state behaviour should be independent of the initial fabric, while the quasi steady state line is dependent on fabric (Verdugo, 1992). There are both benefits and drawbacks of this difference, models that use the quasi steady state as a reference tend to require further calibration of the model parameters to the specific soil specimen, compared to those that use the critical state and therefore ignore the influence of the initial fabric on the response.

2.1.4   UNDRAINED CYCLIC LOADING

For cyclic loading, the behaviour is even more complex than monotonic loading. The initial contractive behaviour of sand means that liquefaction or cyclic softening can occur even in dense soils. However, in contrast with monotonic loading, liquefaction triggering during cyclic loads is controlled not just by the density but also by the stiffness and cyclic energy dissipation. During load-unloading-reloading stages, the soils undergoes non-reversible deformations and degradation of the elastic moduli (Molina-Gómez et al., 2016). If the shear stress demand is kept constant than the soil goes through larger shear strains and large volumetric strains as the soil stiffness degrades. In real in situ conditions the demand is not often a uniform cyclic load and the change in soil stiffness and energy dissipation tends to modify the shear stress, however, it is useful to understand the soil behaviour in terms of uniform cycles of shear stress.

LIQUEFACT
Deliverable D3.1
State of the art review of numerical modelling strategies to simulate liquefaction-induced
structural damage and of uncertain/random factors on the behaviour of liquefiable soils
v. 1.0

Figure 2.4 presents the results of torsional cyclic tests developed to illustrate the cyclic behaviour during liquefaction process in Toyoura sand. Essentially, the soil stress and density state as well as the fabric control the number of cycles required to reach liquefaction (Ishihara, 1993). This is typically quantified by liquefaction resistance curves, which quantify the number of cycles at a given uniform shear stress before liquefaction occurs.
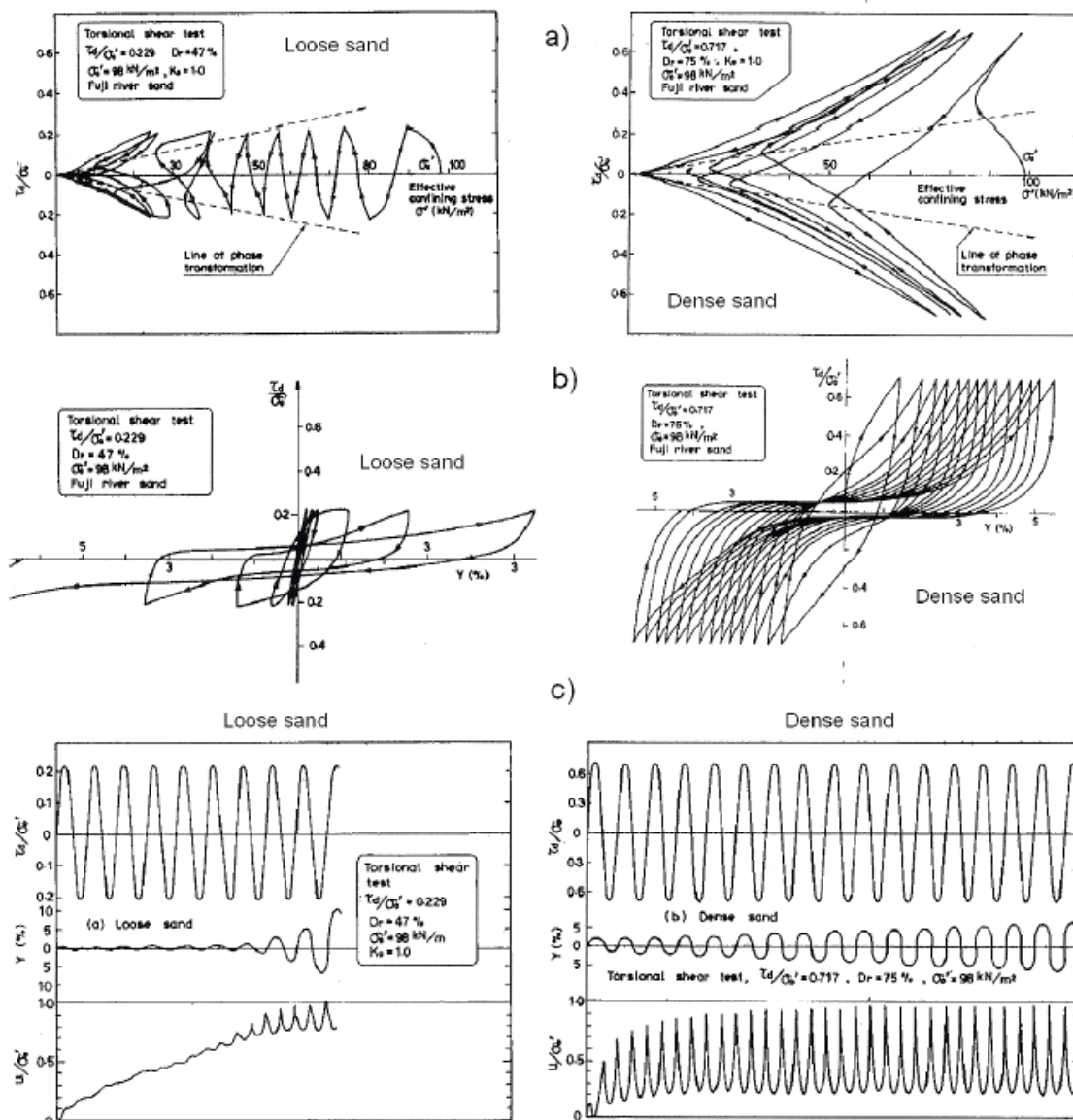
Figure 2.4. Behaviour of Toyoura sand in cyclic torsional tests: (a) Stress-strain curve (b) Stress-path (c) Excess pore pressure generation (Ishihara, 1985)

The behaviour of the soil after liquefaction is highly dependent on the tendency of the soil to dilate. Under large cyclic strain the soil dilates and causes a cyclic reduction in excess pore pressure and cyclic increase in the stiffness of the soil (strain hardening). The cyclic pore pressure reduction has twice the frequency of the

cyclic loading, as large strains are reached twice during each cycle (**Figure 2.4**). The amplitude of the pore pressure reduction and subsequent strength and stiffness increase is controlled by the soil density and confining stress, among other soil parameters.

2.1.5   RESIDUAL STRENGTH

The estimation of residual strength is one of the most debated aspects of liquefaction behaviour (e.g. Castro and Poulos, 1977; Olson and Stark, 2002; Robertson, 2009a; Anderson et al., 2012; Boulanger et al., 2013; Kramer and Wang, 2015; Phan et al., 2016). The residual soil strength is often back-calculated from slope failures; however, this often incorporates a large amount of uncertainty due to the varying soil properties throughout the slope as well as variations in stress and water content. The other major issue is whether the strength is representative of the quasi steady state or critical state of soil, or some other partially drained, varying stress state (**Figure 2.5**).
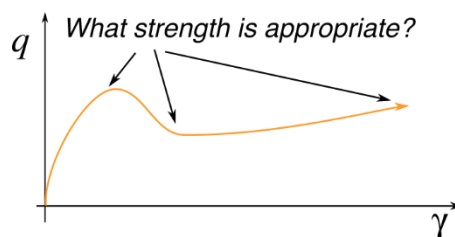
Figure 2.5: Strength of undrained monotonically loaded soil

Unfortunately, the estimation of soil residual strength is essential to many geotechnical problems (e.g. bearing capacity failure). The sensitivity of the strength to pore pressure makes it highly dependent on the situation and therefore the residual strength determined for slope failure may not be appropriate for bearing capacity failure due to the different deformation mechanisms of the soil and the different hydraulic pressures that develop.

There are several empirical methods available to estimate residual strength, such as the one proposed by Kramer and Wang (2015), that establish an empirical procedure to predict residual strength as a nonlinear function of both penetration resistance and initial effective stress, based on the steady-state concepts and calibrated through historical cases. There are also simplified analytical assumptions based on the pore pressure ratio to develop an equivalent friction angle (Cascone and Bouckovalas, 1998). Finally, the residual strength can be back calculated using soil constitutive models for problem dependent situations, such as simulating bearing capacity failure of a shallow foundation (Karamitros et al., 2013a).

2.2   MANIFESTATION OF LIQUEFACTION IN FREE-FIELD CONDITIONS

2.2.1   ESTIMATION OF LIQUEFACTION TRIGGERING

The estimation of the occurrence of liquefaction is a critical part of most procedures for estimating liquefaction related damage. Liquefaction triggering can be estimated through advanced constitutive

modelling or by means of simplified procedures that estimate equivalent demand and resistance for one dimensional soil profiles. The focus of this section is on the simplified procedures, while advanced constitutive modelling is discussed in Section 2.3.

Simplified liquefaction triggering procedures are a very practical tool for assessing the soil susceptibility to liquefaction using easily obtainable field data. The most common simplified procedures are based on Standard Penetration Test (SPT) and Cone Penetration Test (CPT) data, while there are also methods that make use of the soil shear wave velocity and other testing instruments (Viana da Fonseca et al., 2016). The choice of field-testing device is often governed by financial and availability requirements; however, there are some advantages and drawbacks for different devices for different scenarios, e.g. CPT struggles to penetrate gravelly material compared to other devices. Given the wide availability of SPT and CPT testing equipment, the methods based on these devices are often used as a benchmark, especially stress-based methods (e.g. Seed and Idriss, 1971; Seed et al., 1984; Youd et al., 2001; Moss et al., 2006; Boulanger and Idriss 2014; Robertson, 2015).

Conceptually, the stress based method estimates an equivalent cyclic stress demand applied to a layer of soil based on the peak ground surface acceleration (a_{max}), earthquake magnitude (M_W) and total vertical stress (σ_v). That demand is expressed as an equivalent Cyclic Stress Ratio (CSR, see **Equation (3)**), which is normalised by the effective vertical stress (σ_v') and corrected by terms to account for the soil column mass participation factor (r_d), and the influence of both initial static shear stress (K_α) and overburden pressure (K_σ).

$$\text{CSR} = \frac{0.65\sigma_v}{\sigma_v{'}} \frac{a_{max}}{g} r_d \cdot K_\alpha \cdot K_\sigma \tag{3}$$

The resistance of the soil to liquefaction (cyclic resistance ratio, CRR) is quantified by the soil type and density among other soil characteristics, determined through a series of correlations from the measured values from the CPT and SPT devices. The correlations to resistance are typically determined for cyclic loading equivalent in duration to a magnitude 7.5 earthquake event. Therefore, the CSR should be adjusted to an equivalent magnitude 7.5 event using a magnitude scaling factor (MSF). The factor of safety against the triggering of liquefaction is determined based on the ratio of the stress demand and resistance, through **Equation (4)**.

$$\text{FS} = \frac{\text{CRR}_{M7.5}}{\text{CSR}} \cdot \text{MSF} \tag{4}$$

The form of the simplified procedure has remained largely unchanged since its inception by Seed et al. (1971); however, the expressions for r_d, K_α, K_σ, $\text{CRR}_{M7.5}$ and MSF have experienced numerous updates and modifications to better account for the site response, the soil type and the fines content, to name just a few of the influencing factors. In particular, the influence of static shear stress is widely debated. The

change in behaviour can be partially understood by recalling the behaviour of soil under monotonic loading (**Figure 2.2**), where for dense sand the soil dilates under large strain. The addition of static shear stress can also dramatically reduce the building up of pore pressure by limiting the soil from going through stress reversals (switching the direction of shear loading), which is an important part of the contractive behaviour where soil particles are rearranged.

There are several other common correction factors, normally related specifically to the testing apparatus. One correction is the thin layer correction factor for CPT where the sleeve friction is measured across the length of the sleeve and therefore struggles to capture the friction from very thin layers (Moss et al., 2005). Another correction is the influence of fines content; this correction is both related to influence of fines on the measure of stresses on the device and to the influence of fines of the liquefaction resistance of the soil (Cubrinovski et al., 2010). The plasticity of the soil and the limit at which a soil is too plastic to liquefy is often debated (e.g. Seed et al., 2003).

The main drawback of the stress-based method is that liquefaction is ultimately a cumulative strain based phenomenon, where cyclic shear strain results in contraction of the soil skeleton causing liquefaction.

To better account for the dependence on cumulative strain, several alternative methods have been proposed. The energy-based concept relies on a correlation between soil hysteretic energy dissipation and volumetric strain and typically uses Arias Intensity or Cumulative Absolute Velocity as an intensity measure (Bán et al., 2017). Energy-based methods have the advantage of using a single intensity measure and using a cumulative intensity measure gives an indication of the build-up of pore pressure throughout the motion. The main drawback is that the majority of seismic design standards and codes do not provide estimates of these cumulative intensity measures.

The main limitation of the simplified procedure is that it is one-dimensional, and in many cases does not even account for vertical interaction between layers. Cubrinovski et al. (2017a) compared the liquefaction severity using the simplified procedure (Boulanger and Idriss, 2014) and the Liquefaction Severity Number (van Ballegooy et al., 2014) against field data from 55 sites from the Christchurch September 2010 and February 2011 earthquakes. For sites where liquefaction was observed from both events, the simplified procedure underpredicted the severity in 11 out of the 22 cases, and for cases where no liquefaction was observed, the simplified procedure overpredicted the liquefaction severity in 32 out of the 34 cases. Further investigation by Cubrinovski et al. (2017a) using fully coupled effective stress modelling, identified the system response (or vertical interaction of layers) to be the key contributor to this poor comparison. Essentially upward flow of pore water was increasing the severity of some cases, while liquefaction at deep layers was reducing the shaking demand in upper layers, and highly stratified soil was reducing the build-up and liquefaction severity in other cases, none of which is accounted for in the simplified procedure.

The issue of vertical and horizontal interaction is even more important for the estimation of triggering under a building, where the additional shear and confining stresses from the foundation can dramatically change the pore pressure build up and cause pore water flow from high pressure to low pressure regions. The point at which simplified procedures are no longer applicable to buildings is highly dependent on the applied load and geometry of the building and there is currently no clear consensus on the limits.

2.2.2 INDICATORS OF LIQUEFACTION SEVERITY

The purpose of calculating liquefaction triggering is typically to estimate the resulting ground damage. The ground damage can be quantified in terms of ground settlement and lateral spreading, as well as general indices that can qualitatively describe ground damage.

There are several liquefaction severity indices proposed in literature. The methods vary in terms of their weighting of importance of near surface liquefaction and their consideration of soil type and the liquefaction factor of safety increments with depth. The majority of the procedures have a maximum contribution from the near surface layers, this is justified since deformations in surface layers can more easily result in deformations at the surface and manifest surface ejecta. There is no consensus about the best liquefaction intensity indicator and often the indices are used in conjunction to account for some of the uncertainty in the expected level of ground damage.

Zhang et al. (2002) provides a method for estimating the level of one-dimensional consolidation settlement (S_{V1D}, see **Equation (5)**) using volumetric consolidation strains (ε_v) from Ishihara and Yoshimine (1992). More recently, Chiaradonna et al. (2017) propose a simplified procedure based on an effective stress approach, validated through in-situ investigation on real sites. The pore water pressure model requires the definition of two semi-empirical curves: the cyclic resistance curve (as functions of SPT and CPT results) and the pore pressure ratio curve (as functions of the relative density and fine content). The calculated excess pore pressure distribution with depth is used to compute a post-earthquake volumetric settlement.

$$S_{v1D} = \int \varepsilon_v dz \tag{5}$$

The Liquefaction Potential Index (LPI) was developed by Iwasaki et al. (1978) and is a simple depth (z) weighted average of the liquefaction factor of safety (FS) (see **Equation (6)**).

$$\text{LPI} = \int_0^{20m} F_1 \cdot w(z) dz \quad , \quad F_1 = \begin{cases} 1-\text{FS} \ , & \text{FS} \leq 1 \\ 0 & , \ \text{FS} > 1 \end{cases} \quad , \quad W(z) = 10 - 0.5z \tag{6}$$

The Ishihara-inspired Liquefaction Potential Index (LPI$_{ISH}$, see **Equation (7)**) is a correction to LPI developed by Maurer et al. (2014). The major difference is the consideration of the height of the superficial, non-liquefiable crust (H_c) that can reduce land damage.

$$\text{LPI}_{ISH} = \int_{H_1}^{20m} F(\text{FS}) \frac{25.56}{z} dz \ , \quad F(\text{FS}) = \begin{cases} 1-\text{FS} \ , & \text{FS} \leq 1 \cap H_c \cdot m(\text{FS}) \leq 3 \\ 0 & \text{otherwise} \end{cases} , \quad m(\text{FS}) = \exp\left(\frac{5}{25.56(1-\text{FS})}\right) - 1 \tag{7}$$

The Liquefaction Severity Number (LSN) was developed by van Ballegooy et al. (2012) and is similar to of one-dimensional consolidation settlement (see **Equation (5)**) but the volumetric strain of the layer is weighted against the depth of the layer, as shown in **Equation(8)**.

$$LSN = \int \frac{\varepsilon_v}{z} dz \qquad (8)$$

The cumulative thickness of liquefying layers (CTL) was used by van Ballegooy et al. (2012) as a liquefaction severity indicator when examining damage to low-rise residential buildings. The indicator is simply a sum of all layers that where expected to liquefy using a given triggering method and a given hazard.

The choice of indicator or correlation of indicator to infrastructure damage is dependent on the area of influence of the infrastructure and its sensitivity to differential and total settlements and horizontal displacements. There is on-going research in this subject to refine and improve liquefaction severity indicators.

2.3   SOIL CONSTITUTIVE MODELS

The inherent difficulties and costs associated with experimental and field based research justify why numerical modelling of soil liquefaction is a cornerstone of liquefaction research. However, the complex interplay between the soil fabric and the pore water makes this task extremely demanding for the user and the software. In order to simulate the seismic response of liquefiable soils, comprehensive constitutive models which have the ability to describe salient physical phenomena of the soils cyclic response have to be employed. According to Kramer and Elgamal (2001), a soil liquefaction constitutive model should account for the following features:

a) nonlinear inelastic shear stress-strain response;
b) dependence of shear and volumetric stiffness on effective confining pressure;
c) contraction of the soil skeleton during the early stages of loading;
d) dilation of the soil skeleton at large strain excursions;
e) the critical state at which shearing occurs with neither contractive nor dilative tendencies,
f) controlled accumulation of cyclic shear strain when cyclic loading is superimposed upon static stresses;
g) post-liquefaction void-ratio redistribution (dilative and, as the liquefied soil re-consolidates, contractive) ;
h) the coupling response of the soil skeleton and porewater;
i) the effect of the permeability of the soil on the rate at which volume change can occur.

This feature set is beyond the capabilities of current constitutive models (NASEM, 2016), but the list provides a useful set of criteria for the development and validation of current and new models. It should also be noted, that the importance of various features depends on the situation and modelling goal. The modelling of soil site response is highly sensitive to stiffness and the evolution of liquefaction but less

sensitive to residual strength. Bearing capacity failure is highly sensitive to residual strength and less sensitive to evolution of liquefaction and void ratio change. Foundation settlements on deep liquefiable deposits are more sensitive to consolidation and permeability, while foundations on shallow liquefiable deposits are more influenced by soil residual strength and the evolution of liquefaction.

Due to the various problem-dependent requirement sets for constitutive models, each model has trade-offs between the simulation of the different features as well as considering usability. Finally, one of the most important requirements of all constitutive models is the simplicity in which the model parameters can be obtained from field or laboratory tests.

In the following, several constitutive material models for liquefiable soils are reviewed by examining three of the most commonly used software products for simulation of soil liquefaction and soil-structure interaction:

i)   OpenSees
ii)   FLAC
iii)   PLAXIS

2.3.1 OPENSEES

OpenSees (2017) is an open-source software developed at the Pacific Earthquake Engineering Research (PEER) Center which is aimed at the simulation of the performance of structural and geotechnical systems subjected to earthquakes. The software is capable of modelling the coupling response between the soil skeleton and the pore fluid, and can model the redistribution of pore pressure during shaking in either two- or three-dimensions. The open-source nature of the software enables the user to modify existing constitutive models and to implement new models through Tcl-scripting. The software also offers several different solver algorithms as well as the ability to implement a user defined solver.

Some recent examples of the use of OpenSees for liquefaction and soil-structure interaction include:

- Aygün et al. (2011) employed the *PressureDependMultiYield* material model for fragility analysis of a multi-span continuous bridge on liquefiable soils.
- Karimi and Dashti (2016) used the *PressureDependMultiYield02* material model for a fully coupled 3D evaluation and validation of the liquefaction-induced settlements of a single degree of freedom (SDOF) structure founded on a rigid mat.
- The *Manzari Dafalias* material model was used by Shahir and Pak (2010), and Ayoubi and Pak (2017), for a 3D dynamic fully coupled u-p analysis of the liquefaction-induce settlement of shallow foundations.

PDMY02

The *PressureDependMultiYield02* material model, named PDMY02 material in the following, is implemented in OpenSees and is an extended version of the *PressureDependMultiYield* material (Yang et al., 2008). The constitutive model was elaborated in previous studies by Elgamal et al. (2003) and Yang et al.

LIQUEFACT
Deliverable D3.1
State of the art review of numerical modelling strategies to simulate liquefaction-induced
structural damage and of uncertain/random factors on the behaviour of liquefiable soils
v. 1.0

(2003), and is specially tailored for simulation of shear-induced volume contraction and dilatation and non-flow liquefaction (cyclic mobility). Plasticity is formulated based on a number of open conical-shaped yield surfaces (nested surfaces) with the apex located at the origin of the principal stress space. The model uses a nonlinear kinematic hardening and non-associative flow rule that produces volumetric dilation and contraction under shear deformation. The yield surfaces are of the Drucker-Prager type. In this model, no plastic change of volume takes place under a constant stress ratio, since the yield surfaces are open-ended.

The material is usually employed in solid-fluid fully coupled elements which allow, depending on the assumed permeability values, the simulation of, both, undrained (low permeability assumed) and partially drained soil response (actual permeability values). Based on model calibration, the authors provided standard modelling parameters for sands of different relative density (Yang et al., 2008). Gingery (2014) and Gingery et al. (2015) discuss the PDMY02 calibration protocols and the appropriateness of the element-level calibration for the simulation of site response analysis. The results obtained by Gingery et al. (2015) show good agreement between the site response pore pressure values and the calculated factors of safety, indicating that the element-level calibrations are valid for liquefaction triggering analysis of prototype soil systems. Additional calibration parameters for PDMY02 material in the case of Nevada sand, Silica Silt and Monterey sand of different relative densities were proposed by Karimi and Dashti (2016).

STRESS-DENSITY

The *Stress Density* material model was recently implemented in OpenSees. The model was developed by Cubrinovski and Ishihara (1998a, 1998b), and was later extended to 3D conditions by Das (2014). The constitutive model is based on the state concept, where the sand stress-strain behaviour is characterised based on its combined density and confining stress state, using the state index (Ishihara 1993), and using a modified elastic–plastic formulation with continuous yielding and hypo-plasticity using multiple nested yield surfaces. The major benefit of this is that a single set of model parameters can be used to describe the soil at all relevant stresses and densities. There are four different categories of parameters for the model (Cubrinovski et al., 2017a):

- Critical state line, parameters to define the critical state line
- Plastic stress-strain: parameters used to define the shear stress versus strain behaviour
- Stress-dilatancy: parameters to link the plastic shear strain with the volumetric strains
- Elastic: parameters to define the elastic behaviour

The parameters can be obtained through a series triaxial tests defined in Cubrinovski and Ishihara (1998a), the parameters can also be obtained from CPT data using the procedure in Cubrinovski et al. (2017a) where liquefaction resistance curves are determined using the relationships defined in Boulanger and Idriss (2014).

2.3.2   FLAC

FLAC, Fast Lagrangian Analysis of Continua, is a numerical modelling software for advanced geotechnical analysis of soil, rock, groundwater, and ground support, developed by Itasca Consulting Group Inc.

(Itasca, 2017). It utilizes an explicit finite difference formulation that can model complex problems, such as problems that consist of several construction stages, large displacements and strains, non-linear material behaviour or unstable systems (Itasca, 2017). The software is capable of modelling the coupling response between the soil skeleton and the pore fluid, and can model the redistribution of pore pressure during shaking in either two- or three-dimensions. It also features the so called "FISH scripting", which enables the user to interact with and manipulate the numerical models, as well as Python scripting. User-defined constitutive models can be also implemented in the software.

Some recent examples of the use of FLAC for liquefaction and soil-structure interaction include:

- Luque and Bray (2015, 2017) who employed the PM4Sand model for a 2D numerical simulation of liquefaction-induced settlements of a shallow-founded building in Christchurch observed during Canterbury earthquake sequence.
- The PM4Sand model was also used by Ziotopoulou and Montgomery (2017) for a numerical study on the earthquake-induced liquefaction settlement of shallow foundations.
- The NTUA-Sand constitutive model was also used by Dimitriadi et al. (2017) for a study on the seismic performance of strip foundation on liquefiable soils with a permeable crust.

PM4SAND

The *PM4Sand* is a sand plasticity model implemented in FLAC specially developed for geotechnical earthquake engineering applications (Boulanger and Ziotopoulou, 2013). The model follows the basic framework of the stress-ratio controlled, critical state compatible, bounding surface plasticity model for sand presented by Dafalias and Manzari (2004). Modifications to the Dafalias-Manzari model were developed and implemented to improve its ability to approximate stress-strain responses important for geotechnical earthquake engineering applications.

The calibration of *PM4Sand* model and its implementation in the software FLAC was presented by Ziotopoulou and Boulanger (2013), later updated to Version 3.0 (Boulanger and Ziotopoulou, 2015). Ziotopoulou and Boulanger (2015) discuss validation protocols for constitutive modelling of liquefaction, and emphasise the importance of rigorous element-level validations against experimental data. A comparison of the performance of *PM4Sand* model against other constitutive models, i.e. the Dafalias-Manzari model, the PDMY model, and the UBCSAND model, was presented by Ziotopoulou et al. (2014). The formulation of the model focuses on approximating the empirical correlations and design relationships that are frequently adopted to represent the engineering behaviour of sand.

NTUA-SAND

The NTUA-Sand model combines bounding surface plasticity theory with a vanished elastic region (Andrianopoulos et al., 2010). The constitutive model is based on the state concept, where the sand stress-strain behaviour is characterised based on its combined density and confining stress state. Unlike the stress-density model (see above), which uses the state index (Ishihara 1993), the NTUA-Sand model uses the state parameter (Been and Jefferies, 1985). A single set of model parameters can be used to describe

the soil at all relevant stresses and densities. The model has three deviatoric-stress ratio surfaces (critical state surface, the bounding surface and the dilatancy surface) with their apex at the origin to define the continuous yielding behaviour (See **Figure 2.6**). Note that the yield criterion is defined as a single point. An empirical index is used to simulate fabric evolution that scales the plastic modulus, to quantify the rate of excess pore pressure build-up (Andrianopoulos et al., 2010). The Ramberg–Osgood formulation is used for the basis of the hysteretic behaviour and governs the non-linear soil response under small to medium cyclic strain amplitudes.

The accuracy of the constitutive model has been evaluated against experimental data from Arulmoli (1992) and several soil-foundation centrifuge tests (Andrianopoulos et al., 2010).
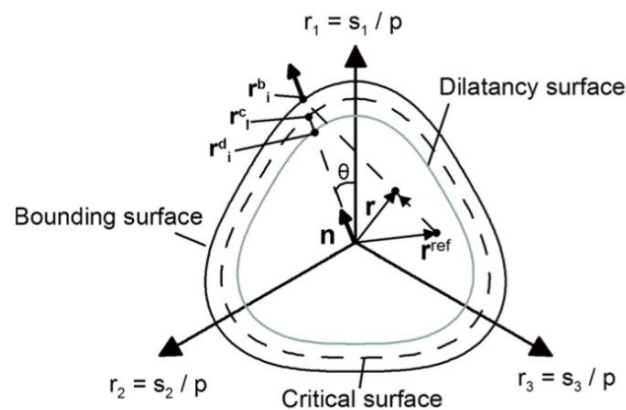
Figure 2.6: Model surfaces and adopted mapping rule in the p-plane of the deviatoric stress ratio space, based on a relocatable projection centre (Andrianopoulos et al., 2010)

UBCSAND

The UBCSAND model is implemented in FLAC and is an effective stress plasticity model which was developed for use in advanced stress-deformation analyses of geotechnical structures (Puebla et al., 1997; Beaty and Byrne 1998; Byrne et al., 2004). The model predicts the shear stress-strain behaviour of the soil using an assumed hyperbolic relationship, and estimates the associated volumetric response of the soil skeleton using a flow rule that is a function of the current stress ratio (Beaty and Byrne 2011).

2.3.3 PLAXIS

PLAXIS is a powerful and user-friendly finite element package intended for two- or three-dimensional analysis of deformation and stability in geotechnical engineering and rock mechanics (PLAXIS, 2017). The software is capable of modelling the coupling response between the soil skeleton and the pore fluid, but cannot model the redistribution of pore pressure during shaking. The software is available in either 2D or 3D versions. As an alternative to the user-friendly interface, PLAXIS also features a remote scripting interface based on Python language, which allows automated model changes or model building. The software also implements a facility for user-defined soil models, which allows users to implement a wide range of soil models using the FORTRAN programming language.

LIQUEFACT
Deliverable D3.1
State of the art review of numerical modelling strategies to simulate liquefaction-induced
structural damage and of uncertain/random factors on the behaviour of liquefiable soils
v. 1.0

Some recent examples of the use of PLAXIS for liquefaction and soil-structure interaction include:

- Daftari and Kudla (2014) reporting the use of the UBC3D-PLM material model for numerical prediction of soil liquefaction observed during the 1987 Imperial Valley earthquake event for case study location.
- Souliotis and Genolymos (2016) calibrated the parameters of the UBC3D-PLM model, and used it for the reproduction of the liquefaction-induced lateral spreading of a quay wall observed during the 1995 Kobe earthquake.
- Bhatnagar et al. (2016) performed a numerical analysis of an embankment on liquefiable soils in PLAXIS, and studied the influence of different remedial measures on response of the embankment.

UBC3D-PLM

The most commonly used constitutive model for simulation of soil liquefaction in PLAXIS is the UBC3D-PLM model (Petalas and Galavi 2013), which is a 3D generalization of the previously described UBCSAND model (Puebla et al., 1997; Beaty and Byrne 1998).

UBC3D-PLM is an elastoplastic constitutive model, which utilizes isotropic and simplified kinematic hardening rules for primary and secondary yield surfaces, in order to take into account the effect of soil densification and predict a smooth transition into the liquefied state during undrained cyclic loading.

2.3.4 ADDITIONAL CONSTITUTIVE MODELS

The *Manzari Dafalias* material was implemented in OpenSees based on the work performed by Dafalias and Manzari (2004). It is a simple stress-ratio controlled, critical state compatible sand plasticity model suitable for simulation of soil liquefaction. The suggested input parameters for the model are provided in the paper by Dafalias and Manzari (2004). Shahir et al. (2012) provide specific calibration parameters for the Nevada sand.

The *CycLiqCPSP* material is implemented in OpenSees and is an extended version of the previous material *CycLiqCP*. The constitutive models were proposed by Zhang and Wang (2012) and Wang et al. (2014), respectively, and were specially designed for simulation of large post-liquefaction shear-deformations. Wang et al. (2014) and Wang et al. (2015) presented the implementation of the models in OpenSees, and validated their results against experimental results. A centrifuge experiment on a single pile in liquefiable ground was examined and the model showed promising prediction capabilities.

The effective stress (modified) Mohr-Coulomb model is implemented in FLAC as the Finn-Byrne model and adopts the pore pressure generation model presented by Martin et al. (1975), later modified by Byrne (1991).

Multi-spring and *Cocktail glass* models are formulated on a basis of strain space multiple mechanism model. This model consists of a multitude of simple shear mechanisms with each oriented in an arbitrary direction and can describe the behaviour of granular materials under complicated loading paths, including the effect of rotation of principal stress axes (Iai et al., 2011).

This project has received funding from the European Union's Horizon 2020 research and innovation programme under grant agreement No. 700748

LIQUEFACT
Deliverable D3.1
State of the art review of numerical modelling strategies to simulate liquefaction-induced structural damage and of uncertain/random factors on the behaviour of liquefiable soils
v. 1.0

2.4 FUTURE RESEARCH OPPORTUNITIES

- Characterise more in-situ sands according to critical state parameters
- Improve correlations between different testing apparatus both in the field and in the laboratory
- Improve the understanding of the influence of static shear stress on liquefaction susceptibility
- Improve the understanding of the influence of fines content, grain angularity, particle size, plasticity and other soil parameters, on liquefaction susceptibility and subsequent behaviour after liquefaction has occurred
- Improve the correlations between liquefaction severity indices and field observation of liquefaction intensity and damage to structures
- Improve simplified triggering procedures to better represent the development of pore water pressure
- Improve the consideration of soil fabric within the critical state framework
- Develop more robust techniques to directly model sedimentation and consolidation for liquefiable soil
- Develop criteria and standard tests for validating constitutive models and numerical models for different scenarios
- Account for vertical interaction of layers and three dimensional effects in the simplified triggering procedures
- Understand the response of soils during partial drainage
- Development of a robust framework for the estimation of soil residual strength under various loading conditions
- Development of efficient numerical methods for sand ejecta simulation.

3. LIQUEFACTION-INDUCED PERMANENT DEFORMATIONS IN BUILDINGS

In the previous chapter, the phenomenon of soil liquefaction and their triggering potential in free-field conditions are summarised. However, in the presence of buildings, the behaviour of liquefiable deposits is even more complex. A building not only modifies the initial stress field in the soil, but also alters its potential to develop excess pore pressure, its dilatancy, the gradient of water flow, the initial seismic demand, etc. On the other hand, the soil can substantially modify the ground motion at the foundation level and the dynamic properties of the structure. Hence, different strategies and methodologies are required for the assessment of the performance of buildings in liquefiable areas rather than for free-field.

The assessment of earthquake-induced liquefaction damage to buildings requires:

I) A proper simulation of the soil behaviour and its interaction with the structure, able to reflect the modification of the global dynamic response and permanent deformations suffered by the building.

II) The definition of damage levels accounting for not only the damage experienced by the structural members but also for the loss of functionality related to rigid-body movements: global settlements and tilting.

In this chapter, a review of the different strategies to evaluate permanent deformations of buildings is presented, while their dynamic response is studied in Chapter 4.

3.1 MANIFESTATION OF LIQUEFACTION IN THE PRESENCE OF BUILDINGS

Liquefaction in the free-field can be substantially interpreted as a 1D phenomenon along a vertical soil column in which the earthquake induces cyclic shear and compressive forces that cause pore pressure to build-up and thus transient stiffness and strength degradation of the soil. Reconsolidation after liquefaction occurs in the soil due to the dissipation of excess pore pressures (Δu) by means of water flow, which results in vertical settlement of the ground surface. The evaluation of liquefaction triggering potential in the free-field is useful for hazard definition purposes, and the estimation of permanent movements at the soil surface can be used for the evaluation of the performance of infrastructure where their stiffness, geometry and applied stresses are sufficiently low such that they do not substantially modify the behaviour of the soil and pore water or impose restrictions on the deformation (e.g. domestic pipelines).

However, the presence of a building usually alters the behaviour in comparison to the free-field. The main conceptual differences induced by the presence of buildings on top of liquefiable soils are:

- The modification of the spatial distribution of effective confining stress (σ'_{0v}) and shear stress (τ) in the soil under the building, associated to the static bearing pressure (q_f) at the foundation level.
- The addition of time-dependent, inertial soil-foundation-structure-interaction-induced stresses in the soil due to earthquake-induced ratcheting.
- The introduction of discontinuities within the soil volume related to failure mechanisms.

- The prevention of any drainage, sand ejecta or soil uplift to occur below the foundation area.

Preliminary considerations of the performance of a building can be done within the framework of the simplified 1D free-field approach. The increment of mean effective stress in the liquefiable layer due to the presence of the building, leads to less increment of pore pressures during the cyclic action, since the instability stress locus tends to become closer to failure envelope for higher confining pressures (Viana da Fonseca et al, 2011, Robertson, 2017). This, regardless of any other parameter, might result in better performances of the "liquefiable ground + shallow foundation building" system rather than in free-field conditions, especially for superficial layers with high water table and $q_f \leq 100$ kPa (approximately the pressure beyond which potential dilatancy is inhibited, i.e. $K_\sigma \leq 1.0$). The beneficial effect of initial shear stress in the soil, especially for medium-high relative densities (D_R values), might be reflected in the K_α value. Regarding the inertial seismic forces, Rollins and Seed (1990), based on preliminary spectral considerations in which structural inelasticity is neglected, suggested that lower demands are mostly expected for soil below buildings rather than in the free-field. Such simplified evaluations suggest a beneficial effect of the building regarding only the liquefaction triggering, but they neglect the complex 3D and local effects, and they do not provide any information about the expected movements of the building.

In order to fully understand the complex manifestation of liquefaction in the presence of buildings, there are essentially three different approaches: field observation, laboratory modelling and numerical modelling. Then, simplified procedures can be developed based on the observed findings.

Performances of buildings in liquefied soil have been observed after different seismic events (see Chapter 1), leading to some preliminary empirical correlations of observed settlements with respect to some index of the liquefaction triggering potential in free-field (e.g. Yoshimi and Tokimatsu, 1977; Adachi et al, 1992).

Experimental tests have increased complexity with the improvement of testing apparatus. Shaking table tests (e.g. Yoshimi and Tokimatsu, 1977 or Liu and Qiao, 1984) have been replaced by centrifuge tests to model high soil stresses and more intricate superstructure models have been used to better capture the effects of soil-foundation-structure interaction (e.g. rigid foundation, rigid block equivalent SDOF simulating the building, MDOF frame, adjacent models…). Relevant centrifuge tests have been carried out, among others, by Whitman and Lambe (1982), Liu (1992), Popescu and Prevost (1993), Liu and Dobry (1997), Kawasaki et al. (1998), Adalier et al. (2003), Seed et al. (2003), Coelho et al. (2004), Coelho (2007), Dashti et al. (2010a), Hayden et al. (2014), Yasuda (2014), Bertalot and Brennan (2015) or Olarte et al. (2017). Nevertheless, minor information, have been gathered from triaxial or direct shear tests on soil accounting for the influence of normal or shear stresses, mainly within the framework of the free-field approach (e.g. Vaid and Finn, 1979; Boulanger and Seed, 1995; Vaid and Sivathayalan, 1996, Hynes and Olsen, 1999; Viana da Fonseca et al., 2015; Riemer et al., 2017).

Finally, a large amount of numerical analysis, mainly using fully-coupled modelling of the soil and rigid foundations with or without elastic superstructures have been carried out especially in the last 15 years: Popescu and Prevost (1993), Pietruszczak and Oulapour (1999), Elgamal et al. (2005), Popescu et al. (2006), Lopez-Caballero and Farahmand-Razavi (2008), Shakir and Pak (2010), Andrianopoulos et al. (2010), Dashti and Bray (2013), Karamitros et al. (2013b,c), Mehrzad et al. (2016), Karimi and Dashti (2017), Ayoubi and

LIQUEFACT
Deliverable D3.1
State of the art review of numerical modelling strategies to simulate liquefaction-induced
structural damage and of uncertain/random factors on the behaviour of liquefiable soils
v. 1.0

Pak (2017), Bray et al. (2017b), Bouckovalas et al. (2016) and Ziotopoulou and Montgomery (2017) among others.

However, simplified methodologies regarding the performance of buildings in liquefiable sites have been more recent and scarce compared to free field trigger procedures (see section 2.2.1). Full physics-based methodologies have been seldom proposed because of the lack of a complete understanding of the phenomena. In fact, for engineering purposes, approaches based on the free-field behaviour are still commonly used despite the consensus regarding their inappropriateness (Bird et al., 2006).

From the numerous case studies, experimental and numerical studies, there are several repeating aspects that can be summarised:

- Lower degree of liquefaction (i.e. lower r_u) is expected below buildings rather than in the free field.
- Higher settlement is expected below buildings rather than in the free field, and can occur during and after shaking.
- The additional shear and confining stress introduced by the foundation influence the build-up of pore water pressure and subsequent dissipation, which is highly related to the soil strength.
- The strains induced in the soil due to settlement could potential result in dilative soil behaviour
- The direction of water flow gradient under the building may not be easily predictable.

A conceptual example of the stresses in the soil around a foundation on liquefiable soil is presented in **Figure 3.1**, which is aimed at explaining some of the general behaviour observed in centrifuge tests of Shahir and Pak (2010), Dashti et al. (2010a), Cetin et al. (2012), Karamitros et al. (2013a), Bertalot and Brennan (2015) and Merzhad et al. (2016), among others. The evolution with time of the ground and water pressures in two different points of the liquefiable soil (under the foundation axis and in the free field away from the structure), when subjected to a ground motion, is described.

In this example, in the free field, full liquefaction (i.e. r_u = 1.0) is attained soon after the start of the ground motion, and it starts the dissipation a long time after the shaking ends. Under the axis of the foundation (mat or footing), the Δu build-up is quicker, and higher maximum absolute values are attained. The cause of the faster increase is the higher cyclic and static shear stress demand under the building. However, as the soil starts to settle the shear strains can result in some level of dilative behaviour causing the pore pressures to decrease. Eventually the pore pressure equilibrates with the free-field values due to horizontal drainage, thus, full liquefaction is not expected under the building (i.e. $r_u \leq 1.0$). There is a third factor that influences the stresses and pore water pressures under the footing, which is due to stress redistribution. Where the static vertical stress for non-liquefied conditions radiated out from the foundation, however, the soil adjacent to the foundation tends to liquefy and weaken before the soil under the foundation and thus the vertical stress is transferred onto the soil directly below the foundation. In the conceptual example provided, this stress redistribution resulted in some level of dilative behaviour.

The influence of the additional shear stress is complex, as at high static shear stress, cyclic stress reversal is unlikely to happen, thus lower degradation of soil stiffness and strength and even lower Δu are expected (Bertalot and Brennan, 2015). Furthermore, the static shear stress can induce dilative behaviour in the soil,

LIQUEFACT
Deliverable D3.1
State of the art review of numerical modelling strategies to simulate liquefaction-induced
structural damage and of uncertain/random factors on the behaviour of liquefiable soils
v. 1.0

which can result in negative pore pressure (Liu and Dobry, 1997; Adalier et al., 2003). For low static shear stress, low degradation is expected as well, but for moderate values the softening might be maximum, because some reversal is expected (Seed et al., 2003).
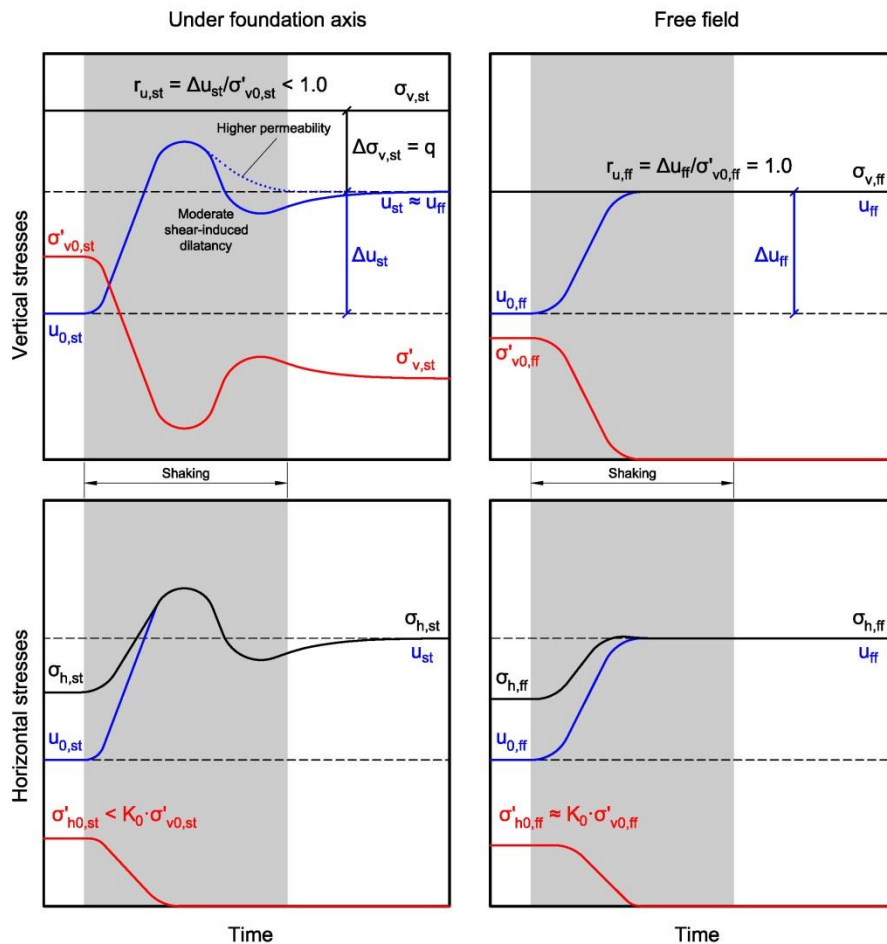
Figure 3.1: Conceptual interpretation of representative stress evolution in two points (free field and under foundation axis) of a liquefiable soil layer subjected to a sufficiently high level of ground motion, after Shahir and Pak (2010), Dashti et al. (2010a), Cetin et al. (2012), Karamitros et al. (2013a), Bertalot and Brennan (2015) and Merzhad et al. (2016)

It is worth noting that the beneficial effects of the absence of full liquefaction and thus lower degradation in the soil under the buildings due to the dilatancy induced by the static and dynamic shear stresses should not be interpreted as a benefit of the building with respect to the free-field. In fact, cyclic mobility due to moderate soil degradation, even when not reaching the maximum values corresponding to full liquefaction, can be enough to cause bearing capacity failure of the foundation (e.g. see Cinicioglu et al., 2006, regarding the Adapazari earthquake). The punching shear mechanism has been suggested to best reflect the failure in liquefiable deposits (e.g. Karamitros et al., 2013a). Still, the presence of a superficial crust has been observed to drastically enhance the performance (Ishihara et al., 1993; Acacio et al., 2001; Karamitros et al., 2013a; Tokimatsu et al., 2017; Bray and Macedo, 2017).

The settlement of the foundation on a liquefied deposit is an accumulation of the volumetric compression of the soil skeleton as well as static and cyclic shear deformation. The compressive and shear strength and stiffness of the soil are highly dependent on the confining pressure, pore pressure, and drainage potential of the soil.

Besides, the evolution of Δu is highly dependent on the permeability of the soil and the drainage conditions. Low drainage, i.e. the difficulty of the water to move away from the contracting soil in order to dissipate Δu values, is a condition for the liquefaction susceptibility of soil. However, totally undrained conditions are not real; partial drainage has been suggested to well represent the phenomenon, given that a portion of the volumetric settlement takes place during the shaking (Dashti et al., 2010a). Some studies (e.g. Shahir et al., 2014) suggest that the liquefied soil shows a large increase of permeability (up to 10 times) rather than in non-liquefied state, due to the loss of contact of soil grains which result in higher porosity and lower tortuosity of the water path.

The degree of permeability of the soil can modify substantially its behaviour under buildings, because horizontal pore water flow, outwards or inwards to the building, can take place during the shaking and thus the Δu-field evolution can be significantly different. In soils with high permeability, the spatial differences of Δu are expected to be immediately balanced; hence, the reduction in Δu from shear-induced dilatancy is expected to be less important, because pore water would occur immediately from the free-field to the soil under the footing.

The reason why larger settlements are expected for increasing permeability (Liu and Dobry, 1997; Karamitros et al., 2013a; Mehrzad et al., 2016) may be that inward flow from the free field keeps large values of Δu during and after the shaking (see dotted line in **Figure 3.1**). However, previous studies suggest an opposite influence on the settlement (Elgamal et al., 2005).

In **Figure 3.2**, the changing direction of water flow during and after the shaking is shown, according to the specified authors. During the shaking, transient flow towards the free field and the foundation edge is observed. After shaking, the soil under the foundation increases u values progressively until equalising to the free field values due to the hydraulic gradient, which is maintained for more time than the previous one. Nevertheless, the magnitude of the shear-induced soil dilatancy and the direction of water flow cannot be easily generalizable, as it is highly dependent on the geometry of the foundation (Bertalot, 2013) and the soil characteristics (Liu and Dobry, 1997).

Regarding the effect of the superstructure inertia, some authors have identified some situations in which it can play an important role, especially for slender buildings (Dashti et al., 2010a; Cetin et al., 2012); while other studies suggest that no relevant effects may be expected because the soil degradation and the potential for the development of a failure mechanism causes sufficient de-amplification of the ground motion in order to overshadow any difference regarding the dynamic properties of the building (Karamitros et al., 2013a).

Furthermore, the effect of the adjacent buildings on the soil degradation and expected movements is still not well understood. Hayden et al. (2014) suggest, based on centrifuge tests in which the distance between

buildings is lower than 3 m, that lower settlement and higher de-amplification rather than for isolated structures are expected. In case of a block of adjacent buildings, lower displacements have been observed, rather in the form of uniform settlements (Bakir et al., 2002). The influence of adjacent buildings on the observed tilting is discussed in Section 3.4.
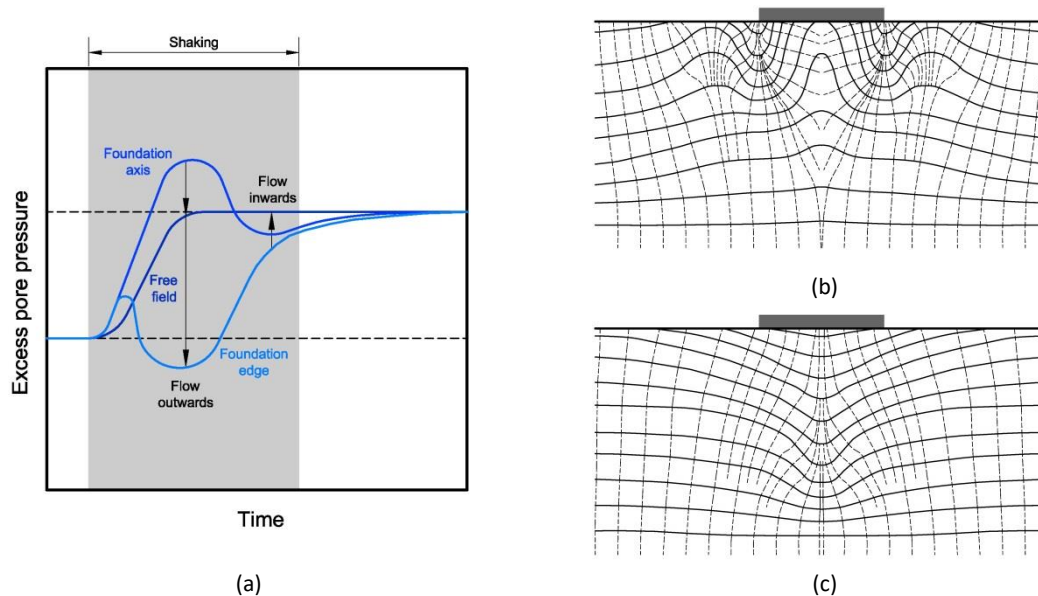
Figure 3.2: Conceptual evolution of u values in three representative points (free-field, under foundation axis and under foundation edge) with indication of the direction of the expected hydraulic gradient (a), and conceptual representation of the u-field (solid line) and water flow direction (dashed line) for the peak value of u under foundation (b) and for the post-shaking situation (c), after Shahir and Pak (2010), Dashti et al. (2010a), Cetin et al. (2012), Karamitros et al. (2013a), Bertalot and Brennan (2015) and Merzhad et al. (2016)

3.2   SETTLEMENTS

Permanent deformations of buildings due to liquefaction-induced soil softening increases seismic vulnerability when compared to non-liquefiable deposits, because those deformations can significantly affect the building operability. Hence, increasing attention has been put onto this issue, especially in the last decade.

Liquefaction-induced settlements under shallow foundations have been observed to be larger than in the free field (e.g. Yoshimi and Tokimatsu, 1977; Liu and Dobry, 1997; Hausler, 2002; Dashti et al., 2010a; Karamitros et al., 2013a; Luque and Bray, 2015; Ziotopoulou and Montgomery, 2017). Moreover, the physical phenomenon has been demonstrated to be radically different: it is primarily controlled by deviatoric strains rather than by volumetric ones (which represent only a small portion of the total settlement). However, in engineering practice it is still common to predict settlement by means of empirical-based approaches originally developed for the evaluation of free-field volumetric settlements, which only account for the mechanism of reconsolidation (e.g. Zhang et al., 2002; Ku et al., 2012).

First, the primary mechanisms contributing to the total settlement are presented, and subsequently a selection of the more recent approaches aimed at the evaluation of the settlements are reviewed.

3.2.1 PRIMARY MECHANISMS CONTRIBUTING TO SETTLEMENT

The different mechanisms causing settlement can be categorised as being volumetric- or deviatoric-induced, depending on the ruling strain component. A major portion of the settlement takes place during the shaking, and it is mostly deviatoric-induced. Still, a part of the volumetric-induced settlement can take place during the shaking for normal ranges of soil permeability; the rest of it develops afterwards, at a minor rate. Centrifuge tests and numerical analyses show consistently a rather linear settlement evolution with time during shaking. Some authors have suggested different intensity measures to be proportional to the settlement, e.g. Arias Intensity (Dashti et al., 2010b) or Cumulative Absolute Velocity (Karimi and Dashti, 2017; Bray and Macedo, 2017).

Deviatoric strains are induced in the soil due to the ground shaking, the static bearing pressure and the structural displacements (soil-structure interaction). Settlement is accumulating due to the development of alternate punching-shear mechanisms able to be modelled as a Newmark-type sliding block (Karamitros et al., 2013a). In each cycle, the relative movement of the foundation is out of phase with the bedrock, causing differential oblique forces applied to the soil surface. Also, rocking of the building causes vertical pulses of axial load in exterior footings or the edges of the mat foundation (Dashti et al., 2010a; Bray and Macedo, 2017), and analogously the rotation of single footings cause localized increases of vertical pressure in their edges.

At the beginning of the shaking, large inertial forces are applied to the soil, in which r_u is still not so high and thus stiffness and strength degradation in the soil is still moderate, thus lower de-amplification of the motion is attained. Consequently, the settlement at the beginning of the shaking is more prone to be ruled by the ratcheting of the superstructure. Afterwards, if the duration of the strong shaking is sufficiently long, both the cyclic mobility of the soil and the failure mechanism act as a natural isolation which de-amplify the seismic excitation in the foundation. Therefore, the settlement at the last phase is more prone to be ruled by static pressure, which can lead eventually to bearing capacity failure even when full liquefaction is not attained. The evaluation of soil residual strength or bearing capacity at the liquefied state is also a critical issue, because the settlement increases drastically when the factor of safety is lower than 1.0 (Shahir and Pak, 2009; Bray and Macedo, 2017). Tsai et al. (2017) statically analysed a 3-story house with a shallow spread footing, from this model it was suggested that a reduction to 10% of the original strength and stiffness was appropriate for the liquefiable soil. Different methodologies are proposed for the estimation of the residual strength of liquefied soil (e.g. based on equivalent degraded friction angle, ϕ_{deg} (Cascone and Bouckovalas, 1998) or assuming empirical relations (Robertson (2009b), Kramer and Wang (2015)). There is currently no consensus on the appropriate way to determine the bearing capacity of a shallow foundation on liquefied soil.

Several authors have identified the most important parameters affecting the deviatoric settlement (Dashti et al., 2010a; Karamitros et al., 2013c; Tokimatsu et al., 2017; Bray and Macedo, 2017;

among others). They refer mainly to the characteristics of the soil (stratigraphic profile, liquefiable thickness...), the building (bearing pressure, geometry…) and the strong motion.

Favourable parameters –i.e. causing lower settlements— are, roughly in order of importance:

- Soil relative density (D_R), which inhibits r_u –although lower de-amplification of shaking is expected.
- Thickness of the superficial crust (H_C), which can hold part of the soil mobilised within the failure mechanism.
- Building width (B), which reduces ratcheting in the first phase of the settlement and can eventually reduce the inward drainage in the last phase.

Conversely, unfavourable parameters are:

- Severity of the seismic excitation (e.g. Peak Ground Acceleration and significant duration), which increases both the inertial forces and the soil degradation.
- Static bearing pressure (q_f), which reduces the safety factor for bearing failure –although large q_f values may induce dilatancy in the soil.
- Thickness of the liquefiable layer (H_L), which allows the whole failure mechanism to be attained within the degraded soil.
- Aspect ratio of the building (H/B), which exacerbates SSI-induced shear forces.

Regarding volumetric-induced settlement, most of it is a consequence of the reconsolidation mechanism, which can be divided into two different phenomena: sedimentation and consolidation. The last one corresponds to the progressive contraction associated to the increase of σ' due to the dissipation of Δu, while sedimentation only takes place when the level of r_u is high enough to cause a rearrangement of the floating particles. Reconsolidation advances from the bottom of the liquefied layer to the shallower part. Besides, hydraulic gradient with horizontal component generated during the shaking can cause localized strains and thus their contribution to the settlement can be of some importance (Dashti et al., 2010a).

Finally, sand ejecta, when present, have shown much higher devastating potential rather than any other mechanism (Bray and Macedo, 2017). Localized fractures in the soil crust induce the seepage of pore water and fine soil contents to the surface, resulting in the removal of a portion of soil underneath the foundation –typically near the edge—, causing settlements of footings or tilting of mat foundations.

3.2.2   METHODOLOGIES FOR ESTIMATING SETTLEMENTS

An accurate simulation of the behaviour of liquefiable soil under the presence of superstructures in order to capture the magnitude of settlement requires rather complex modelling strategies and high levels of computational effort. In section 3.1, a list of some works carrying out numerical analyses is presented.

Based on the performed literature review, it can be concluded that there is still a lack of numerical studies that address soil-foundation-structure interaction considering inelastic structural models and the effects of soil liquefaction. Development of such approaches is crucial for understanding the evolution of damage in buildings.

Nevertheless, several attempts to provide simplified methodologies able to capture the magnitude of building settlements on liquefiable deposits have been proposed so far, especially in the last decade, in order to provide approximate values for design or assessment purposes. In **Table 3.1**, a selection of the main procedures is shown and compared. The first proposed approaches were empirical correlations with observed settlements after important seismic events, while, in the last years, more physics-based procedures have been developed.

Some methodologies estimate the total settlement, while other ones only provide magnitudes of the expected settlement during shaking, which involves the total deviatoric-induced part plus a fraction of the volumetric-induced settlement. The residual, after-shaking fraction of the settlement can be conservatively estimated as equal to the total volumetric settlement, which is commonly accepted to be similar to the free-field settlement (e.g. Bray and Macedo, 2017). Currently, the method proposed by Zhang et al. (2002), based on CPT results, is considered to provide reasonable estimation of free-field settlement (see Section 2.2.2 and **Equation (5)**). However, for sand ejecta there is still a lack of efficient numerical methods for simulation of that phenomenon, due to the inability of continuum-based models to capture the formation of localized (random) fractures in the superficial crust (Luque and Bray, 2015).

THE "CLASSIC CHART" AND OTHER CORRELATIONS

The first attempt of finding a trend between the settlement and some of the aforementioned variables is made by Yoshimi and Tokimatsu (1977) using field data after the 1964, Niigata, earthquake. They observed an inverse relationship between settlement and building width, both normalized by the liquefied thickness: S/Z_L and B/Z_L, respectively (see **Figure 3.3a**). That normalisation has been used very often afterwards (e.g. Adachi et al., 1992; Liu, 1995; Liu and Dobry, 1997; Dashti et al., 2010a; Bertalot et al., 2013), even when other parameters have been identified to have more influence on the observed settlement (e.g. Dashti et al., 2010a; Karamitros et al., 2013a; Bray and Macedo, 2017).
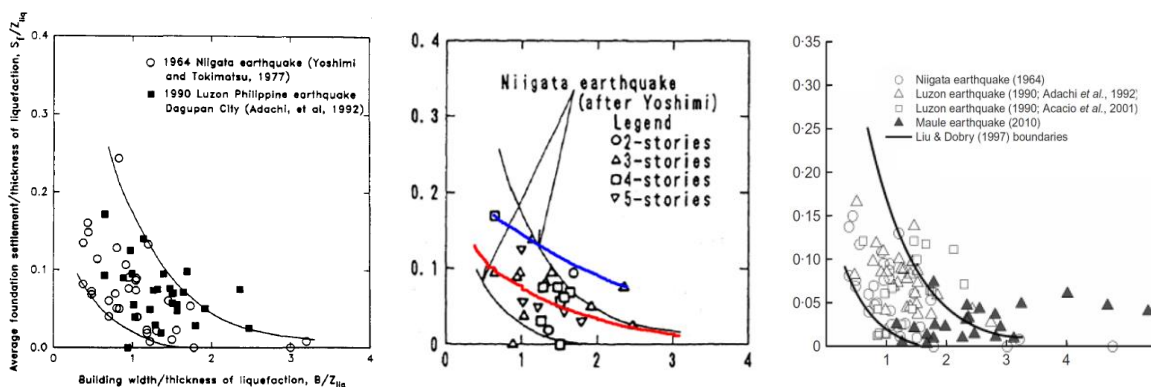
Figure 3.3: "Classic chart" relating observed normalised settlement and normalised building width (from Liu and Dobry, 1997) (a) and Luzon earthquake data plotted together with the boundaries of Niigata data, from Adachi et al. (1992), with upper Luzon boundary (blue) and average trend of Niigata (red) (b); and "classic chart" with the addition of data from Maule earthquake (c, from Bertalot et al., 2013)

Table 3.1: Comparison of different methodologies for the estimation of liquefaction-induced settlements in buildings

Approach	Framework	Methodology	Estimated settlement	Parameters					
				Motion	Liquefaction extent	Soil properties	Static demand	Geometry	SSI effects
"Classic chart" (Yoshimi and Tokimatsu, 1977, and other works)	Chart	Pure empirical	Total		Z_L		-	B	-
Liu (1995)	Formulation	Pure empirical	Total	Intensity	Z_L	D_R	q_f	B	-
Shahir and Pak(2010)	Formulation	Mainly empirical	Total	Z_L, equivalent homogeneous infinite Z_L, H_L			q_f	B	-
Unutmaz and Cetin (2012)	Formulation	Theoretical-empirical	Total, deviatoric or volumetric	τ from inertial forces and in soil mass	-	D_R, $(N_1)_{60}$ (other for cohesive soils)	q_f, α	-	$S_a(T)$/PGA, structure-to-soil stiffness ratio, H/B
Bertalot et al. (2013)	Chart and formulation	Mainly empirical	Total		Z_L		q_f	B, L	-
Karamitros et al. (2013c)	Formulation	Theoretical-empirical	Fraction during shaking	PGA+T_s+N_s or ground velocity time history	-	H_L, φ$_{deg}$	q_f	B, L	-
Lu (2017)	Chart within formulation	Pure empirical	Total	PGA	-	D_R	q_f	B	-
Bray and Macedo (2017) [*]	Formulation and judgement	Mainly empirical	Fraction during shaking	$Sa(T)$, CAV		S, H_L, CPT	q_f	B	-

[*] Only refers to the proposal for the estimation of deviatoric-induced settlement

LIQUEFACT
Deliverable D3.1
State of the art review of numerical modelling strategies to simulate liquefaction-induced
structural damage and of uncertain/random factors on the behaviour of liquefiable soils
v. 1.0

Notwithstanding its widespread use, different interpretations have been identified regarding the definition and calculation of Z_L. Originally, it recalls the thickness of the portion of soil which would liquefy in hypothetical free-field conditions (i.e. in the soil where the building is founded but removing the building and their loads) subjected to the ground motion and deducing all the upper or intermediate portions of the layer in which factor of safety for liquefaction is higher than 1.0. The simplified approach for free-field triggering estimation of Seed and Idriss (1971) is usually suggested for the evaluation of Z_L, which returns increasing Z_L for increasing PGA in homogeneous soil profiles. However, in some works (e.g. Dashti et al., 2010a), Z_L is assimilated to the total thickness of the liquefiable layer (H_L), which is only a geotechnical parameter, independent from the seismic demand. In some cases (e.g. for not so severe motions), not all the thickness of the liquefiable layer reaches liquefactions, so $Z_L \le H_L$.

In Yoshimi (1980), upper- and lower-bound curves are proposed in order to cover the whole range of values of normalized settlement. They are plotted in a classic chart in Liu and Dobry (1997) (see **Figure 3.3a**), together with the data corresponding to the settlement of buildings after the 1990, Luzon, earthquake, according to Adachi et al. (1992). Those upper- and lower-bound curves have become a fundamental reference for the topic, but it should be noted that they apparently suggest a much more pronounced dependence on B than the trend curve for the whole set, which is plotted in red in **Figure 3.3b**. That trend is also more in accordance with the upper bound of Luzon data (plotted in blue) and with some other results, as real measurements on oil tanks after 1983 Nikonhau-Chubu earthquake (Liu, 1995), 2010 Maule earthquake (Bertalot et al., 2013) or Dashti et al. (2010a) centrifuge tests (see **Figure 3.3c**).

On the other hand, a different interpretation of the increase of settlement for low width ratio in the data in Yoshimi and Tokimatsu has been proposed by Shahir and Pak (2010). They suggest that most of the individual footings, which are the most frequent foundation solution within the set, are more likely to have suffered bearing capacity collapse. However, the disaggregated results for the different foundation types suggest that higher values of settlement do not correspond to individual footings but to mat foundations and continuous footings. Furthermore, the identification of single footings with lower values of B is misleading, because B corresponds to the whole building, not to the footing.

Nevertheless, for very reduced H_L, as in centrifuge tests representing the Maule earthquake in 2010 (Dashti et al., 2010a) results are not in agreement with this trend: very low influence of B is shown. Dashti et al. (2010a) infer that the normalization by Z_L should not be employed. Underlying this statement there is the belief that such a normalisation is based on the assumption that the settlement is proportional to the volumetric one, as in free field. Considering that under a building the deviatoric contribution to the settlement is more important than the volumetric one, such a normalisation may not be a good strategy.

However, a different analysis can be done. The trend suggests that, for increasing seismic demand, an increase of settlement is expected only if the liquefiable layer is sufficiently thick and rather homogeneous in order to provide higher Z_L. In other words: the only parameter able to represent seismic demand in this chart is Z_L. Thus, the normalisation can be only used, regardless of seismic demand, if there is sufficient thickness of the liquefiable layer. In the experimental tests performed by Dashti et al. (2010a), the same accelerograms are scaled to two different values of PGA: 0.19g and 0.55g, but the chart in the paper only shows the high-demand results, which are inconsistent with the Yoshimi and Tokimatsu trend. Roughly, the

values of total settlement obtained for low PGA are around half the values for high PGA. Considering that Z_L (= H_L) is similar in both cases, if the low-PGA data were plotted on the chart, they would be closer to the Niigata boundaries and rather consistent with the upper bound of Nikonhau-Chubu data. Actually, most of the data from real earthquakes or centrifuge tests that have been plotted within the original boundaries correspond to values of PGA between 0.15g and 0.35g (Lu, 2017). Hence, the anomaly caused by a very thin liquefiable layer highlights the importance of the seismic demand and the role of deviatoric settlements.

A different empirical-based approach is proposed by Juang et al. (2013), both for free-field and under-building settlements. It is based on Robertson (2009b, 2009c) method, which can be used to compute the factor of safety (FS) against triggering of liquefaction when a deterministic approach is adopted (Youd et al., 2001; Ku et al., 2012) in order to compute the liquefaction potential in terms of the probability of liquefaction. The authors recognise that their formulations are solely based in documented case-histories, with no detailed interpretation of the factors that can influence the settlements in the presence of buildings founded over liquefiable soils; but still their procedure should be valuable in practice.

Herein, the remaining methodologies listed in **Table 3.1**, different from the "classic chart", are reviewed. To enable easy reading, notation is homogenised and some steps are omitted. For more details, the original contributions should be consulted.

LIU (1995)

Aimed at a good correlation between the results of three seismic events in China, Liu (1995) proposed a formulation for soils without a relevant superficial crust, assuming that there is no sand ejecta. Normalised S is approximated as in **Equation (9)**, being S_0 a basic value of settlement depending on the seismic intensity while the other terms stay as weighting factors accounting for the rest of the variables. The relevance of the contribution is that the influence of ground motion severity, soil characteristics and bearing pressure are taken explicitly into account.

$$\frac{S}{Z_L} = S_0 \cdot \frac{0.44}{B/Z_L} \cdot \left(0.001 \cdot q_f\right)^{0.6} \left(\frac{1-D_R}{0.5}\right)^{1.5} \tag{9}$$

SHAHIR AND PAK (2010)

The authors propose a formulation for the case of no bearing capacity failure. It is obtained as a parametric analysis regression by means of a numerical model which was previously calibrated against centrifuge experiments of the other authors. The building is simulated by a rigid block, so the influence of aspect ratio is not fully taken into account, thus the positive influence of B in the reduction of ratcheting contribution to settlement is lower.

A trend of settlement ratio was observed characterised by a rapid increase with the width ratio when it is lower than 0.9 and by a decrease for higher values at a lower rate. It is said to be caused by the intersection of a pressure bulb (with a depth of influence equal to the width of the foundation) with Z_L. Such an

interpretation is not straightforward, because Z_L is measured in free field, away from the building, while the bulb pressure is intersecting a soil which has a rather complex distribution of excess pore pressure ratio.

Nevertheless, it is observed that the variation caused by the different parameters (PGA, D_R and q_f) can be cancelled by adopting different normalisations:

- Influence of PGA and D_R is cancelled by normalising to $Z_{L,m}^{0.5}$, being $Z_{L,m}$ the equivalent Z_L in homogeneous, infinite free field, which can be interpreted as a measure of seismic demand and quality of the soil.
- Settlement is found to be proportional to $q_f^{0.4}$, thus showing always a negative overall influence on settlement notwithstanding the induced dilatancy on the soil for higher values of q. This trend is similar to that observed by Karamitros et al. (2013a) and contrary to Bertalot et al. (2013), who suggest that such a positive influence of high q_f values can be important enough to cause lower settlements.

On the other hand, this methodology accounts for the settlement caused by the soil under the Z_L with an addition of a term. The final expression is shown in **Equation (10)**, where B_f is the width of the foundation element. In recent years, the team has refined this approach in order to capture the response of more complex soil profiles (Ayoubi and Pak, 2017).

$$\frac{S}{Z_L} = Z_{L,m}^{0.5} \cdot q_f^{0.4} \cdot \left[0.0007\exp\left(-0.5\frac{B_f}{Z_L}\right) - 0.0012\exp\left(-3.1\frac{B_f}{Z_L}\right) + 0.0007 \right] + 0.0144\frac{H_L}{Z_L} \tag{10}$$

UNUTMAZ AND CETIN (2012)

The authors propose a methodology based on a preliminary work (Cetin et al., 2012) in which the triggering of liquefaction under buildings is approached by an extension of the simplified approach for free-field (see section 2.2.1). It is a rather complex procedure in which representative values of CSR are obtained, accounting for SSI effects. Then, in Unutmaz and Cetin (2012), strain demands are related to that CSR and thus settlements are obtained as the accumulation of deformation of layers subjected to equivalent uniform strain –volumetric and deviatoric.

First, the value of the equivalent CSR –normalised to the usual values of σ'_{v0} and α— is estimated for the middle point of each soil layer, as in **Equation (11)**. It explicitly separates the contribution of shear stress of building's inertia forces (τ_b) and soil column mass (τ_{soil}), and functions $f(\cdot)$ are used in order to account for soil-structure interaction relevant variables. Soil-to-structure stiffness ratio is represented by the relationship between the soil shear wave velocity (V_s) and the ratio between the effective height of the equivalent SDOF of the structure (H_{eff}) and the fundamental period (T). The rest of the factors –i.e. those accounting for both initial static shear stress (K_α) and overburden pressure (K_σ) — are analogous to the free-field approach.

$$CSR_{eq}(z) = \theta_1 \left(\frac{\theta_2 \cdot f\left(\dfrac{V_s T}{H_{eff}}\right) \cdot f\left(\dfrac{H}{B}\right) \cdot \tau_b(z) + \tau_{soil}(z)}{\sigma'_v(z) \cdot K_\alpha(z) \cdot K_\sigma(z)} \right)^{\theta_3} \tag{11}$$

Vertical dissipation laws of 2:1 and 1.6:1 for overburden pressure and building shear inertial forces are proposed. In the horizontal direction, a simplified static τ-distribution is adopted, thus K_α is obtained. Thus, two different values of CSR(z) are considered to characterize appropriately the demand in an equivalent 1D column under the building: maximum and representative value. The last is understood as an average value weighted by the increment of vertical pressure due to the structure, in order to make a difference with respect to the free-field.

Subsequently, volumetric and deviatoric strains are related to CSR values depending on the soil characteristics, in order to calculate settlement as an accumulation of strain along the soil column. Empirical-based formulations for granular and cohesive soil are suggested. Then, the maximum potential settlement is estimated as an integration of both strains along the equivalent soil column. It is worth noting that the accumulation of both shear distortion and axial strain are summed regardless of their different nature.

Finally, a statistical calibration against field results of settlements in mat foundations after the 1999 Kocaeli earthquake is carried out, accounting for uncertainties by means of random correction terms. Different expressions are proposed, depending on the chosen terms for characterizing settlement (which, in turn, depend on the corresponding CSR): representative or maximum value, with or without subtraction of free-field settlement.

The authors consider the prediction capacity as being satisfactory, because the dispersion is reasonably moderate. However, a deeper examination of the procedure reveals that the model parameters which provide best-fit results correspond to a negligible contribution of deviatoric settlement if compared with the volumetric contribution, which may not be completely in agreement with the observed behaviour.

The authors have extended the simplified approach for free-field to evaluate CSR in a 2D or 3D field. However, the free-field origin of the approach makes it difficult to capture other specific phenomenon such as shear-induced dilatancy or flow behaviour only by means of few correction factors (i.e. K_α or K_σ).

BERTALOT ET AL. (2013)

The presented procedure in Bertalot et al. (2013) included q_f as an input parameter to capture the apparent benefit of high q_f values. Regarding B/Z_L normalisation, they consider that, even when it has been shown that, for sufficient H_L, it can have some influence in the capacity of developing punching and shear settlement, the understanding of the phenomenon is not so deep. Thus, they remove this normalisation for B compared to the classic chart, but they kept it for S. However, it is pointed out that the method should

LIQUEFACT
Deliverable D3.1
State of the art review of numerical modelling strategies to simulate liquefaction-induced
structural damage and of uncertain/random factors on the behaviour of liquefiable soils
v. 1.0

move from this normalization towards the explicit consideration of seismic demand and soil profile (geometry and mechanical properties) in an independent way, instead.

Thus, they re-plot all the available data from real earthquakes (Niigata, Luzon and Maule) in a chart dependent on S/Z_L, B and estimated q_f. They obtain some higher-bound envelope (see **Figure 3.4a**) by interpolating the maximum values of normalised settlement, which is quite a conservative assumption more orientated to design rather than assessment.

The most arguable decision is how to estimate q from the field databases used for the calibration. Also, there are not many cases of high q (i.e. $q_f > 100$ kPa) in the database, so the initial goal is hard to achieve. The authors consider a linear relationship with the number of storeys, which would correspond to the case of similar contact area of the foundation for all the cases, i.e. for mat foundation, as other authors do (e.g. Bray and Macedo, 2017). The reliability of that assumption regarding pad footings is arguable. Average values for the Maule earthquake are 15 kPa/storey, while the value is higher (21 kPa/storey) for Dagupan earthquake (Acacio et al., 2001).
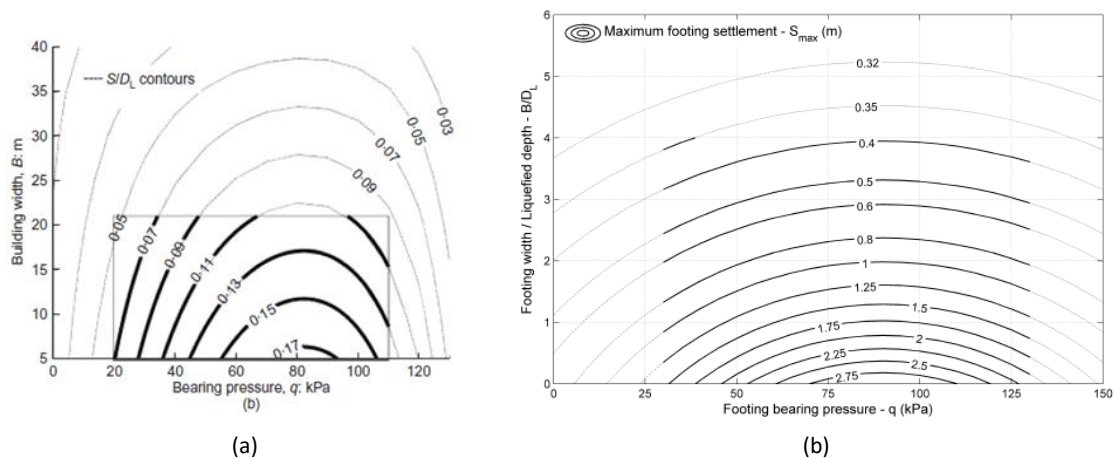
Figure 3.4: Proposed charts in Bertalot et al. (2013) and in Bertalot (2013)

It does not seem reasonable to estimate pressure using a linear relationship with number of storeys. Theoretically, a practitioner should design the building footings in order to have similar settlements in all of them, which usually results also in rather similar q_f. Pressures should be lower than the design value to avoid both collapse and total settlements limit and implicitly also differential settlements. Hence, for the usual ranges of number of storeys in which a mat foundation is not required, the average bearing pressure should be theoretically constant. Only for very few storeys in medium-good soil quality, the bearing pressure may be reduced because geometry of the foundation may be based on minimum geometry rather than in minimum cost. In fact, an analysis of the relation between real field values of q_f with the number of storeys (n) in the buildings of Dagupan, most of them founded on single footings (Acacio et al., 2001), shows that q_f is almost independent of n.

The same author proposes a modified method in (Bertalot, 2013), based on the previous empirical relationships found in field cases but also from experimental tests (see **Figure 3.4b**). It better captures the

LIQUEFACT
Deliverable D3.1
State of the art review of numerical modelling strategies to simulate liquefaction-induced
structural damage and of uncertain/random factors on the behaviour of liquefiable soils
v. 1.0

results with relatively thin liquefiable layers. The normalisation of settlement disappears and *B* is normalised instead. Still, this normalisation is shown not to be precise in order to capture the effect of variability in soil relative density.

KARAMITROS ET AL. (2013c)

The authors propose an analytical method with strong physical basis whose main advantage is to account for each relevant influencing parameter separately, thus their corresponding roles can be calibrated against experimental or numerical simulation one by one.

The foundation bearing capacity failure mechanism is simulated by the Meyerhof and Hanna (1978) model for a crust on a weak layer, even though the collapse is more similar to a punching shear mechanism rather than a Prandtl type helix. Superficial crust is beneficial and there is an upper bound beyond where failure occurs entirely within the crust and does not get affected by the liquefiable layer.

The proposed expression for the dynamic settlement S_s (i.e. the settlement during shaking) is shown in **Equation (12)**, being c a foundation aspect ratio correction, a_{max} the peak bedrock acceleration, T_s the representative period of the motion, N_s the number of cycles of the excitation and FS_{deg} the degraded static factor of safety of the foundation. The variables corresponding to the input motion refer to an equivalent sinusoidal excitation, but any heterogeneous seismic record can be used by relating those variables to the velocity time-history.

$$S_s = c\left(a_{max}T_s^2N_s\right)\left(\frac{H_L}{B_f}\right)^{1.5}\left(\frac{1}{FS_{deg}}\right)^3 \tag{12}$$

The calculation of FS_{deg} (ratio between the degraded bearing capacity and q_f) relies on the adoption of an equivalent degraded friction angle (ϕ'_{deg}) within the Meyerhof and Hanna failure mechanism framework. A linear degradation with r_u ranging from 0 to 1 is assumed for the calculation of ϕ'_{deg}. r_u is estimated as a weighted average of the values in free field and under the footing, considering conservatively full liquefaction in free field and assuming that r_u under the footing is well represented by the value measured at a specific point C under the centre of the foundation, when a simplified value can be estimated based also on the expected settlement. Thus, the settlement per cycle (S_{cyc}) depends on FS_{deg}, which in turn depends on r_u and it finally depends on S_s. Consequently, an iterative (yet simple) procedure is required.

The authors have calibrated the method against available centrifuge tests and post-earthquake data. The main disadvantage of this method is the difficulty of application for site profiles in which there is no clay crust, as in Adazapari city (near the Kocaeli earthquake).

Aimed at solving that shortcoming, a refinement of the approach made by some of the authors for the case of non-cohesive, permeable crust, is presented in Dimitriadi et al. (2017). Numerical analyses show that, thanks to the permeability of the crust, an upper portion of the liquefiable layer, immediately below the crust, behaves as a "transition zone" in which lower r_u and lower strength degradation is observed. Thus,

LIQUEFACT
Deliverable D3.1
State of the art review of numerical modelling strategies to simulate liquefaction-induced
structural damage and of uncertain/random factors on the behaviour of liquefiable soils
v. 1.0

the FS_{deg} depends not only on ϕ'_{deg} of the three zones, but also on the relative thickness of the transition zone and on a normal stress parameter related to the lateral friction developed within a punching-like failure mechanism through the permeable crust and the transition zone. For most of the required variables, analytical (best-fit) expressions are proposed.

Finally, a new formulation for the assessment of the dynamic settlement is suggested (see **Equation (13)**). If compared with the original formulation in Karamitros et al (2013c), T_s has been replaced by the average of itself and the soil fundamental period (T_{soil}), which is considered to be representative enough of the zone in which the sliding plane occurs, in order to be consistent with the rigid sliding block approach. Also, H_L and B_f are considered implicitly within the expression of FS_{deg}, which is more complex.

$$S_s = 0.017a_{\max}\left(T_s + T_{soil}\right)^2 N_s \left(\frac{1}{FS_{\deg}}\right)^{0.5}\left[1+0.15\left(\frac{1}{FS_{\deg}}\right)^5\right] \tag{13}$$

LU (2017)

The empirical approach developed by Lu (2017) is based on calibration from a large number of results found in literature –centrifuge tests, numerical analysis and field data. The agreement with the results used for calibration is rather satisfactory, however, the method does not have a strong a mechanical framework.

The author proposes, for the sake of ease, the adoption of the framework of the classic Meyerhof equation for settlements, assuming superficial water table and replacing the term related to SPT ($N/0.00284$) by an "index of strength" of liquefiable soils, N_{LR} (see **Equation (14)**, in which C_D is a correction factor for the depth of embedment).

$$S = C_D \frac{q_f}{N_{LR}}\left(\frac{B}{B+0.33}\right)^2, \quad B > 1.2\,\text{m} \tag{14}$$

N_{LR} depends on D_R (between 30% and 60%), the level of q_f (low, 10-30 kPa; medium, 30-80 kPa; high, 80-120 kPa) and PGA (0.10-0.40 g), and can be obtained from the chart shown in **Figure 3.5a**. The shortcoming lies on the lack of criteria for selecting the value, depending on PGA, within the corresponding boundaries for each given q_f-based region. The generic chart (**Figure 3.5a**) is plotted without any guidance for the influence of PGA. Then, aimed at applying the method to a field case study – a 2016 Taiwan earthquake-, a fuzzy scale of PGA is added within the corresponding band, suggesting a nonlinear (e.g. logarithmic or similar) relationship with PGA (see **Figure 3.5b**). But also they suggest that the choice should be based on the observation (or prediction) of "strong interaction between soils and buildings" and "liquefaction severity". Moreover, it is worth noting that the thicknesses of the bands are so large that N_{LR} can reach such low values that the sensitivity of settlement results with respect to different qualitative assumptions is very high.

LIQUEFACT
Deliverable D3.1
State of the art review of numerical modelling strategies to simulate liquefaction-induced
structural damage and of uncertain/random factors on the behaviour of liquefiable soils
v. 1.0

Notwithstanding this major drawback, the author maintains that, when applied to a very large database, the method returns more accurate results than the approach proposed in Bertalot et al. (2013), also capturing the beneficial effect of high q level on the inhibition of excess pore pressure and thus causing a decrease of settlement. However, similar simplified linear relationship between q_f and number of storeys is done, which could be criticized.
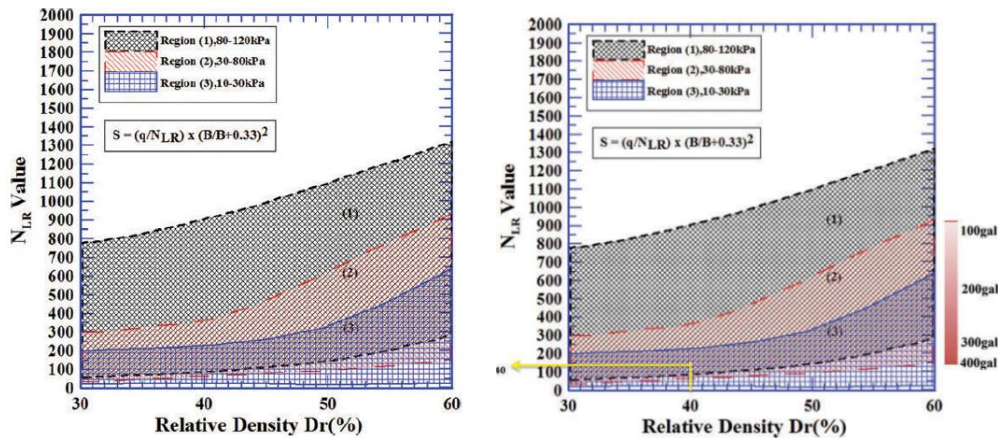
Figure 3.5: General chart for the estimation of NLR (a) and example of use with guideline for the influence of PGA (b), from Lu (2017)

BRAY AND MACEDO (2017)

The simplified procedure proposed by Bray and Macedo (2017) is the result of an extensive in-situ, experimental and analytical work developed in the University of Berkeley in the last decade. As a result of it, a numerical procedure has been satisfactorily calibrated for the evaluation of liquefaction in soil below buildings; and simultaneously, it has been identified which intensity measures provide better prediction of settlements.

Consequently, a parametric set of over a thousand numerical analyses was conducted, and the influence of the different parameters on the deviatoric settlement was disaggregated, showing rather consistent trends. The influence of the degraded bearing capacity was shown to be very important: buildings near to the liquefaction-induced bearing collapse show a dramatic increment of settlement. Hence, the authors suggest that, for low bearing capacity factors of safety, the evaluation of settlements is worthlessness.

A purely empirical expression for the deviatoric settlement (see **Equation (15)**) is obtained as a best-fitting regression of the results of the parametric analyses. Two intensity measures are chosen. CAV_{dp} is the standardised Cumulate Absolute Velocity as defined in Campbell and Bozorgnia (2012). LBS is an index of equivalent liquefaction-induced shear strain on the free-field, defined as the integration along the soil column of the strain –estimated by means of the CPT-based procedure proposed in Zhang et al. (2004)—, weighted by the depth in order to provide more importance to the soil close to the foundation. The model parameters c_1 and c_2 assume values of -8.35 and 0.072 for LBS ≤ 16, respectively, and -7.48 and 0.014 otherwise; ε is a normal random variable with 0.0 mean and 0.50 standard deviation in *ln* units.

LIQUEFACT
Deliverable D3.1
State of the art review of numerical modelling strategies to simulate liquefaction-induced structural damage and of uncertain/random factors on the behaviour of liquefiable soils
v. 1.0

This project has received funding from the European Union's Horizon 2020 research and innovation programme under grant agreement No. 700748

$$\ln(S_s) = c_1 + 4.59\ln(q) - 0.42\ln(q)^2 + c_2 LBS + 0.58\ln\left[\tanh\left(\frac{H_L}{6}\right)\right] - 0.02B + 0.84\ln\left(CAV_{dp}\right) + 0.41\ln\left[S_a(T)\right] + \varepsilon \qquad (15)$$

Finally, the suggested procedure for the estimation of total settlement consists in the following steps:

1) Obtain the safety factor for liquefaction triggering in free-field.
2) Calculate the liquefaction-induced degraded bearing capacity safety factor, and judge the performance as unsatisfactory if it is lower than 1.0 for light or low buildings or lower than 1.5 for heavy or tall buildings.
3) If the likelihood of sediment ejecta is significant, based on the magnitude of ground failure indices, estimate the ejecta-induced settlement (S_e) as a direct result of loss of ground, based on case histories or engineering judgement.
4) Estimate the volumetric-induced settlement (S_v) by means of Zhang et al. (2002) or similar.
5) Estimate the deviatoric-induced settlement (S_s) using Equation (15).
6) Estimate the total liquefaction-induced building settlement: $S = S_e + S_v + S_s$

3.3   DIFFERENTIAL SETTLEMENTS

In the case of liquefiable deposits, the definition of damage levels in buildings should account not only for the damage experienced by the structural members –typically expressed in terms of flexural demand— but also for the loss of functionality related to rigid-body movements which do not cause structural damage.

Usually, flexural damage is related to ground motion, while rigid-body movements are attributed to ground movements. However, frames founded on pad footings instead of rigid mat foundation can experience flexural damage due to differential settlements, which are complex SSI phenomena showing high degree of uncertainty due to heterogeneity of soil, scarce field data, structural variability and intrinsic uncertainty of seismic hazard and liquefaction triggering.

The behaviour of buildings in liquefiable soils regarding the time-history Δu build-up suggests that there might be an initial, probably narrow "window" of time in which both sources of flexural damage –due to ground shaking and due to differential settlements— may coexist. However, coupled procedures are not usually considered due to their inherent difficulty. In Bird et al. (2006), the following simplification is considered to be sufficiently accurate: "all damage due to ground shaking occurs in the first part of the earthquake and the liquefaction-induced ground deformation will occur towards the end of, or subsequent to the earthquake".

In general, regardless of the liquefaction potential of the soil, the estimation of differential settlements for design purposes traditionally follows a very simple rule of thumb in which differential settlements within assumed homogeneous soil layers are equal to a fraction of the total settlement: $\Delta S = a \cdot S$. Many authors have proposed different characteristic (i.e. conservative) values for a, ranging between $0.4 - 1.0$ (e.g. Bjerrum, 1963; Kramer and Holtz, 1991; Viggiani, 1993; Coduto, 1994, 2001; Terzaghi et al., 1996). Then,

those values of ΔS might be imposed alternatively to the different column bases in order to design the rest of the structural members.

In Schneider et al. (2015) it is suggested that values of $a = 0.5$ may constitute a higher bound after a numerical calibration; still, only inherent heterogeneity of soil is accounted as a source of uncertainty, as most of the probabilistic studies carried out so far do (Fenton and Griffiths 2002, Akbas and Kulhawy 2009, Ahmed and Soubra 2014, Schneider et al., 2015). They model the inherent heterogeneity of soil by assuming different probabilistic distributions of a chosen mechanical property acting as an indicator: Young modulus, compressibility, SPT or CPT measures. In most cases, they account for the distance between the footings as an input value for the probabilistic model (Kayser and Gajan 2014).

Most of those proposals arise from empirical observation of adjacent isolated footings without any structural connection between them (e.g. D'Appolonia et al., 1968). Only Coduto (1994, 2001) and Viggiani (1993) consider the structural stiffness as an input parameter. In general, it is more feasible to obtain relevant information from experimental tests rather than from field data, considering the difficulty in the measurement of S due to the lack of suitable reference points. Moreover, if any measurement of ΔS in real or simulated structures is carried out in order to obtain regression values of a for further linear design purposes, real movements causing nonlinear incursion in structural members should not be accounted for.

Ignoring the structural stiffness does not adequately reflect common cases (Dutta and Roy 2002). In fact, any design methodology relying on the imposition of vertical movements sequentially to each single footing, regardless of any consideration about the stiffness of the building, does not return homogeneous safety factors for all the cases: it would lead to more conservative design for stiffer frames rather than for more flexible ones. Most vulnerability methodologies assume that all the "potentiality" of the soil to settle in a differential manner is fully becoming effective to the frame (Bird et al., 2005, Negulescu and Foerster 2010).

Moreover, in some cases of very high seismicity and loose soil, thus large member cross-sections, the imposition of $\Delta S = a \cdot S$ can lead to absurd, unreal flexural demands on members, because the imposed relative displacement could be eventually higher than the maximum settlement than the footing would experience if there was not any bearing capacity of the soil under it.

In liquefiable sites, ground movements are not only a consequence of the building mass, thus free-field displacements can be important. Hypothetical free-field settlements coincident with the position of contiguous footings could eventually show different magnitudes if the soil shows different characteristics. Some approaches (e.g. Bird et al., 2005) suggest the use of free-field differential settlements for design or assessment purposes instead of using other probabilistic-based approaches, which may not be conservative considering that real differential settlements considering SSI could reach higher values rather than in the free-field.

The imposition of fixed ΔS values to the frames regardless of their stiffness may be more realistic for lateral movements rather than for settlements, although some reduction of lateral displacement demand is

LIQUEFACT
Deliverable D3.1
State of the art review of numerical modelling strategies to simulate liquefaction-induced
structural damage and of uncertain/random factors on the behaviour of liquefiable soils
v. 1.0

observed in some studies on bridges founded on piles (McGann and Arduino 2015). No further information regarding common buildings is available.

In the case of significant post-shaking liquefaction-induced volumetric settlement (or also if sand ejecta occurs), the foundation of buildings with sufficient stiffness can experience a detachment from the ground surface due to incompatibility of deformations (Cubrinovski et al., 2011), which is not possible in the non-liquefiable case.

Conversely to the assumption of free-field displacements, other works explore the "a-approach" ($\Delta S = a \cdot S$). In Stuedlein and Bong (2017), a random field model of inherent soil variability has been adopted for the analysis of settlements in free-field after shaking, for increasing seismic demand. Results show that potential a values may reduce dramatically for larger ground motions. It seems that for sufficiently high seismic demand, able to cause high excess pore pressure ratios and thus severe stiffness and strength degradation of soil, any variability of soil mechanical properties gets greatly overwhelmed, while for lower values of peak ground acceleration (PGA) the degradation is not so homogeneous and differences may exacerbate. Suggested maximum and average values of a (only accounting for soil heterogeneity) are, approximately: 0.30 and 0.15 for PGA = 0.13g, respectively, and 0.15 and 0.05 for PGA = 0.25g, respectively.

3.4   TILTING

3.4.1   MECHANISMS

Foundation tilting is caused by very similar phenomenon to differentially settlement and often have similar design limit states (Task Force Report, 2007), even though rigid-body tilt can occur with no induced structural damage. Rigid body tilting can be considered a special case of foundation tilt. Because rigid-body tilt can occur without deforming the structure, the influence of structural stiffness is less important to the magnitude of foundation tilt.
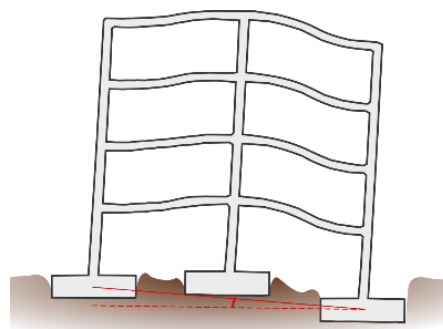
Foundation tilt

Figure 3.6: Definition of foundation tilt

In frame structures the interaction between rigid body tilt, local footing rotations and differential settlement is difficult to separate. The difficulty with interpreting and estimating the differential deformations is partially due to poorly defined reference points, here we will consider tilt as the difference

LIQUEFACT
Deliverable D3.1
State of the art review of numerical modelling strategies to simulate liquefaction-induced structural damage and of uncertain/random factors on the behaviour of liquefiable soils
v. 1.0

This project has received funding from the European Union's Horizon 2020 research and innovation programme under grant agreement No. 700748

in vertical displacement of the outer most edges of the foundation divided by the horizontal distance between them. However, as shown in **Figure 3.6**, this makes it difficult to decouple from differential settlement.

The use of this simple definition does not directly infer any level of structural stresses, which is dependent on the deformation of the superstructure, the level of global foundation tilt and the local displacements of the footings (**Figure 3.7**).

$$\theta_{f,local} < \theta_{f,global}$$
Increased column curvature

$$\theta_{f,local} = \theta_{f,global}$$
Balanced: No increased deformation

$$\theta_{f,local} - \theta_{f,global} \le \theta_{ss,plastic}$$
Reduced column curvature

$$\theta_{f,local} - \theta_{f,global} > \theta_{ss,plastic}$$
Impossible: Increased drift
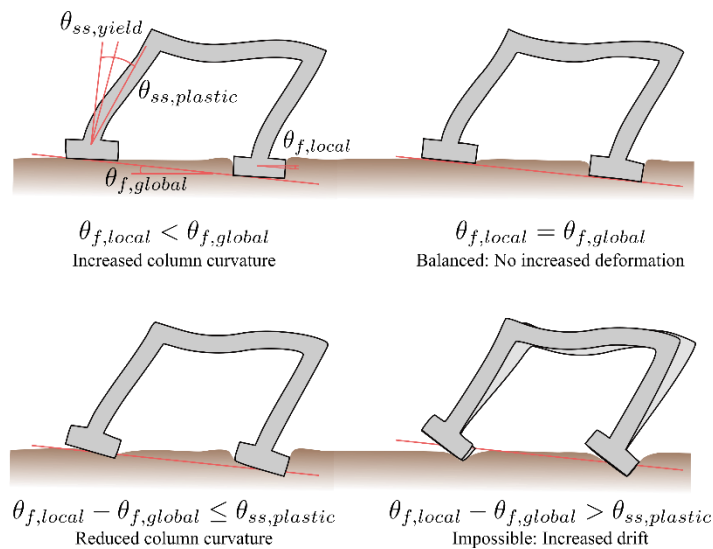
Figure 3.7: Interplay between dynamic tilt, foundation deformation and structural deformation
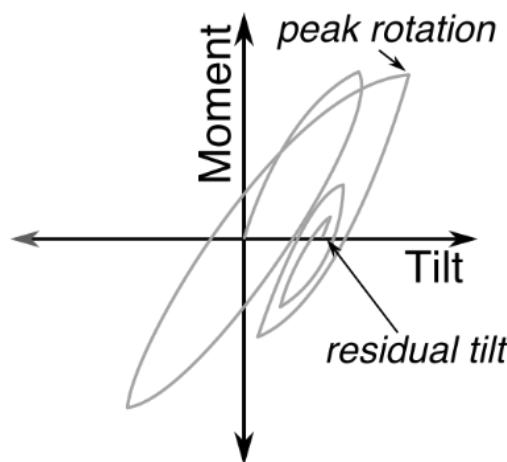
Figure 3.8: Definition of peak foundation rotation and residual foundation tilt

Dynamic inertial forces in the structure or deformations in the soil can drive foundation tilt. Another special case of foundation tilt, is transient tilt where the foundation rotates due to inertial forces, the maximum rotation that occurs during an earthquake is often referred to as the 'peak foundation rotation'. The peak

foundation rotation is different from the residual or permanent foundation rotation because some of the peak deformation is restored through the soil rebounding and when the foundation rotation causes uplift the gravity forces tend to act to restore the foundation back to the full compliant condition (**Figure 3.8**).

This section focuses on the causes of residual foundation tilt, while Section 4.2 covers the role of peak foundation rotation in the dynamic response of the structure.

Horizontal soil heterogeneity leads to different soil deformations across the foundation. This was one of the main causes of differential foundation movement for the buildings studied by Luque and Bray (2017).

The **pore pressure** influences the soil strength and stiffness and therefore plays an important role in the estimation of foundation deformations. The presence of high water pressure can exacerbate the other effects that cause foundation tilt simply by weakening the soil. If the pore pressure is non-uniformly distributed then the asymmetric stiffness and strength can also result in foundation tilting. Pore-water can be non-uniformly distributed at the start of shaking due to the soil conditions as well as due to source and sink effects, where water is flowing from one place to another. Pore-water can also flow non-uniformly once excess pore pressure builds up, this is due to variability in the permeability of the soil and drainage. Final pore water flow after shaking can cause further tilting if it flows under the foundation. In Adapazari, a building tilted for more than 60 degrees and the tilt of this building was about 30 degrees on the day next to the earthquake and increased to present state for about 10 days (Yoshida et al., 2001).

Superstructure inertial forces also referred to as SFSI (soil-foundation-structure interaction)-induced residual foundation deformation. The overturning moments applied by the superstructure on the foundation result in the foundation soil yielding and the foundation uplifting. The contribution of foundation uplift compared to soil yielding influences the level of residual deformation that can be expected as foundation uplift can be considered as a nonlinear elastic deformation (Chatzigogos et al., 2011) while soil yielding typically results in permanent soil deformation. The level of foundation uplift is largely controlled by the axial load on the foundation, and therefore the foundation residual tilt can be linked to the level of peak foundation rotation and the applied axial load (Deng and Kutter, 2012; Deng et al., 2012).

Eccentric stiffness and mass in the structure and foundation result in an imbalance in capacity and demand. Eccentricity can result in foundation tilt even under static non-liquefied conditions. However, eccentricity is even more important under dynamic loading, where the build-up of pore pressure is dependent on the level of applied stress and variations in stiffness can result in additional load being applied to certain parts of the structure. The cyclic loading tends to result in increasing asymmetric displacement under each cycle.

Lateral spreading or asymmetric horizontal earth pressure results in non-uniform soil deformations and foundation tilt. The imbalance of earth pressure due to either a free-face of sloping ground results in static shear stress in the soil and favoured movement in the less supported direction. An extreme case of this is when cracks open from laterally spreading soil and part of the foundation completely loses support.

Adjacent structures is another case of imbalanced earth pressures, the stresses imposed in the soil from adjacent foundations can overlap with the soil that supports the foundation of interest. The asymmetry can influence the strength, stiffness of the soil underneath the foundation and result in tilting. Adjacent structures can also prevent or modify pore water flow and thus can the change the extent of liquefaction and weakening of the soil.

P-delta effects. This is a second order effect, where foundation tilt results in asymmetric loading of the foundation due to the horizontal movement of the superstructure mass. The applied overturning moment on the foundation from P-delta effects can be approximated by **Equation (16)**. There for if some level of foundation tilt occurs, the additional P-delta moment can contribute to further rotation.

$$M_{p\Delta} = M_{ss,eff} \cdot H_{eff} \cdot g \cdot \theta_f \tag{16}$$

3.4.2   ESTIMATION OF TILT STRATEGIES

Given the number of variables that contribute to foundation tilt there is currently no robust simplified analytical frameworks for determining foundation tilt in liquefied soils. Some empirical correlations exist based on the total settlement or factor of safety against overturning moment (Kiyota et al., 2014; Karimi and Dashti, 2016; Tokimatsu et al., 2017). Expressions for non-liquefied soil exist that account for SFSI-induced permanent tilt (e.g. Deng et al., 2012, Millen et al., 2016). More recently, Montgomery and Boulanger (2017) presented an interesting study on the effect of spatial variability of penetration resistance on the liquefaction-induced settlement in which the soil characterised with spatially correlated Gaussian random fields. Such an approach allows the estimation of differential settlements due to inherited variability of soil properties. However, the paper examined settlement only under free-field conditions.

The most common approach to estimating foundation tilt is through numerical simulation where soil heterogeneity, pore pressures, superstructure inertial forces, mass and stiffness eccentricities, lateral spreading, adjacent structures and p-delta effects can all be modelled directly. However, successful numerical simulations of this complexity are limited and tend to focus on understanding case study buildings (e.g. Bray and Luque, 2017). For broad parametric studies some of the above effects tend to be disregarded. Recent examples are the numerical studies by Karimi and Dashti (2016) and Hong et al. (2017) that investigated building tilt but did not consider soil heterogeneity. There are also some contradictory results from recent numerical simulations, suggesting that further understanding of the driving mechanisms is needed. Numerical studies by Barrios et al. (2017) showed that adjacent buildings tended to tilt away from each other, while Yasuda (2014) based on field observation and numerical analyses, suggest that buildings closer than 3 m may tilt inwards.

Another approach to estimating residual foundation tilt is to use centrifuge testing, although very limited due to the excessive costs. Foundation tilt was a key parameter of interest for the centrifuge studies conducted by Hayden et al. (2014) when examining the performance of adjacent buildings. The buildings in the centrifuge tests tended to tilt away from each other.

3.5   FUTURE RESEARCH OPPORTUNITIES

- Develop a simplified procedure for estimating pore water pressure build-up underneath foundations
- Develop a procedure to estimate shear strains underneath foundations, accounting for pore pressure build-up
- Develop a framework for the estimation of total settlement, differential settlement and tilt, that accounts the various different mechanisms and their interaction
- Develop mitigation techniques to reduce foundation permanent deformations

LIQUEFACT
Deliverable D3.1
State of the art review of numerical modelling strategies to simulate liquefaction-induced
structural damage and of uncertain/random factors on the behaviour of liquefiable soils
v. 1.0

4. LIQUEFACTION-INDUCED MODIFICATION OF THE DYNAMIC RESPONSE OF BUILDINGS

The modelling of an infinite soil medium that is coupled not only in in terms of shear and volumetric strains but also coupled with the water pressure and is highly non-linear and stress dependent, is an impressively challenging task. Not just for the user but for the software and computer as well! The combination of the complexities of fully coupled effective stress soil modelling with the dynamic non-linear response of a structure, which is made of multiple brittle and ductile materials, has discrete and continuous joints between different elements, and can partially uplift from the soil under strong shaking, is at the limits of the ability of numerical modelling. There are always trade-offs with numerical modelling, where some phenomena are not considered or are captured through a series of separate numerical models. This section explains the major mechanisms involved with dynamic soil-foundation-structure interaction, and covers common numerical modelling approaches. Three subsections are used to split the problem into ground motions effects, soil-foundation interface effects, and structural modelling considerations.

4.1   GROUND MOTION MODIFICATION

4.1.1   MECHANISMS AND PHENOMENA

The primary damage to buildings during earthquakes is shaking damage, therefore the modification to the ground shaking due to liquefaction is extremely important in the context of quantifying building performance.

Ishihara and Cubrinovski (2005) investigated the ground motions recorded at the Kobe Port Island Vertical Array site during the 1995 Kobe earthquake, illustrating that liquefaction caused a reduction in shaking amplitude, a loss of high frequency content and a shift to longer period motion in comparison to the adjacent Pack House site which experienced less liquefaction. In Adapazari, the heaviest concentrations of damage in the city generally coincided with surface soils that were less sensitive to liquefaction, whereas in areas with higher susceptibility to liquefaction, the building damage was relatively reduced (Bakir et al., 2002). These perceived beneficial effects have even prompted interest in deliberately using liquefaction to isolate buildings from strong shaking (Mousavi et al., 2016).

However, liquefaction does not always result in less shaking. As matter of fact, Bouckovalas et al. (2016) demonstrated that liquefaction of the soil can cause an amplification in the seismic shaking especially in lower frequencies which is highly dependent on the depth of the liquefied layer. Moreover, investigations by Wotherspoon et al. (2015) of the ground motion station NNBS during the 2011 Christchurch earthquake demonstrated post-liquefaction acceleration spikes that were double the amplitude of the pre-liquefaction acceleration values.

The current understanding is that liquefaction causes a reduction in soil shear stiffness (and resistance), increase in soil shear strain, and can amplify and reduce particular frequencies of the surface shaking. Therefore, the amplification or reduction of the surface shaking, in terms of peak values, due to

liquefaction is function of the frequency content of the outcrop motion and of the geotechnical specificities of the site.

Conceptually, the reduction in stiffness can provide protection to buildings similar to base isolation techniques used within structural engineering and it is often referred to as "natural seismic isolation" (**Figure 4.1**).
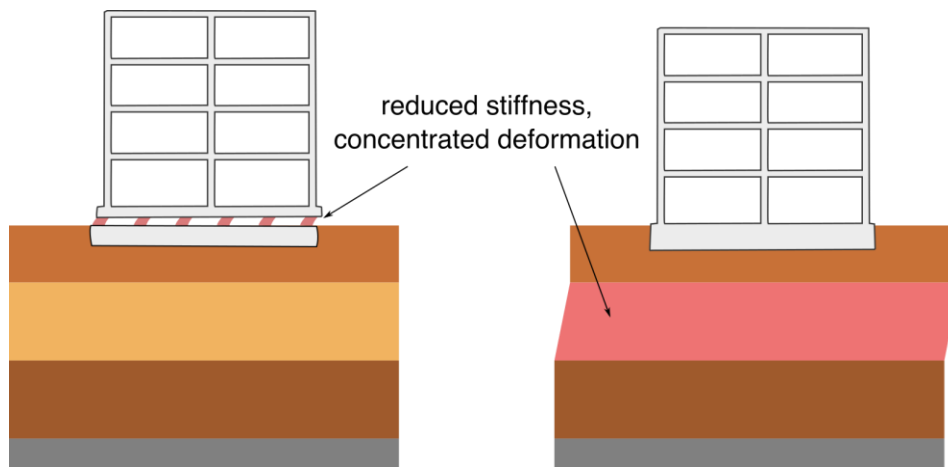
Figure 4.1: Conceptual natural seismic isolation due to liquefaction

The reduced stiffness lengthens the characteristic site period and means that shear waves dissipate more energy over the same distance because shear wave speeds have reduced (and consequently the wavelength), this is particularly evident for small cycle (high frequency) waves. The energy dissipation per cycle is also increased because the softer soil undergoes larger nonlinear strains and therefore the liquefied layer can act as a low-pass filter. Not all frequencies are reduced. In some cases, particular frequencies can be amplified. The amplification of frequencies is dependent on the characteristic site period (fundamental frequency) of the soil deposit. When shaking frequencies are close to the fundamental frequency of the deposit the up-going wave reflects off the surface and superimposes forming a standing wave that increases the surface shaking amplitude (**Figure 4.2**).
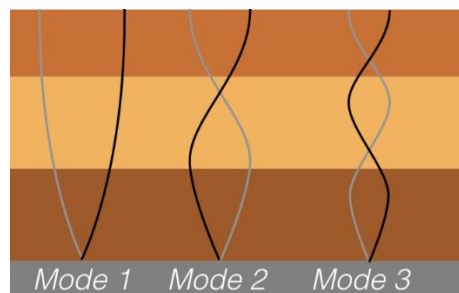
Figure 4.2: Standing wave modes that cause site amplification

The major parameters influencing the amplitude of amplification/de-amplification are the base soil stiffness contrast (i.e. how much wave energy is reflected back into the soil deposit) and the level of energy dissipation per cycle. In terms of which frequencies are amplified, the major parameters are the shear wave velocity (Vs) and height of the deposit (H), as the natural modes of a homogeneous site deposit can be determined from **Equation (17)**, where m is the wave number (Kramer, 1996).

$$T_m = \frac{4H}{(2m+1)V_s} \tag{17}$$

When the soil deposit liquefies, the change in stiffness results in a change in the natural frequency of the soil deposit so different frequencies are superimposed. Kramer et al. (2011) investigated the ground motion recorded in the of Kawagishi-cho apartment building in 1964 Niigata earthquake and observed a shift in the dominant frequency of the motion from approximately 0.1 to 5 seconds once liquefaction occurred under the structure. Additionally, the interface between liquefied and non-liquefied layers develops a stiffness contrast, which causes waves to reflect off the interface and can potentially cause superposition in the upper deposit (**Figure 4.3**).
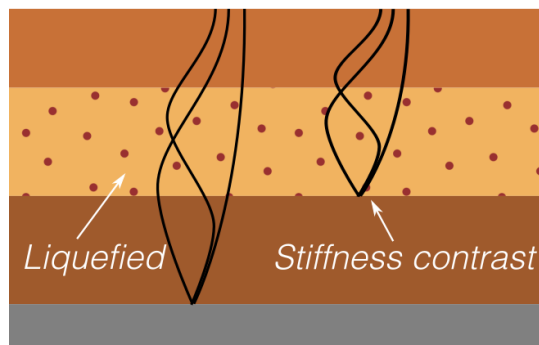
Figure 4.3: Site amplification occurring due to the stiffness contrast between liquefied and non-liquefied layers

Bouckovalas et al. (2016) investigated the amplification of the shaking response of a two-layered visco-elastic soil deposit resting on a rigid bedrock. The top layer represented a non-liquefied crust and the lower layer represented a liquefied deposit, with a soil shear wave velocity ratio between the two layers (Vs,L/Vs,c) of 0.15, the densities were equal, the liquefied layer was three times thicker than the crust (H_L/H_C), and the viscous damping of the crust and lower deposit set to 10% and 15% respectively.

This simple analytical model indicated that amplification of the excitation frequency would occur when the ratio of the height of the liquefied layer to the excitation wave length in the liquefied layer ($H_L/\lambda*L$) was less than 0.25, while de-amplification would occur above this ratio. The properties were then varied and the simple model indicated that changing the ratio of densities, the ratio of shear wave velocities and changing the crust damping all had negligible effect on the transfer function. Increasing the liquefied layer damping

reduced the amplitude of amplification and changing the ratio of crust thickness to liquefied layer thickness caused a major change in the relationship.

Typically, we can observe that ground motions from liquefied deposits have less high frequency content and can have larger displacement demands than their non-liquefied equivalents. However, liquefied ground motions also have a unique signature that is not observed in other ground motions. Liquefied ground motions have acceleration spikes. It is believed that these high frequency acceleration spikes are a result of soil dilation (strain hardening) as explained by Kramer et al. (2011):

"As the amplitude of the shear stress increases, dilation causes the effective stress, and stiffness, to increase so that the later portion of the stress pulse travels faster than the early (…) energy in the pulse. The resulting high-frequency spikes of acceleration superimposed upon the long-period response of the softened soil."

The peculiar characteristic in liquefied soil of increasing in stiffness at large strain rather than decreasing means that acceleration peaks are unique to liquefied soils.

Robust methods to quantify the level of strain hardening and the modifications to frequency content have not yet been developed. However, acceleration spikes in liquefied soil deposits were observed during the 2011 Tohoku earthquake and Roten et al. (2013) showed the behaviour was linked to soil-dilatancy. Since this phenomenon is related to soil dilation, we can expect more pronounced acceleration spikes in denser sand. Potentially the manifestation of acceleration spikes is also dependent on the depth of the liquefied layer. Shallower liquefied layers typically undergo larger shear strain (increasing the potential for dilative behaviour), however, an acceleration spike also requires an accumulation of superimposed waves that can only develop by travelling through deeper deposits, furthermore, deeper deposits would dissipate more energy due to the extended travel distance.

The majority of liquefaction related site response research has focused on ground shaking in the free-field. However, several centrifuge studies (e.g. Dobry and Liu, 1994; Dashti et al., 2010b; Bertalot and Brennan, 2015) have demonstrated that the presence of a building can dramatically change the pore pressure build up, and potentially cause dilation resulting in increased strength and stiffness rather than contraction and liquefaction!

Even in non-liquefied soil the presence of a building can increase the soil shear wave velocity through the additional confining stress. In many cases the presence of a building reduces pore pressure build up and subsequently limits the stiffness degradation and energy dissipation (while the opposite is also possible). In the context of the above framework, this affects the amplitude and frequency content of surface shaking. The additional shear stress of a building can also cause further strain hardening and the potential to increase the amplitude of acceleration spikes, however, the limited research on this topic does not allow solid conclusions.

Another interesting aspect of the interaction between site-response and liquefaction is the influence of ground improvement. Increasing demand to occupy potentially liquefiable land and recent events such as the Christchurch earthquakes (2010-2011) has increased the number of novel techniques proposed for ground improvement to mitigate liquefaction. These techniques have been developed without a full

LIQUEFACT
Deliverable D3.1
State of the art review of numerical modelling strategies to simulate liquefaction-induced
structural damage and of uncertain/random factors on the behaviour of liquefiable soils
v. 1.0

understanding of the theoretical principals behind building performance in liquefiable soil deposits (MBIE, 2017). The majority of these ground improvement methods are focused on reducing permanent settlement and tilt, which could have dire consequences in terms of ground shaking. Centrifuge tests performed by Liu and Dobry (1997) investigated soil compaction as a ground improvement measure against liquefaction, the surface ground shaking increased remarkably when the ground improvement reached a depth of more than 70% of the depth of the liquefied layer. The ground improvement allowed the shaking energy to more easily travel to the surface and potentially increased the level of shearing in the non-liquefied zone (**Figure 4.4**). There is an urgent need to develop a robust theoretical framework to understand ground shaking in liquefied deposits and for assessing the trade-offs between optimising for minimal settlement compared to minimal ground shaking.
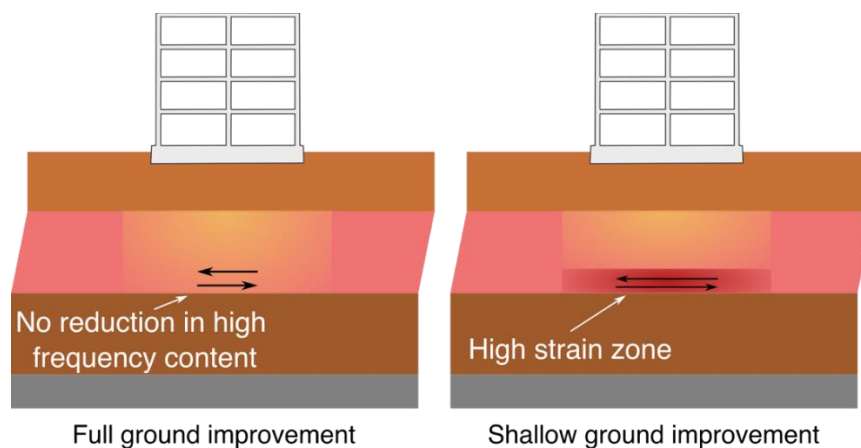
Figure 4.4: Influence of ground improvement

There are many other mechanisms and phenomena that contribute to the response and ground shaking of a site. These phenomena have not been covered here as there are no specific interactions with liquefaction (i.e. they occur independently of whether liquefaction occurs). Several earthquake geotechnical engineering textbooks (e.g Kramer, 1996) cover these effects which have been non-exhaustively listed below:

- Fault rupture mechanics

- Distance to fault

- Orientation incident shear waves

- Influence of surface waves

- Topographic amplification

- Basin effects

4.1.2 MODELLING STRATEGIES

There are many software applications that enable site response analysis. These different software applications can be considered under three different classes, in increasing level of complexity and ability (Kramer, 1996):

- Linear/Equivalent linear analysis: The soil shear modulus is considered linear and typically represents a secant stiffness. The soil hysteretic behaviour is modelled through viscous damping, where the equivalent viscous damping is based on the energy dissipated through a cycle of loading and is usually dependent on the expected level of shear strain.

- Total stress analysis: The soil behaviour is modelled in the time domain following a nonlinear stress-strain path that allows the hysteretic energy dissipation to be modelled directly. The soil stiffness and resistance is entirely based on the total stress (or initial effective stress) and it does not account for the generation of excess pore pressures during earthquake motion.

- Effective stress analysis: is modelled in the time domain following a nonlinear stress-strain path where the current stress state accounts for changes in pore pressure. These models can directly model the hysteretic energy dissipation and capture complex material behaviour such as cyclic liquefaction.

Inside of each of these classes the ability of the software application can vary considerably, however, the classification provides a basis to discuss some of the major benefits and drawbacks of the different analysis approaches.

LINEAR/EQUIVALENT LINEAR ANALYSIS

Equivalent linear analysis is obviously limited in that it cannot accurately capture nonlinear stress-strain paths and therefore is typically only used at low shear strain levels where liquefaction is not expected to occur. Kaklamanos et al. (2013) analysed the Japanese Kik-net downhole array and showed that for analyses with large peak ground acceleration, large shear strain or long site predominant periods the linear and equivalent analysis methods resulted in biased predictions in behaviour. Kaklamanos et al. (2013) provides some guidance on the usefulness of linear and equivalent linear modelling for estimating spectral acceleration at different periods, where the max shear strain is less than 0.1%, the equivalent linear method provides suitable estimates across the full range of spectral periods. The equivalent linear method can still provide suitable estimates of spectral acceleration for periods greater than 0.5s up to 1% shear strain. At lower periods when the maximum shear strain is within 0.1% and 0.4% is not clear whether a suitable prediction can be achieved with equivalent linear analysis, while above 0.4% a nonlinear analysis is necessary.

The major biases that occur with equivalent linear analyses are that the equivalent shear modulus over predicts the extent of shear modulus reduction in high frequencies and at the start of the motion, and under predicts the nonlinearity of low frequencies and at the end of the motion. Another major drawback of the equivalent-linear approach is that the stiffness remains constant throughout the entire ground

motion, which means that greater superposition tends to occur at the natural frequencies of the equivalent deposit than would develop in reality (Kramer, 1996). Other than being the simplest and most interpretable analysis approach, equivalent linear analysis has the distinct advantage of being able to capture the frequency dependent dynamic stiffness and damping of the soil when the analysis is conducted in the frequency domain.

TOTAL STRESS ANALYSIS

There are many different variations of non-linear models, the most common for site response analysis is the strain based model (also referred to as an unload-reload model), where the non-linear stiffness is approximated based on the backbone curve of the soil response (e.g. Ramberg and Osgood, 1943; Pyke, 1980). While these models can model a gradual reduction in stiffness with increasing strain, the unloading stiffness is typically intrinsically related to the backbone curve (e.g. using the Extended Masing Rule), thus the modelling of energy dissipation is limited (Kramer et al., 2011).

Other total stress-based models use linear elasto-plastic response to capture the soil response, where the soil remains linear until it reaches a yield/failure point where the tangent stiffness reduces dramatically (e.g. Drucker and Prager, 1952). Elasto-plastic models are most applicable to soil strength related problems (e.g. foundation bearing capacity failure) and are not appropriate for site response analysis where the stiffness rather than strength is the most important characteristic.

The third type of non-linear model is the advanced constitutive model. Advanced constitutive models can model continuous yielding, typically formulated in terms of hypo-plasticity or nonlinear elastoplastic frameworks where the nonlinear soil response is determined based on the current stress state in relation to one or more yield and failure stress surfaces (Kolymbas and Wu, 1993). Using more complex constitutive equations allows the soil to be modelled in greater detail especially in relation to the estimation of energy dissipation and residual deformations. The additional complexity of an advanced constitutive model is often not warranted in non-liquefying soil but tends to be more widely used in effective stress analysis for the simulation of liquefiable deposits.

EFFECTIVE STRESS ANALYSIS

The effective stress analysis class is an extension of non-linear total stress analysis, except that it accounts for the change in pore pressure (e.g. the initiation of liquefaction) and the stiffness and strength are defined based on the effective stresses. The techniques to account for pore pressure build up vary significantly (e.g. based on number of cycles, cumulative elastic or inelastic shear strain), many of the most advanced models are discussed in Section 2.3 on soil constitutive models. Advanced constitutive models can capture the strength and stiffness degradation associated with the initiation of liquefaction, and can model the phase transformation of a soil changing from contractive to dilative, which is an important aspect in capturing acceleration spikes (Kramer et al., 2011). The majority of effective stress models are advanced constitutive models, however, there are also backbone curve-based effective stress models, which are simpler in that the shape of the backbone response is modified based the level of pore pressure build up (e.g Matasovic and Vucetic, 1993).

There is another approach to soil-fluid modelling that does not require a macro level constitutive model of the soil, as the individual soil particles are modelled directly. This approach is the discrete particle method, however, these models have not matured enough to been used in practice or even widely within research circles (NASEM, 2016). There are also various advantages of using two-dimensional and three-dimensional models compared to the typical one-dimensional site response models, such as the ability to capture the influence of non-vertically oriented shear waves and capture basin effects, further discussion on this can be found in Kramer (1996).

A study by Markham et al. (2016) investigated the site-response of several ground motion stations during the Christchurch earthquake sequence using equivalent linear, total stress and effective stress modelling techniques within the site-response analysis software DEEPSOIL. For the Christchurch hospital site the obtained surface acceleration response spectra over a period range of 0.067-10s were very similar for all three different types of models. However, the time series behaviour was quite different in terms of frequency content and changes throughout the time history. This apparent similarity highlights the importance of the purpose of the site response analysis. If the purpose is to obtain spectral accelerations for the seismic design of modern buildings, the difference between the different methods can be less important because strong shaking at the start of a motion can dominate the spectral response before the nonlinear behaviour and liquefaction influence the response. However, if the purpose is to use site response analysis to obtain surface shaking time series to conduct further response history analyses of structures that are sensitive to shaking duration (e.g. un-reinforced masonry buildings) or equipment that is sensitive to high frequency content (e.g. oscillating machinery), then the differences would be more important. Markham et al. (2016) also conducted effective stress analyses with the advanced constitutive model PM4Sand (Boulanger and Ziotopoulou, 2015) in FLAC2D, and found that this model better approximated the record surface shaking than the effective stress model used in the DEEPSOIL. Another conclusion from the study was the importance of quantifying the input motion, which can introduce considerably bias to the surface motion, especially in the case of the Christchurch February 2011, where considerable directivity and near-field effects were apparent in the recorded motions.

When conducting site response analysis of liquefiable deposits, it is important to evaluate the abilities of the method against the phenomena described in Section 2.1. **Table 4.1** provides a guide on the abilities of the different techniques.

Table 4.1: Advantages and drawbacks of different techniques for site response analysis

Class	Equivalent linear	Total stress			Effective stress	
Type	**Back-bone**	**Back-bone**	**Elasto-plastic**	**Constitutive model**	**Back-bone**	**Constitutive mode**
Pros	Simple to implement and use	Can capture the evolution of nonlinear behaviour			Can capture the evolution of nonlinear behaviour	
	Can account for frequency dependent impedance	Simpler than constitutive models	Simpler than constitutive models	Potential to capture full stress-strain behaviour of soil	Can simulate pore pressure build up	
		More stable than many constitutive models	Can capture stress based failure		Simpler than constitutive models	Potential to capture full stress-strain behaviour of soil
Cons	Cannot simulate the build-up of pore pressure	Cannot simulate the build-up of pore pressure			Limited ability to model phase transformation	More complex than other total stress methods
	Cannot simulate evolution of nonlinear behaviour	Limited ability to model hysteretic behaviour	Poor estimate of stiffness and energy dissipation		Limited ability to model hysteretic behaviour	
	Biases for high frequency and low frequency content	Limited ability to capture residual deformations	Calibration parameters based on expected level of nonlinearity	More complex than other total stress methods	Calibration parameters based on expected load path (e.g. number of cycles)	
	Tend to over amplify frequencies that are close to the site frequencies	Limited ability to model asymmetric loading paths	Can over amplify the frequencies close to the elastic site frequencies			
Summary	Suitable for non-liquefiable deposits with low strain demands	Suitable for non-liquefiable soils, with relatively simple loading	Limited applicability to site response analysis	Suitable for non-liquefiable soil deposits, necessary at large strains	Suitable for liquefiable soils, with relatively simple loading	Suitable for all types of site response analysis

LIQUEFACT
Deliverable D3.1
State of the art review of numerical modelling strategies to simulate liquefaction-induced
structural damage and of uncertain/random factors on the behaviour of liquefiable soils
v. 1.0

4.2 SOIL-FOUNDATION-STRUCTURE IMPEDANCE MODIFICATION

4.2.1 MECHANISMS AND PHENOMENA

The influence of the soil profile on the dynamic response of the superstructure has two major aspects. The first influence is the amplification/de-amplification and changing of phase of different frequencies of the ground motion due to it travelling through the soil deposit, often referred to as 'site-response'. The second influence is the modification to the dynamic properties of the soil, foundation structure system due to the consideration of the deformation of the soil and foundation, often referred to as soil-foundation-structure interaction (SFSI).

This section of the report focuses on the second aspect, while the influence of the site response is the focus of Section 4.1.

Conventional SFSI analysis considers the change in building response through two separate phenomena, kinematic interaction and inertia interaction. The kinematic interaction considers the change in ground-motion due to the difference in stiffness between the soil and foundation/structure. In deep foundations, kinematic interaction can result in significant amplification and de-amplification of different frequencies and even provide additional over-turning moments to the foundation. For shallow foundations, the response is almost negligible and many researchers have demonstrated that kinematic interaction often de-amplifies horizontally propagating shear waves (e.g. Lin and Miranda, 2007).

The inertial interaction is due to the generation of inertial effects in the structure that will give rise to additional soil-structure interaction forces. The difference in inertia causes the heavy structure to lag behind the soil and push against it and eventually oscillates out-of-phase to the soil. The simulation of inertial interaction is often achieved by modelling the soil impedance through dynamic stiffness and damping. The inclusion of additional flexibility and damping at the foundation level results in an overall increase in system flexibility and typically greater system energy dissipation, thus many researchers have shown that inertial interaction reduces seismic demand and improves performance for elastic systems (e.g. Pecker, 2007). However, there is also a considerable body of research demonstrating the detrimental effects of soil-foundation-structure interaction (e.g. Mylonakis and Gazetas, 2000; Moghaddasi et al., 2011).

Regardless of the beneficial and detrimental effects of SFSI, there is growing support for the use of nonlinear soil and foundation deformations to limit shaking energy from entering the structure (e.g. Pecker and Pender, 2000; Deng et al., 2012). This is supported by considerable evidence that the behaviour can be reliably predicted in terms of nonlinear stiffness, foundation moment capacity, level of settlement and residual tilt (e.g. Deng and Kutter, 2012; Liu et al., 2013), although reliable estimates of performance have not yet been developed for liquefiable soil. For non-liquefiable soil the foundation moment capacity can be estimated using the **Equation (18)** from Gajan et al. (2005).

LIQUEFACT
Deliverable D3.1
State of the art review of numerical modelling strategies to simulate liquefaction-induced
structural damage and of uncertain/random factors on the behaviour of liquefiable soils
v. 1.0

$$M_f = \frac{N \cdot B}{2}\left(1 - \frac{1}{FS_v}\right)$$

(18)

Where N is the axial load applied to the foundation, B is the foundation width and FS_v is the bearing capacity factor of safety under purely vertical load. The estimation of foundation rotational stiffness and residual tilt can be determined based on the contributions from three rotation mechanisms (elastic deformation, foundation uplift and soil yielding (**Figure 4.5**)) (e.g. Gajan et al., 2005).
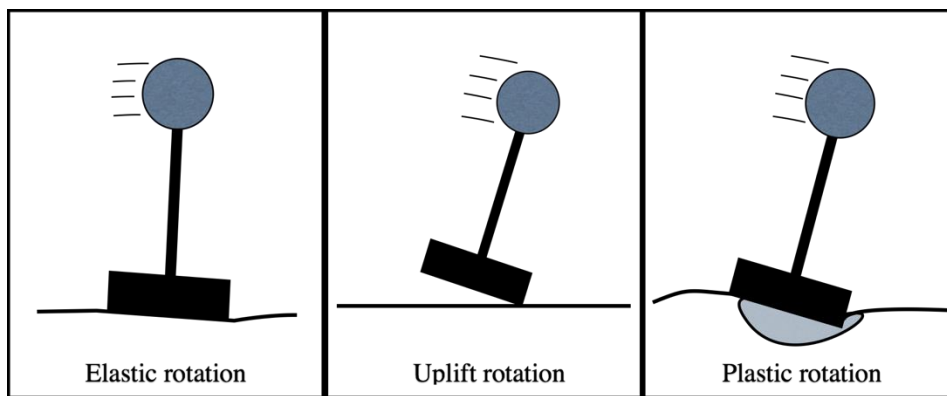
Figure 4.5: Mechanisms of foundation rotation

An important consideration for design and assessment when considering SFSI is the level of energy dissipation of the system. Seismic design procedures often reduce design loads based on the structural ductility, however, if the dominant deformation mode is foundation rocking then the system may not dissipate as much energy compared to a yielding structure. The shared energy dissipation between the superstructure and the foundation needs to be quantified (**Figure 4.6**) (Millen et al., 2015).
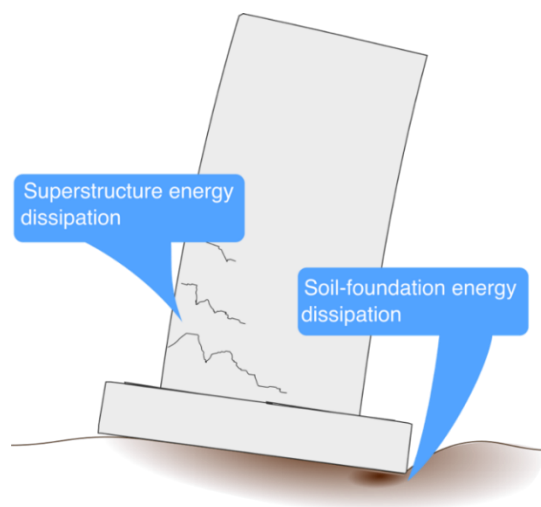
Figure 4.6: Shared energy dissipation between the superstructure and foundation

LIQUEFACT
Deliverable D3.1
State of the art review of numerical modelling strategies to simulate liquefaction-induced
structural damage and of uncertain/random factors on the behaviour of liquefiable soils
v. 1.0

Other SFSI mechanisms can also have an important influence on the structural response. The potential for foundation rocking to reduce the shaking energy entering the structure is based on the formation of a non-linear mechanism at the base of the structure limiting the development of the first mode of response. However, for tall structures the second and third mode can contribute with significant energy and are not capped by foundation rocking and are only shifted to slightly longer vibration periods (**Figure 4.7**) (Millen, 2016).

Fixed base   Pinned base

$$f_1 = \frac{v}{4H} \qquad f_2 = \frac{3v}{4H} \qquad f_3 = \frac{5v}{4H} \qquad f_1 \approx 0Hz \qquad f_2 = \frac{v}{H} \qquad f_3 = \frac{3v}{2H}$$
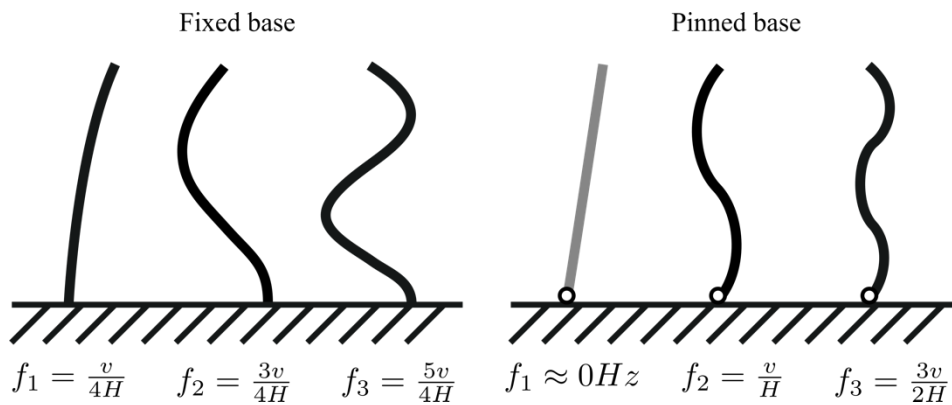
Figure 4.7: Behaviour of cantilevers with hinge at base

The Influence of SFSI on frame structures is even more complex, as soil-foundation deformation can occur both as a rigid body displacement and within the foundation. The additional flexibility of the foundation alters the overall flexibility of the soil-structure system (**Figure 4.8**).

Rigid foundation = high system stiffness

Flexible foundation = low system stiffness
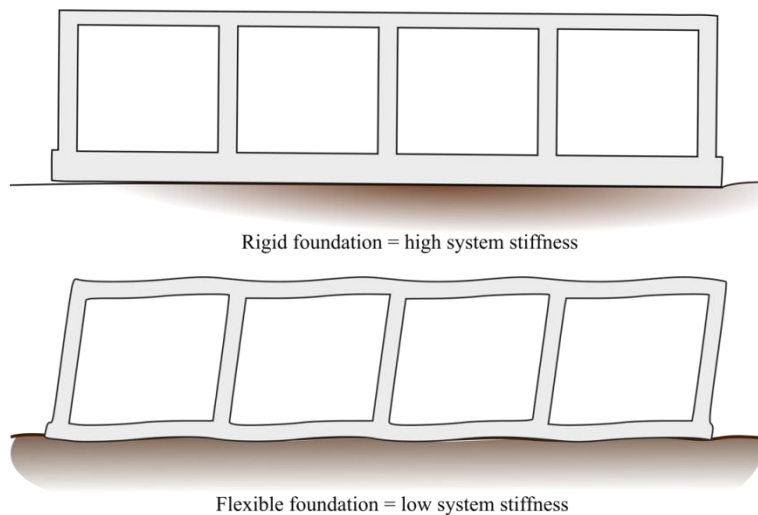
Figure 4.8: Foundation flexibility influences the system stiffness

LIQUEFACT
Deliverable D3.1
State of the art review of numerical modelling strategies to simulate liquefaction-induced
structural damage and of uncertain/random factors on the behaviour of liquefiable soils
v. 1.0

The relative flexibility of the soil-foundation elements with respect to the structure determines the distribution of stresses within the structure. Foundation elements with low rotational stiffness can shift stresses to the beam elements (Gelagoti et al., 2011) (**Figure 4.9**).

Loading direction

Loading direction

Low rotational to axial stiffness ratio

High rotational to axial stiffness ratio
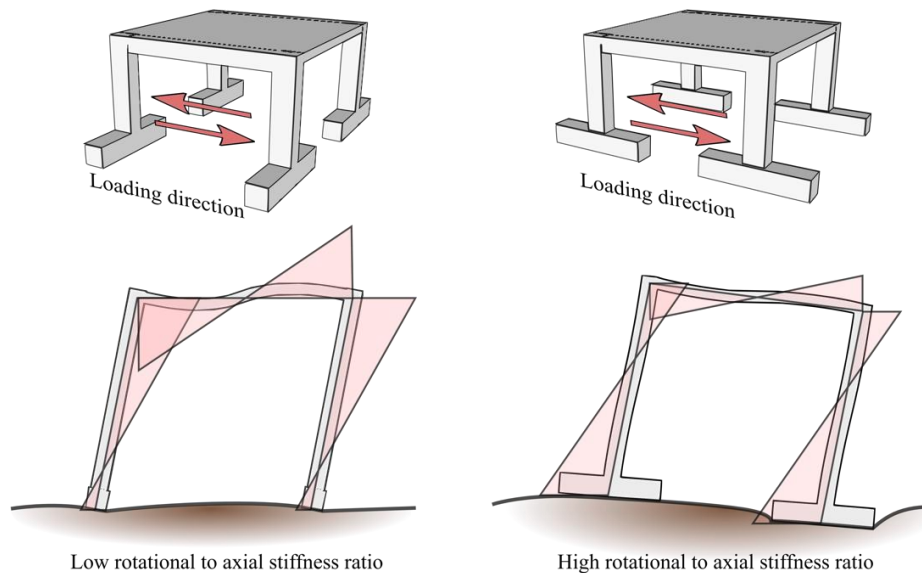
Figure 4.9: Influence of relative stiffness of foundation elements on the distribution of stresses

The influence of liquefaction changes the stiffness and strength of the soil surrounding the foundation. Therefore, liquefaction should result in an increase in the level of energy dissipation and deformation at the soil-foundation interface (if all else remains equal). However, the reduction in shaking energy caused be liquefaction can counteract this behaviour such that a reduction in dynamic soil-foundation deformations is possible.

The location of liquefaction is also important, where horizontal heterogeneity can result in different footings having different stiffness and resistance and therefore causing a stress concentration within the structure. The location of liquefaction vertically also has an influence on the behaviour. The impedance of the soil-foundation interface is dependent on the propagation of waves through the soil and is strongly influenced by stiffness contrasts. The reduction in stiffness in liquefied layers tends to increase the stiffness contrast and make the conventional soil-foundation impedances terms (e.g. Gazetas, 1991) less applicable.

4.2.2 CURRENT MODELLING STRATEGIES

There are three distinct approaches to modelling soil-foundation-structure (SFS) systems:

- Direct approach: The soil, foundation and structure are all modelled within the same simulation, also referred to as the integrated approach, where kinematic and inertial interactions are taken into account in a natural way.

- Sub-structured (De-coupled) approach: The soil and (massless-) foundation are modelled in one simulation and then the foundation and structure are modelled in the second step with simplified consideration of the soil, but taking into account the generation of inertial effects in the structure.

- Simplified analytical approach: The various interactions between the soil, foundation and structure are considered at a macro-level through a series of expressions that capture their influence.

Direct approach

The major advantage of the direct approach (**Figure 4.10**) is that it implicitly considers the site-effects, the kinematic interaction and inertial interaction, as well as the interdependence of each of these phenomena on each other. However, integrated models are often not practical due to several practical difficulties. One such difficulty is that for numerical stability and accuracy the computation time-step must be proportional to the size of the material elements and inversely proportional to the stiffness of the material (ITASCA, 2017). Given that a structure typically has small stiff structural elements while soil is relatively weak and is essentially infinite in size, separate numerical models for different aspects are often used to efficiently solve these problems. Even when integrated modelling is used, the structure is often modelled again in greater detail to better understand its response.
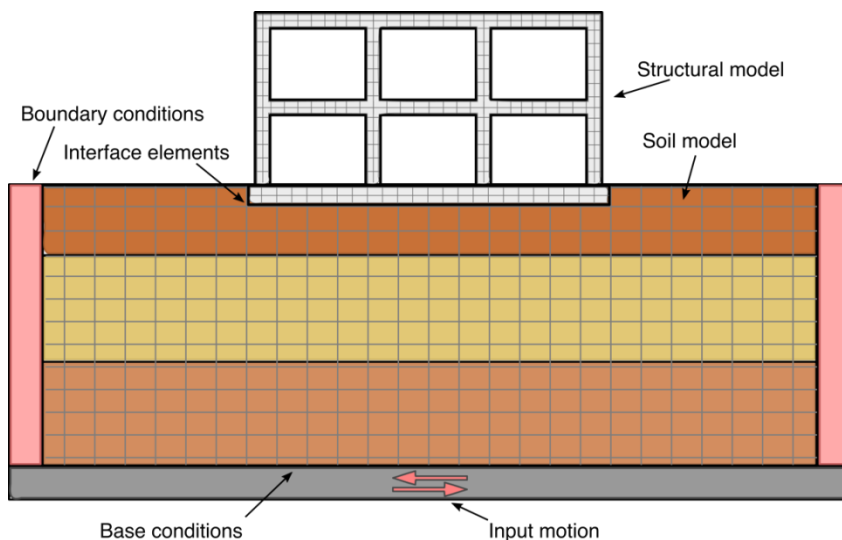
Figure 4.10: Schematic interpretation of a direct/integrated model

A further complication to the direct modelling approach is the choice of damping used for the simulation. Damping is used to both simulate energy loss through other mechanisms not directly considered in the model (e.g. heat or geometric dissipation in a two-dimensional model compared to a three-dimensional reality) and it is used to stabilise time history based calculations against un-realistic numerical oscillations. Damping can be modelled through dashpot elements which absorb energy based on the difference in velocity between the two nodes at the ends of the dashpot. However, the force generated by the dashpot

is passed to the ends of the element which may not be realistic. The alternative is to apply the damping model globally, where energy is lost through a velocity dependent matrix and the force calculated by this matrix is applied directly to nodes thus can better simulate loss from radiation damping. Unfortunately, in the majority of numerical software applications the global damping matrix does not allow the simulation of different levels of critical damping for different parts of the model.

Further issues occur with the modelling of the interface between the soil and foundation, where gaps form between the soil and foundation and then close with some impact, making it difficult to model with a single constitutive model, however, the majority of software applications have overcome these peculiarities with the use of special interface elements. There are several software applications that facilitate the direct modelling of the SFS system (e.g. PLAXIS, OPENSEES, FLAC), with many examples of successful modelling (e.g Borozan, 2017; Luque and Bray, 2017). The constitutive models used within these applications are reviewed in Section 2.3.

Sub-structure approach

The sub-structure approach to simulating SFSI first focuses on modelling the soil and then uses the soil response as an input for a model that focuses on the superstructure. The soil-(massless) foundation is often modelled directly with a finite element mesh (or other appropriate numerical technique like Boundary Element Method (BEM), Method Fundamental Solution (MFS) or even by the coupling of different methods) and is further explained in Section 4.1 on site response analysis. For shallow foundations, the modelling of the structure with consideration of SFSI typically focuses on the inertial interaction, where the effects of kinematic interaction are either ignored or are often superimposed on the results of the inertia interaction. While superposition is not theoretically possible for an inelastic SFS systems, the assumption is often suitable because the influence of inertial interaction dissipates in short distances from the foundation and kinematic interaction influences the motion based on the wave length, thus typically influencing high frequency content that is less important to the structural response (Gazetas and Mylonakis, 1998).

Several structural analysis software applications facilitate the modelling of inertial interaction (e.g. Ruaumoko, OpenSees). The modelling of inertial interaction based on lumped parameter models has two different numerical approaches, one is the conventional Winkler-beam model and the other is the macro-element (**Figure 4.11**). The Winkler beam model uses a series of un-coupled translational springs to represent the soil. The location of the stiffness and location of the springs under the foundation provides the axial and rotational stiffness. The springs can also yield to provide the plastic response and detach to capture the uplift response (El Ganainy and El Naggar, 2009; Harden and Hutchinson, 2009).

The macro-element simulates the axially, moment and shear stiffness with single springs (dashpots and masses) that are coupled together and attending to a constitutive model to capture the soil plastic response and uplift behaviour (e.g. Chatzigogos et al., 2011; Figini et al., 2012; Prisco and Maugeri, 2013).

The major advantage of the Winkler-beam compared to the macro-element is that it can directly model the foundation flexibility, while its major drawback is that it can be difficult to model nonlinear vertical and

LIQUEFACT
Deliverable D3.1
State of the art review of numerical modelling strategies to simulate liquefaction-induced
structural damage and of uncertain/random factors on the behaviour of liquefiable soils
v. 1.0

rotation of behaviour of the foundation over a large range of foundation moment demands due to the implicit coupling between the vertical and rotational stiffness. There are currently no suitable macro-element or Winkler-beam models that can simulate the effects of liquefaction on SFSI.
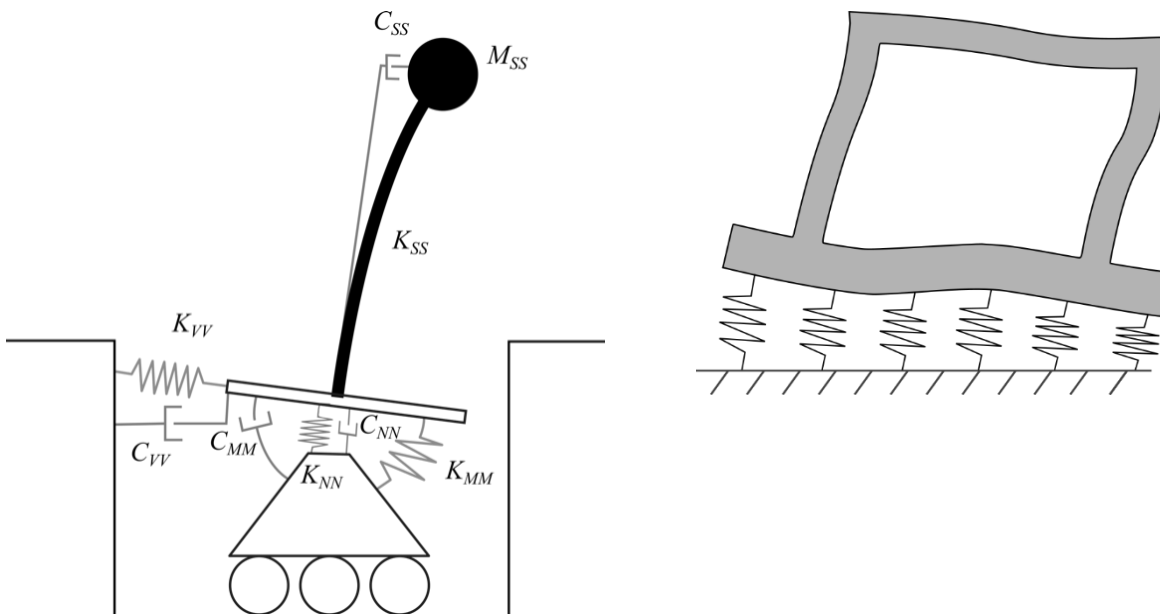
Figure 4.11: (a) [Left] Soil-foundation macro-element attached to SDOF structure; (b) [Right] Soil-foundation Winkler-beam model

Simplified approach

Several analytical procedures have been developed recently to further understand and design for SFSI (e.g. Paolucci et al., 2013; Deng et al., 2014; Millen et al., 2016). Conceptually these displacement-based procedures are explained in **Figure 4.12**, where the first step uses the displaced shape of the structure-foundation-soil system (Δ_i) based on a first mode response at peak design drift and mass distribution (m_i), to determine an equivalent SDOF displacement (Δ_e), equivalent mass (m_e), effective height (H_e) using **Equations (19) - (21)**. The nonlinear behaviour is converted to an equivalent linear behaviour in steps two and three, where the secant-to-peak stiffness is used as the effective stiffness and the energy dissipation is usually accounted for through an equivalent viscous damping. The effective period is determined based on the interception of the design displacement with the reduced spectral displacement, where the spectral displacement is reduced based on the energy dissipation. The final step is to compute the base shear from the effective stiffness (K_{eff}) and the design displacement. Currently none of these simplified analytical procedures directly account for liquefiable soils, however, their simplified analytical approach provides a rapid approach to assessing SFSI effects and could be extended to account of liquefaction.

$$\Delta_e = \frac{\sum_{i=1}^{n} m_i \Delta_i^2}{\sum_{i=1}^{n} m_i \Delta_i} \qquad (19)$$

$$m_e = \frac{\sum_{i=1}^{n} m_i \Delta_i}{\Delta_e} \qquad (20)$$

$$H_e = \frac{\sum_{i=1}^{n} m_i \Delta_i H_i}{\sum_{i=1}^{n} m_i \Delta_i} \qquad (21)$$
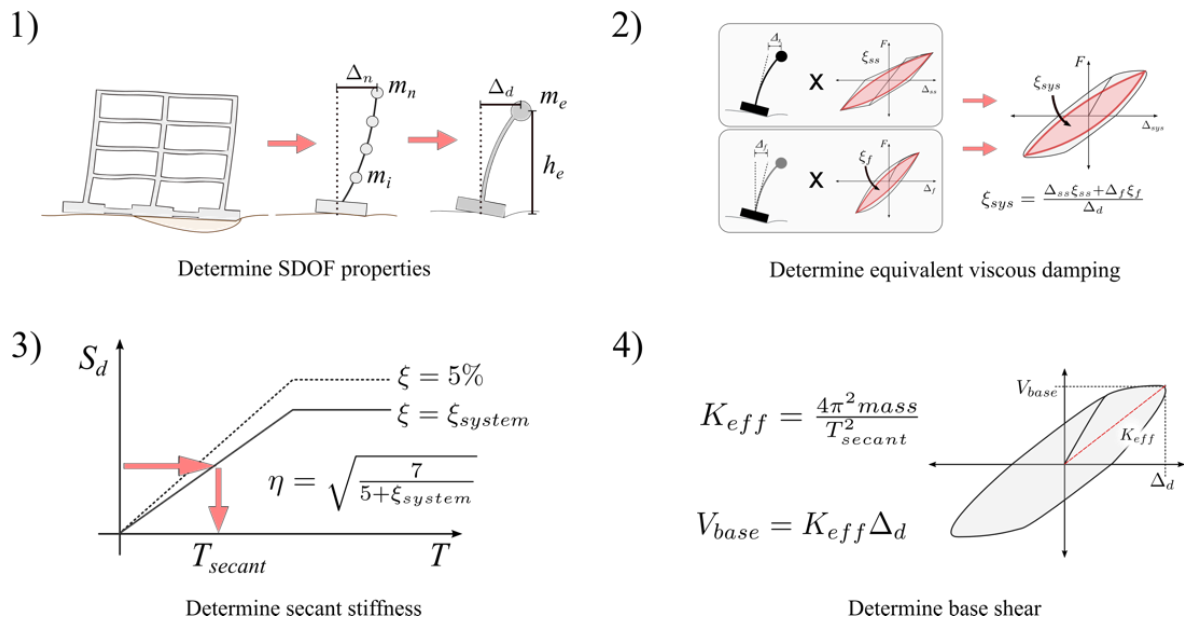
Figure 4.12: Displacement-based design with consideration for SFSI

Another approach to the simulation of SFSI effects is physical modelling; however, this is often very expensive due to the stress dependent behaviour of soil, thus requiring large scale models or centrifuge modelling. Several successful centrifuge campaigns have been conducted recently that simulate SFSI and liquefaction (e.g Liu and Dobry, 1997; Dashti et al., 2010b; Bertalot and Brennan, 2015). Despite the recent success of these projects, the benefits and pitfalls of experimental work is beyond the scope of this report. **Table 4.2** summarises the three different numerical analysis approaches.

Table 4.2: Analysis approaches to simulate SFSI effects

	Direct approach	Substructure approach	Simplified analytical
Pros	Directly accounts for the interactions between the soil, foundation and structure Can model soil heterogeneity and asymmetric structural configurations Can provide time history output for the assessment of non-structural elements	Can incorporate many different methods for the assessment of various aspects of the problem Can iteratively improve accuracy of the most influential aspects Can provide time history output for the assessment of non-structural elements	Quick and easy to implement Easily incorporate many different methods for the assessment of various aspects of the problem Easily interpreted, can understand the importance of various contributions
Cons	Need advanced software that can deal with the numerous difficulties of modelling SFSI and liquefaction Can be difficult to understand the important of different mechanisms Usually situation specific, model is not applicable to other situations	Issues with superposition especially in highly nonlinear systems Can fail to capture important interactions between the structure and soil Multiple steps can be slow due to data transfer Can overcome some difficulties of the direct approach with suitable simple assumptions	Limited detailed output, no time series output Not possible if mechanisms are not understood enough to be simplified Not suitable for unusual configurations
Summary	Suitable for assessment of all systems, depending on software and user capabilities	Suitable for most soil-structure systems, but struggles with strongly interacting nonlinear soil-structure systems	Suitable for preliminary assessment and the assessment of low importance structures

4.3   STRUCTURAL MODELLING CONSIDERATIONS

4.3.1   MECHANISMS OF STRUCTURAL DEFORMATION AND DAMAGE

The mechanisms leading to structural deformation and damage in earthquake-relevant building members (i.e. beams, columns and walls) are connected to the underlying options governing their structural design. Generally, these options can be assigned to two main groups of design rules according to the type of structure that is obtained: non ductile and ductile design rules. Non ductile design is often referred to as "force-controlled" and refers to design procedures in which structural member capacities are governed by strength. In such members, the ductility or energy-dissipation capacity is expected to be low, which means that their ability to remain an active part of the structural system after reaching their peak strength is low, therefore experiencing a "brittle" failure. Non ductile design rules are usually associated to structural design approaches that do not account for earthquake action and focus mostly on gravity loads. Therefore,

the presence of this type of construction in earthquake-prone areas can be seen as the result of one of four possible scenarios:

- the construction was built before the enforcement of modern seismic design standards that establish adequate earthquake design rules leading to ductile constructions;
- the construction is recent but was built in a region where modern seismic design standards do not exist or are not enforced;
- the construction is recent and was built in a region where modern seismic design standards exist but were disregarded in the design;
- The construction is recent and was built in a region when the seismic hazard was underestimated.

Non ductile design of framed buildings usually leads to a certain type of structural behaviour where the known weak-column-strong-beam mechanism is likely to occur. This mechanism reflects the fact that, for a given beam-column joint, the capacity of the adjoining columns is lower than that of the adjoining beams. Since columns are critical members for the survival of buildings, once damage concentrates in the columns' end regions due to an earthquake, they may not be able to support the weight of the construction above and lead to global collapse.

The modern approach to the seismic design of ordinary structures is based on ductile design considerations that are established in practice by the capacity design procedure. A structure designed according to this procedure involves a mixture of members with high load capacity and members with high inelastic deformation capacity to optimise the response of the structural system. The capacity design procedure involves identifying a failure mechanism, the members and regions responsible for its development, and providing these members and regions with adequate ductility. Simultaneously, the rest of the members are protected by providing them with adequate strength to ensure nearly elastic behaviour. In an ordinary building structure, beams are the members in the first group while walls and columns are the nearly elastic members. Beams are therefore designed to have a high ductility or energy-dissipation capacity, which means that their ability to remain an active part of the structural system after reaching their peak strength is high, therefore experiencing a "ductile" failure.

Structural damage can be analysed at the local (member) level or at the global (system) level in both ductile and non-ductile constructions. When adopting a local level approach, damage is analysed using demand values associated to the behaviour of structural members which also depend on the type of damage mechanism being analysed. If this damage mechanism is ductile, the most common approach is to check member chord rotation demands (EC8-3, 2005). In case the damage mechanism is brittle, the common approach is to check if member capacity in terms of shear strength is not exceeded by the corresponding demand. When using a global level approach, structural damage is usually correlated with peak values of interstorey drift ratios (e.g. see Ramirez and Miranda 2009, FEMA, 2012, D'Ayala et al., 2015 and references cited therein). However, the performance of buildings in previous earthquakes indicates that significant residual displacements may also occur. In particular, the amplitude of these residual displacements or interstorey drift ratios is seen to be critical for determining the technical and economic feasibility of repairing damaged structures. Often structures perform well in terms of preventing collapse, since they were able to remain standing after an earthquake. However, from a loss perspective, these structures

exhibit poor structural performance since their cost-efficient repair is not possible and they need to be demolished. The likelihood of experiencing residual deformations is seen to increase as the level of inelastic deformation increases (e.g. see Ramirez and Miranda, 2012 and references cited therein). This suggests that lateral force resisting systems that are capable of sustaining large lateral displacements and are designed just to avoid collapse are very likely to experience high levels of damage in the form of residual deformations when subjected to earthquake ground motions.

Several studies have proposed the explicit consideration of residual drifts in seismic performance-based assessment. For example, Christopoulos and Pampanin (2004) proposed the use of a residual deformation damage index, which is a non-dimensional parameter, ranging from 0 to 1 computed as a function of residual deformations in the structure. Uma et al. (2010) extended the performance matrix approach to compute a performance level as a function of the joint probability distribution of peak and residual deformations by defining a probabilistic seismic demand model that allows the estimation of experiencing a given combination of peak and residual deformation conditioned on the level of ground motion intensity. More recently, Ramirez and Miranda (2012) improved the Pacific Earthquake Engineering Research (PEER) Centre performance-based assessment methodology by explicitly accounting for residual deformations when computing the probability that a building may have to be demolished after an earthquake due to excessive damage. Their approach computes the economic loss conditioned on the level of ground motion intensity defined by the sum of three terms: losses resulting if the building collapses, losses associated with repairs given that the structure has not collapsed, and losses resulting from having to demolish the building given that is has experienced excessive residual drifts.

Aside from structural damage, modern earthquake-damage analysis approaches equally focus the quantification of damage to non-structural elements and to the contents of a construction. Non-structural elements can be divided into two categories (D'Ayala et al., 2015): elements that will contribute to the response of the structure under earthquakes (e.g. masonry infill walls for the case of reinforced concrete -RC-buildings) and elements that will not contribute to that response (e.g. plumbing fixtures, lighting and branch wiring, partitions, doors, windows). Elements of the first category need to be considered when developing the numerical model of the construction in order to obtain realistic results from the earthquake response analysis. However, both types of elements need to be considered in the damage analysis since both will play a significant role when assessing economic losses. A distinction between non-structural elements of the second category and construction contents can also be made using the definitions suggested by Porter et al. (2012): non-structural elements include equipment that is typically delivered by the general contractor with a new construction; contents are added by the owner or a vendor after construction is completed. Given the multitude of non-structural elements and of their characteristics, non-structural component-based damage (and loss) analyses require the use of common response measures in order to relate damage and earthquake demand. Currently, two demand parameters are found to be adequate to quantify non-structural damage (Ramirez and Miranda 2009; FEMA, 2012; D'Ayala et al., 2015): peak interstorey drift ratio and peak floor acceleration. Therefore, non-structural elements are categorized into drift-sensitive and acceleration-sensitive components, depending on which of the parameters induces damage. Given that structural damage is also primarily caused by peak interstorey drift ratios, earthquake-induced damage in a construction can be assigned to the three

following categories of elements: drift-sensitive structural elements, drift-sensitive non-structural elements, and acceleration sensitive non-structural elements.

4.3.2   METHODS OF ANALYSIS

Given that moderate- or large-intensity earthquake ground motions are expected to produce some damage to constructions, the corresponding structural demand is inherently expected to be nonlinear. As such, a nonlinear structural model is usually required to obtain a realistic representation of that demand and, consequently, of the damage to the construction. Still, under certain conditions, a linear (or an equivalent linear) elastic model can provide admissible results. If the level of ground shaking is expected to be low, or if the structure is extremely stiff and strong, it is possible to assume that structural demand will remain elastic and that structural deformation-based damage maybe irrelevant. On the other hand, damage related to brittle mechanisms may not be irrelevant (e.g. shear failure) and a different interpretation of the problem may also be required if non-structural damage is of concern.

The use of an equivalent linear SDOF model remains the main method for the design of structures where the seismic demand is estimated based on the response of a SDOF with an equivalent period based on the structure, and the seismic demand is reduced based on the ductility of the structure. The most widely used approach is the "equal displacement rule", typically for structures that have a moderate fundamental period of vibration (e.g. between 0.5s and 3s according to Newmark and Hall, 1982) and where the dynamic behaviour is largely governed by this fundamental mode of vibration, the inelastic peak displacement is assumed to be equal to that of an equivalent elastic structure with the same elastic vibration period. This assumption can also be applied to structural assessment. For example, this rule is the underlying assumption behind the criteria defined by EC8-3 (2005) to enable the use of static linear elastic analysis to perform the seismic safety assessment of existing buildings. Another equivalent linear SDOF approach is "displacement-based assessment" where the equivalent SDOF has a vibration period based on the secant-to-peak displacement stiffness of the structure, and an equivalent viscous damping based on the level of hysteretic energy dissipation (Priestley et al., 2007).

The inherent simplifications in the equivalent linear SDOF approaches mean that further assumptions are required to estimate the distribution of stresses and deformations within the structure, which is a non-trivial exercise, especially in the case of irregular structures. Therefore, the development of an inelastic model of the structure with an adequate level of detail is the most common choice to determine structural demand under any level of ground shaking with an acceptable level of realism, particularly if economic losses need to be derived from those damage levels. In light of this, a subsequent decision needs to be made regarding the type of analysis to be used: static or dynamic. This selection needs to be made by thinking about the type of data that is required in the subsequent stages where the seismic fragility analysis and the economic loss assessment are performed. These stages require structural response to be described not by a single value but by a distribution of values or by measures representing the central value of that distribution (e.g. a mean or a median) and its dispersion. Furthermore, these measures need to be obtained for several levels of seismic intensity. Given these constraints, to analyse a model and evaluate the distribution of its structural response in terms of a certain engineering demand parameter, for a given level

of the seismic intensity measure, the following three options can usually be established (D'Ayala et al., 2015):

- Nonlinear dynamic analysis: this type of analysis requires a set of ground motion records to perform dynamic response history analysis of a mathematical model (a 3D or a 2D model) representing the structure (and the non-structural elements that may influence structural behaviour). The subsequent repetition of this multi-ground motion analysis for several intensity levels in which the ground motion set is scaled to match those intensities is usually called an Incremental Dynamic Analysis - IDA (Vamvatsikos and Cornell, 2002).

- Nonlinear static analysis: this type of analysis is based on the use of a first-mode load pattern to perform a pushover analysis of a 3D/2D structure, and then fit the resulting capacity curve with an elastic-plastic, elastic-plastic with residual strength or a quadrilinear backbone curve response model. Structural demand can then be evaluated. The evaluation of seismic performance is then conducted using one of the following options:
  - Nonlinear static analysis with dispersion information: the procedure uses a set of ground motion records to estimate the distribution of the demand (see D'Ayala et al. (2015) for details)
  - Nonlinear static analysis without dispersion information: the procedure uses smoothed design response spectrum that only provide central values of the demand (see D'Ayala et al. (2015) for details).

Recently, Dolšek (2016) provided a review of analytical methods for seismic fragility analysis based on nonlinear static procedures. The fragility parameters are generally computed based on simulations which are used to account for the effects of record-to-record variability and modelling uncertainties (or other knowledge-based uncertainties). In order to account for the knowledge-based uncertainties, the pushover-based simulations can be performed at the level of MDOF model (e.g. Fragiadakis and Vamvatsikos 2010; Dolšek 2012) or by taking into account the variation of the force-displacement relationship of the SDOF model (Kosič et al., 2014). Many different simulation methods can be used to perform pushover analysis with consideration of knowledge-based uncertainties (e.g. Barbato et al., 2010; Jalayer et al., 2013). It is convenient and straightforward to utilize Monte Carlo simulation with Latin Hypercube Sampling (e.g. Dolšek 2009; Fragiadakis and Vamvatsikos 2010). However, all the referenced procedures are based on the simulations which are performed at the level of MDOF model either by conducting pushover or dynamic analysis. As an alternative, an approximate procedure utilizing the pushover analysis for the deterministic MDOF model and the uncertainty analysis at the level of SDOF model was recently proposed (Kosič et al., 2014). Such approach is computationally less demanding, since all the simulations are performed at the level so called probabilistic SDOF model. Therefore, it can be attractive for fragility analysis of a building stock. One of the simplest approaches for derivation of fragility curves based on pushover analysis is to combine the N2 method (e.g. Fajfar 2000), which is the most common approach in Europe for determination of expected seismic response based on pushover (implemented in Eurocode 8 (CEN 2004)), with default dispersions which account for record-to-record variability and modelling uncertainty. Such values were recently proposed for reinforced concrete frames based on an extensive numerical study (Kosič, Dolšek and Fajfar, 2016).

LIQUEFACT
Deliverable D3.1
State of the art review of numerical modelling strategies to simulate liquefaction-induced
structural damage and of uncertain/random factors on the behaviour of liquefiable soils
v. 1.0

Nonlinear dynamic analysis generally provides a more realistic representation of structural response to ground shaking. As such, it can provide a more reliable assessment of earthquake performance than nonlinear static analysis. Nonlinear static analysis cannot capture transient dynamic behaviour, and can struggle to estimate peak and residual deformations, especially when the structural elements degrade in strength and stiffness during loading. Nevertheless, nonlinear static analysis is less time-consuming, thus often more convenient, and can provide an adequate representation of structural response for structures whose dynamic response is mostly governed by the first-mode of vibration. In general, nonlinear static analysis provides adequate results for low-rise buildings (less than about eight storeys (Dolšek, 2016)) with symmetrical regular configurations. Further discussion on the advantages and disadvantages of both methods can be found in Deierlein et al. (2010).

4.3.3   CURRENT NONLINEAR MODELLING STRATEGIES

Inelastic models of structural elements are usually differentiated by how models are able to simulate the distribution of plasticity through the member cross sections and along its length. As such, two major categories of models are available for flexure-critical elements (i.e. elements where performance is expected to be governed by flexure-related conditions): concentrated plasticity models and distributed plasticity models. **Figure 4.13** presents five idealized models that fall into these categories and that are commonly used for simulating the inelastic response of structural members such as beams, columns, braces and some flexural walls. The main characteristics of each models are briefly summarized as follows (Deierlein et al., 2010):

- The simplest models concentrate inelastic deformations at the end of the element through a rigid-plastic hinge (**Figure 4.13a**) or an inelastic spring with hysteretic properties (**Figure 4.13b**). By concentrating the plasticity in zero-length hinges with a behaviour defined by a moment-rotation model, these elements exhibit condensed and numerically efficient formulations.

- Models with a finite length hinge (**Figure 4.13c**) provide an efficient distributed plasticity formulation with designated hinge zones at the member ends. The behaviour of cross sections in the inelastic hinge zones is usually defined through either nonlinear moment-curvature relationships or explicit fibre-section integrations. The inelastic hinge length can be fixed or variable, as determined from the moment-curvature characteristics of the section together with the concurrent moment gradient and axial force. Integration of deformations along the hinge length captures the spread of yielding more realistically than the concentrated hinges, while the finite hinge length facilitates the calculation of hinge rotations.

- Fibre formulation models (**Figure 4.13d**) distribute plasticity by numerical integrations through the member cross sections and along the member length. Uniaxial material models are defined to capture the nonlinear hysteretic axial stress-strain characteristics in the cross sections. The plane-sections-remain-plane assumption is enforced and uniaxial material "fibres" are numerically integrated over the cross section to obtain stress resultants (axial force and moments) and incremental moment-curvature and axial force-strain relations. The cross section parameters are then integrated numerically at discrete sections along the member length using displacement or

LIQUEFACT
Deliverable D3.1
State of the art review of numerical modelling strategies to simulate liquefaction-induced
structural damage and of uncertain/random factors on the behaviour of liquefiable soils
v. 1.0

This project has received funding from the European Union's Horizon 2020 research and innovation programme under grant agreement No. 700748

force interpolation functions. Distributed fibre formulations are usually not capable of reporting plastic hinge rotations; they instead report strains in the material fibres (e.g. in the steel and concrete fibres for the case of a RC cross section). These can be can be difficult to interpret relative to acceptance criteria that are typically reported in terms of hinge rotations and deformations.

- More complex models (**Figure 4.13e**) discretize the continuum along the member length and through the cross sections into small finite elements with nonlinear hysteretic constitutive properties that have numerous input parameters. This fundamental level of modelling is the most versatile, but it is also the most challenging in terms of model parameter calibration and computational resources. As with the fibre formulation, outputs are also defined in terms of strains in the materials and similar difficulties in the interpretation of the results apply.
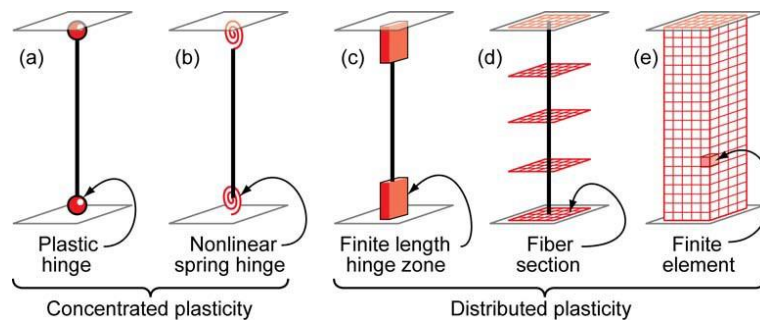
Figure 4.13: Idealized models of beam-column elements (adapted from Deierlein et al., 2010).

One key aspect of model selection for vertical elements such as columns is the ability to simulate axial force-moment interactions. Concentrated and finite length hinge models can account for this interaction through yield surfaces (e.g. see Deierlein et al., 2010 for additional details). On the other hand, fibre and finite element models are able to capture this interaction directly. While distributed plasticity models are able to simulate variations of the stress and strain through the section and along the member in more detail, important local behaviours, such as strength degradation or the nonlinear interaction of flexural and shear, are difficult to capture without sophisticated and numerically intensive models. On the other hand, phenomenological concentrated hinge/spring models may be better suited for capturing the nonlinear degrading response of members through calibration using member test data on phenomenological moment-rotations and hysteresis curves. Thus, when selecting a type of model, it is important to understand: (*i*) the expected behaviour, (*ii*) the assumptions, and (*iii*) the approximations inherent to the selected type of model. Further discussion on several aspects such as model sensitivity, parameter calibration for monotonic and cyclic loading, among others, can be found for example in Deierlein et al. (2010), Shoraka (2013), Huang and Kwon (2015), Hamburger et al. (2016) and references cited therein.

When dealing with non-ductile or low-ductility constructions, accounting for shear-critical elements (i.e. elements where performance is expected to be governed by shear-related conditions) is important due to the brittle nature of the mechanisms involved. Therefore, special models are required to account for the complex flexure–shear–axial interactions in shear-dominated elements. There are sophisticated models based on finite element discretization available to deal with these behaviour phenomena. However, such

models are numerically intensive and, therefore, difficult to use in the dynamic analysis of complete structures (Huang and Kwon, 2015). Therefore, more practical and efficient approaches using lumped plasticity, finite hinge length or fibre models combined with shear aggregated sections and lumped shear springs are usually considered (e.g. see Shoraka (2013), Huang and Kwon (2015) and references cited therein for a review of several of these models). To illustrate the characteristics of some of these models developed for the case of RC elements, **Table 4.3** summarizes the main features of the models analysed by Shoraka (2013). Given that non ductile columns are mainly susceptible to shear failure followed by axial failure, some of these models also include an additional lumped axial spring to capture axial failure.

As a result of inadequate structural detailing practices that are often found, modelling the behaviour of beam-column joints is also seen to be critical for predicting the earthquake response of RC non ductile structures. Among other aspects, many structures exhibit little or no transverse shear reinforcement within the beam-column joints, and the beam bottom reinforcement is often terminated within the beam-column joints with a short embedment length (Celik and Ellingwood, 2008). Therefore, in these structures, beam-column joint behaviour is governed by shear and bond-slip which requires additional modelling to capture the inadequate joint shear capacity resulting from a lack of transverse shear reinforcement and the insufficient positive beam bar anchorage. To address these issues, the modelling of beam-column joints has been receiving considerable attention and different models have been proposed to simulate their behaviour under cyclic loads (e.g. see the reviews in Celik and Ellingwood (2008), Sharma et al. (2011) and Shafaei et al. (2014)). A few of the more relevant modelling approaches are briefly summarized herein.

Alath and Kunnath (1995) modelled the joint shear deformation with a rotational spring model with degrading hysteresis. The finite size of the joint panel was taken into account by introducing rigid links. The envelope to the shear stress-strain relationship was determined empirically and the cyclic response was captured with a hysteretic model that was calibrated to experimental cyclic response. Biddah and Ghobarah (1999) modelled the joint shear and bond-slip deformations with separate rotational springs. The shear stress-strain relationship of the joint was simulated using a trilinear idealization based on a softening truss model, while the cyclic response of the joint was captured with a hysteresis relationship with no pinching effect. The bond-slip deformation was simulated with a bilinear model based on previous analytical and experimental data. The cyclic response of the bond-slip spring was captured with a hysteresis relationship that accounts for pinching effects. Youssef and Ghobarah (2001) proposed a joint element in which two diagonal translational springs connecting the opposite corners of the panel zone simulate the joint shear deformation; twelve translational springs located at the panel zone interface simulate all other modes of inelastic behaviour (e.g. bond-slip, concrete crushing) and elastic elements were used for the joining elements. This model requires a large number of translational springs and a separate constitutive model for each spring, which may not be available and restricts its applicability. Lowes and Altoontash (2003) proposed a four-node twelve-degree-of-freedom joint element. Eight zero-length translational springs simulate the bond–slip response of beam and column longitudinal reinforcement; a panel zone component with a zero-length rotational spring simulates the shear deformation of the joint; and four zero-length shear springs simulate the interface-shear deformations.

Table 4.3: Comparison of three models to simulate shear failure in non ductile columns (adapted from Shoraka, 2013).

	Model 1: Haselton et al. (2008)	**Model 2: Leborgne and Ghannoum (2009)**	**Model 3: Shoraka (2013)**
Failure types	Flexure, flexure–shear	Shear, flexure–shear	Shear, flexure–shear
Elements	Elastic beam–column element + zero-length flexural spring	3 nonlinear elements + zero-length springs	Nonlinear element + zero-length springs
Model description	The model provides regression-based equations that are used to estimate linear and nonlinear parameters of flexural springs based on column properties and loading conditions.	The shear spring model has the ability during analyses to monitor the deformations between two nodes bracketing the plastic hinge region and forces in the adjacent column element. The model compares the shear force in the column with a limiting shear force and the rotation of the plastic hinge region with a limiting rotation.	This model detects shear or flexure–shear failure based on shear strains in the plastic hinge zone of the columns element. The model can detect when shear capacity is sufficient and flexural deformations govern response; however, it does not currently capture flexural failures (i.e. degradation due to rebar buckling/fracture).
Cyclic modelling	Calibrated for the full cyclic behaviour, including in-cycle and cyclic degradation	The model can simulate the full degrading behaviour, including in- cycle and cyclic degradation.	The model can simulate the full degrading behaviour, including in-cycle and cyclic degradation; however, cyclic parameters are not calibrated.
Input by user vs. adaptive model	All model parameters are fixed by user input at the model building phase. Thus, the model does not adjust behaviour to varying boundary conditions during analysis.	The user can either input fixed values for rotation and shear-force limits or use the calibrated version of the model that automatically evaluates limits during analysis.	During analysis the model monitors column forces and deformation demands between integration points and adjusts the limit state that triggers strength degradation

The modified-compression field theory is used to define the envelope for the shear stress–strain relationship of the panel zone. The model, however, is not suitable for the analysis of the joints of non-ductile frames with no transverse reinforcement. Sharma et al. (2011) proposed a model where two shear springs in the column portion of the joint and a rotational spring in the beam region relate the panel joint deformation to the principal stress on which the joint failure criteria is based. However, this model is developed for bent-in deformed bars and it does not separate the shear joint deformation from the bond-slip effect. Metelli et al. (2015) developed a model where the total deformation of a beam-column joint is given by the sum of two contributions: the shear deformation of the panel zone and the rotation at the interface sections between the joint and the structural members converging in the joint, due to the slip of the reinforcing bars within the joint core.

As referred before, to obtain an adequate representation of the behaviour of constructions subjected to earthquakes, certain types of non-structural elements need to be considered in the nonlinear model. For the case of RC buildings, the more important of non-structural elements are masonry infill walls. Available numerical modelling approaches for masonry infills are normally divided into two categories: finite element (micro) models that use continuum elements and macro-models based on strut elements or other types of simplified structural element arrangements. Given that the first category of models is much more computationally demanding, its usage is restricted to the simulation of detailed but small-sized structures (e.g. one-bay-one-storey infilled frames) in order to validate a given constitutive model by attempting to replicate experimental results or to simulate detailed behaviour results that can then be used to calibrate a simpler mode of the second category (e.g. see Mohamed, 2017) and references cited therein). Given their numerical efficiency, models of the second category are generally used when simulating the nonlinear dynamic behaviour of full-size structures under earthquake loading. Macro-modelling approaches involving single strut or multi-strut models have been proposed to simulate the in-plane behaviour of masonry infills in framed structures since the 1950s. Reviews on the details of several macro-models and of their practical implementation can be found in (Asteris, et al., 2011; Catherin, et al., 2013; Tarque, et al., 2015; Buch and Bhat, 2015; Mohamed, 2017; Noh et al., 2017) and specific parameter calibration approaches proposed for several macro-models can also be found in (Mohamed, 2017). Aside from modelling the in-plane behaviour of masonry infills, the simulation of the out-of-plane behaviour has also been recently addressed by research due to the large levels of infill damage seen in recent earthquakes as a result of this type of behaviour. Still, the level of development of models accounting for the out-of-plane behaviour of infills is still far from that of in-plane models. Detailed reviews of existing models and discussions on the phenomena and challenges that are involved can be found in (Anić et al., 2017; Asteris et al., 2017; Zhai et al., 2017).

Finally, a further note is added regarding the modelling of viscous damping for nonlinear dynamic analysis under earthquake loading. Damping modelling is one of the several aspects of nonlinear structural modelling that remain challenging and unresolved. Chopra and McKenna (2016) and Luco and Lanzi (2017) provide detailed reviews and discussions on several damping formulations and aspects that need to be accounted for when modelling viscous damping, along with possible solutions for different types of problems.

4.4 FUTURE RESEARCH OPPORTUNITIES

- Robust methods have not yet been developed to quantify the level of strain hardening and the modifications to frequency content (e.g. acceleration spikes) of surface shaking on liquefied deposits.

- The influence of liquefaction-related modifications to ground shaking are not well understood in terms of how the affect the seismic performance of different buildings.

- The presence of the building influences the level of liquefaction and the amount of soil stiffness reduction, as well as causing wave reflections off the stiff foundation. These effects must be considered when estimating the surface input motion for the analysis of buildings.

- The influence of the timing of liquefaction on the performance of a buildings needs to be quantified, as the building can experience strong shaking before liquefaction occurs.

- A framework is needed for the considering benefits and side-effects of ground improvement methods

- Develop dynamic soil-foundation impedance terms that account for liquefaction at various depths and in the presence of buildings

- Quantify the nonlinear foundation rotation deformation in terms of a back-bone response for use in displacement- based design and assessment procedures

- Quantify the expected distribution of stresses within the structure in relation to the expected level of deformations in the foundation

- Determine the extent that horizontal variability in soil conditions could result in stress concentrations with the structure

- Quantify the influence of the cyclic vertical load from frame-action on the expected level settlement and changes in soil stiffness

- Develop a simplified procedure to account for the dramatic changes in soil stiffness that can occur during the shaking due to soil liquefaction

- Development of simplified numerical models to simulate the soil-foundation interface for liquefiable soils

- Develop simplified spectrum based approach to account for liquefaction in the seismic response of a structure

5. LIQUEFACTION EFFECTS ON OTHER CRITICAL INFRASTRUCTURE

5.1 EMBANKMENTS

5.1.1 PHENOMENA

During seismic shaking the general movement of an embankment is towards the free face or down the slope. The movement is driven by an in-balance of support force where the earth-pressure is less on the free face or downward slope, thus under cyclic loading the embankment more easily overcomes the static resistance in one direction and moves more in that direction. Cyclic loading, especially in the case of loose liquefiable soil deposits, can result in severe weakening of the soil and can trigger flow-like behaviour where the static shear stress caused by a free face or downward slope can result in large strains and contractive soil behaviour, eventually leading to a dramatic loss of soil shear strength. The behaviour under these conditions is extremely complex as the shear strains are very large and variable throughout the deposit, and some level of drainage, pore pressure dissipation and void redistribution can be expected (Kramer and Wang, 2015). Given these difficulties, the estimation of soil residual strength and embankment movements typically relies on case study data.

Earth structures such as highway and railway embankments can spread laterally and settle, resulting in opening of cracks in the road pavement or displacement of the railway tracks. The list of possible damage patterns is unlimited.

Therefore, as it is expressed by Pitilakis and Argyroudis (2014) in their synthesis of Syner-G project, classification of damage and the subsequent definition of specific damage states are important in the vulnerability assessment as the seismic intensity is correlated to the expected damage level through the fragility or vulnerability functions. Again, the form of the fragility functions depends on the typology of the element at risk. For common structures (e.g. buildings, bridges) and other not extended elements (e.g. cranes, tanks, substations), the fragility curves describe the response and damage level of particular subcomponents (e.g. columns, transformers) or of the entire structure. For linear elements of extended networks such as gas pipelines, the fragility functions describe the number of expected damages along a certain length (i.e. per km). Examples and further details are given in the next section.

5.1.2 MODELLING STRATEGIES

Methods for deriving fragility curves generally describe damages on a discrete damage scale. In the empirical procedures, the scale is used in survey efforts to produce post-earthquake damage statistics, and sometimes it is rather subjective (i.e. there is often a discrepancy between the damage levels that any two different inspectors would assign for the same incident). In analytical procedures the scale is related to the limit state of selected mechanical properties that are described by appropriate indices, such as the displacement capacity or the storey drift in the case of buildings or simple drift in pier bridges. For other elements at risk, the definition of the performance levels or the limit states may be more vague and follows

LIQUEFACT
Deliverable D3.1
State of the art review of numerical modelling strategies to simulate liquefaction-induced
structural damage and of uncertain/random factors on the behaviour of liquefiable soils
v. 1.0

other criteria related, for example, in the case of pipelines, to the limit strength characteristics of the material used in each typology.

The definition and consequently the selection of the damage thresholds, i.e. limit states, are among the main, yet, unavoidable sources of uncertainties (Pitilakis and Argyroudis, 2014). The authors refer that (quoting), an important issue related to the fragility curve construction and implicitly to the risk assessment is the selection of an appropriate earthquake intensity measure (IM) that characterizes the strong ground motion that best correlates with the response of each element, for example, building, pipeline, or harbour facilities like cranes. Several measures of the intensity of ground motion (IMs) have been developed. Each intensity measure may describe different characteristics of the motion, some of which may be more adverse for the structure or the system under consideration. The use of a particular IM in seismic risk analysis should be guided by the extent to which the measure corresponds to damage to the components of a system. Optimum intensity measures are defined in terms of practicality, effectiveness, efficiency, sufficiency, robustness, and computability (Mackie and Stojadinovic 2003).

In general, IMs are grouped in two general classes: empirical intensity measures and instrumental intensity measures. With regard to the empirical IMs, different macroseismic intensity scales could be used to identify the observed effects of ground shaking over a limited area. Instrumental IMs are, by far, more accurate and representative of the seismic intensity characteristics and the severity of ground shaking. For example, for bridges the spectral response value at a specific period (i.e. T ¼ 1.0 s) is typically used. For other lifeline components, it may be the peak ground acceleration (e.g. buildings, tanks, electric power substations), peak ground velocity (e.g. pipelines), or even the permanent ground deformations (e.g. pipes, embankments, roadways, railways). The correlation between damages of specific elements at risk and intensity measures is not simple and never unique. Several other descriptors like peak ground strain, Arias intensity, cumulative absolute velocity, and other parameters of the ground motion have been also used for different structures composing a lifeline system.

Giving an insight to this problem, the same authors state that there is a trend to use two descriptors instead of one, and hence the fragility curve is transformed in fragility surfaces (Seyedi et al., 2010; Douglas et al., 2014).

The selection of the adequate intensity parameter is also related to the approach that is followed for the derivation of fragility curves and the typology of elements at risk. The identification of the proper IM is determined from different constraints, which are first of all related to the adopted hazard model, but also to the element at risk under consideration and the availability of data and fragility.

5.2 PIPELINES

5.2.1 PHENOMENA

The occurrence of large displacement amplitudes in surface soils during strong ground shaking is caused by the occasional fractured and buckled pavements as well as heavily damaged water supply and sewage

LIQUEFACT
Deliverable D3.1
State of the art review of numerical modelling strategies to simulate liquefaction-induced
structural damage and of uncertain/random factors on the behaviour of liquefiable soils
v. 1.0

This project has received funding from the European Union's Horizon 2020 research and innovation programme under grant agreement No. 700748

systems as observed in the central zone of Adapazari (Bakir et al., 2002, Yoshida et al., 2001, Toprak and Taskin, 2007).

As expressed in Pitilakis and Argyroudis (2014), lifelines (or, sometimes, referred as critical infrastructures) may be distinguished in two major categories: (i) utility systems including potable water, natural gas, oil, electric power distribution, wastewater, or communication systems and; (ii) transportation systems comprising roadways, railways, airport, and port facilities. Sometimes the terms infrastructures or critical facilities are used instead, at least for some of them.

Compared to buildings, addressed specifically in the previous sections, lifeline systems present three distinctive features: (a) higher spatial variability and topology and exposure to different geological and geotechnical hazards; (b) eventually wide, but certainly different, variety of component typologies and materials used; and, (c) specific functionality requirements, which make them, eventually more, dependent to highly hierarchical networks. The referred authors, as well as the works of Pitilakis et al. (2014a. 2014b), present an overall synthesis of SYNER-G project (http://www.vce.at/SYNER-G/) where they discuss the vulnerability assessment of the two big classes, links (e.g. pipelines, roads) and nodes (e.g. tanks, power substations), concluding that an important parameter is the presence of synergies between components within the same system (intra-dependencies) or between different systems (interdependencies). In their conclusions, "the physical damage of a component of a system interacting with another one may affect seriously the second system's performance and functionality. Therefore, it is essential to define the taxonomy of each interacting lifeline system that describes the individual components of each system and their role in the network as well as the way other systems affect its performance" (sic).

Finally, Pitilakis and Argyroudis (2014) address the variability of seismic ground motions due to spatial extent of lifeline systems and to geotechnical hazards, with significant differences in permanent ground deformations, resulted from fault crossing, landslides, and liquefaction (e.g. lateral spreading, settlements, buoyancy effects).

One of the important learnings from the recent earthquakes is that some earthquake resistant design methods and technologies prove to be working. Data from literature was presented to show the repair rate versus lateral strain for different pipelines (Toprak et al., 2015).

The behaviour of buried pipelines under earthquake action can depend in general on very different factors: intensity measure of the earthquake (either acceleration, velocity or displacement); type of the travelling waves (e.g. P-, S-, R-waves …) (Newmark, 1967; Newmark and Rosenblueth, 1971; St. John and Zahrah, 1987; Hashash et al., 2001); ground conditions (Kachadoorian, 1976); pipe material, strength and ductility, thickness, diameter, operational pressure, type of connection and conditions (age, state of corrosion, past damages …)(Wengstrom, 1993; Ballantyne, 1995; O'Rourke and Liu, 1999).

Past earthquakes have shown that the main cause of damage to buried pipelines is due to permanent ground deformations, PGD (i.e. faulting, landslides or liquefaction) (Eguchi, 1987; Hall, 1987), whilst a few earthquakes have induced damages to pipelines only by the effect of seismic wave propagation

LIQUEFACT
Deliverable D3.1
State of the art review of numerical modelling strategies to simulate liquefaction-induced
structural damage and of uncertain/random factors on the behaviour of liquefiable soils
v. 1.0

(O'Rourke and Ayala; 1990), mainly to pipelines that were previously weakened either by corrosion or welds of poor quality (EERI, 1986).

Liquefaction can damage pipelines both as a vertical settlement and as a lateral spread or a combination of the two phenomena. The orientation of the pipe relative to the ground movement can affect the amount of damage (O'Rourke and Nordberg, 1990; O'Rourke et al., 2012, 2014; McLachlan et al., 2013).

As an example of a EILD due to the failure of critical infrastructures was the 2010–2011 Canterbury Earthquake Sequence (CES), in New Zealand, that caused unprecedented damage in the city of Christchurch and the largest number of fatalities since the 1931 Hawkes Bay (Napier) earthquake (Bouziou and O'Rourke, 2017). In Christchurch CES (the 2010 Mw7.1 followed by the 2011 - 3 June 2011 and 23 December 2011, MW6.3 - earthquakes and numerous aftershocks) a great number of ground and slope failures, mainly due to liquefaction, produced extensive damages to the water, electricity, and road networks rendering many of them inoperable (O'Rourke et al., 2012, 2014), while the gas system performed rather well.

Bouziou and O'Rourke (2017) present the areas of liquefaction effects presented in **Figure 5.1**, derived from maps of observed liquefaction effects that were documented through aerial photography and site observations, and are available through the Canterbury Geotechnical Database (CGF, 2012).
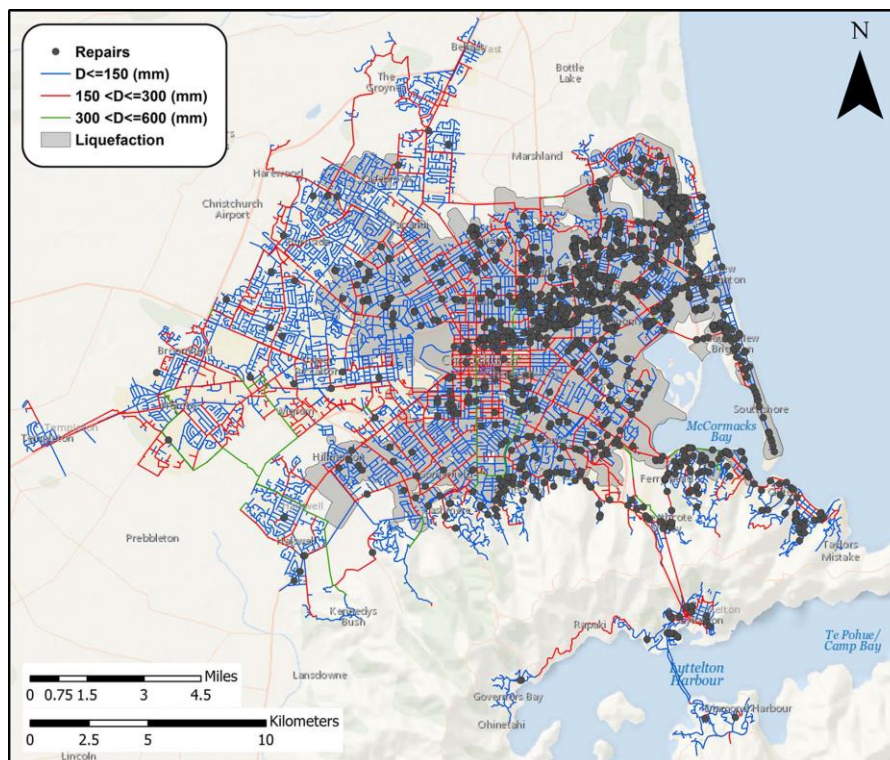

Figure 5.1: Map of Christchurch water distribution system, 22Feb.2011 earthquake (CGD, 2013)

Bouziou and O'Rourke (2017) identify a criterion to define the areas of observed liquefaction through visible surface features and, therefore, they were expanded to account for a zone of influence at their perimeter that affects underground pipelines, being described in that paper as areas of liquefaction effects. The ground motion records related to the 22 Feb. 2011 earthquake from 40 stations in the Christchurch area were selected for spatial analysis and the selected records were fully processed by to provide acceleration, velocity, and displacement time histories and response spectra. Airborne Light Detection and Ranging (LiDAR) data were obtained by AAM Brisbane (AAM) and New Zealand Aerial Mapping (NZAM), before and after each of the main seismic events during the CES, allowing for the determination of horizontal and vertical ground movements, which were then used to develop grids of differential vertical and horizontal ground movement (details in article).

Using the data sets described above, the spatial distribution of damage in the water distribution system during the 22 Feb. 2011 earthquake was quantified, "pertaining to pipeline length, repairs, and RRs for asbestos cement (AC), cast iron (CI), polyvinyl chloride (PVC), and modified polyvinyl chloride (MPVC) pipelines in the water distribution system, including locations inside and outside areas of liquefaction effects" (quoting Bouziou and O'Rourke, 2017). An extensive evaluation of the damages in the pipes, within the areas of liquefaction effects, with respect to the total length of each pipe type was done, using normalized indicators for comparison of the vulnerability of different pipe types relative to their total length. The screening criteria developed by O'Rourke et al. (2014) was used during the regression analysis of pipeline damage to ensure fidelity of the Repair Rates (RR) correlations with the geometric mean peak ground velocity (GMPGV). In fact, the performance of the Christchurch water distribution system in areas affected by transient ground deformations (TGD), during the 22 February 2011 earthquake was evaluated through correlations of pipeline damage with earthquake ground motions. The peak ground velocity (PGV) horizontal orthogonal components that were processed by GNS Science (CERA, 2012) were used to calculate the GMPGV sample values that were introduced in the geostatistical model.

Measurements of ground surface elevation before and after each earthquake during the CES were acquired through high resolution airborne LiDAR surveys. The differential vertical ground surface movements associated with PGD effects during the 22 February 2011 earthquake were used to calculate angular distortion, β, and evaluate the effects of differential vertical ground movement on pipeline damage. Similar to vertical ground movements, lateral ground surface movements were calculated both for individual seismic events as well as for sets of consecutive earthquakes using pairs of LiDAR point clouds.

The combined effects of lateral ground strain and vertical differential ground movement on pipeline damage were evaluated using an approach similar to that developed by Boscardin and Cording (1989) for ground movement effects on buildings.

The Christchurch data for repair rate (RR) vs GMPGV, as presented by Bouziou and O'Rourke (2017), provide improved regressions for future fragility analyses of water distribution pipeline performance during earthquakes and expand the database of historical data.

5.2.2 MODELLING STRATEGIES

The liquefaction effect is typically included in damage analysis of buried pipelines evaluating first the probability that a specific site will liquefy and then the amount of permanent ground deformation (PGD) expected at the site.

When the vulnerability of elements due to ground failure is examined (i.e. liquefaction, fault rupture, landslides), permanent ground deformation (PGD) is the most appropriate Intensity Measure (IM). The consideration of hazard from PGD is essential in modelling the seismic risk to lifeline systems. For pipelines and similar systems with linear elements, fragility models are generally given in terms of PGD (Pitilakis and Argyroudis, 2014), as they are mostly vulnerable to permanent displacement of the ground rather than transient shaking. Four primary causes of permanent ground displacements are commonly considered: liquefaction-induced lateral spread, liquefaction-induced settlement, slope displacement, and co-seismic fault rupture. In addition to strong shaking, another transient effect that poses a potential risk to lifeline systems is the transient ground strain (PGS).

Several models are available for the estimation of PGD; some of them are intended to relate the degree of deformation and the probability of the geotechnical hazard occurring to the intensity of the ground motion (Weatherill et al., 2014). However, it should be noted that most theoretical and empirical models relating PGD to strong shaking require a level of geotechnical detail that may be impractical to obtain for a spatially distributed set of sites. HAZUS methodology (FEMA 2003) provides a rather simple "baseline" model that can be implemented in the widest variety of applications.

The preferred approach for the definition of pipeline damage functions is based on the use of empirical data and the outcome is generally expressed in terms of repair rate (i.e. the number of repairs per unit length of the pipe). A database of observed damages to buried pipelines from past earthquakes is provided by ALA (2001), including 41 data points from 4 earthquakes (one Japanese and three U.S.), with liquefaction as the main failure mechanism.

Data about the liquefaction impact on pipelines during the 1999 Izmit earthquake can be found in Toprak (1998) and Tromans (2004). Several correlations are given in Toprak and Taskin (2007) regarding the pipeline damage estimation correlations for ground shaking effects. Peak ground velocity versus repair rate relationships are presented.

Data and assessment procedures for the evaluation of the liquefaction impacts on pipe networks at Christchurch during the 2010-2011 earthquakes can be found in Cubrinovski et al (2011), O'Rourke et al., (2014).

Documents from the American Lifeline Alliance (ALA, 2001), HAZUS (NIBS, 2004) and SYNER-G summarize the state-of-art of the recent formulations for seismic fragility curves to be used with the most common types of buried pipelines.

6. ASSESSING PERFORMANCE

6.1 PERFORMANCE LEVELS

6.1.1 DAMAGE LEVELS – LIMIT STATES

In earthquake loss assessment models that do not account for damage induced by phenomena related to soil failure, performance levels connected to damage or non-structural damage are usually established using response parameters relating to structural deformations. As mentioned in Section 4.3.1, structural damage, and consequently performance levels, can be established at the local (member) level or at the global (system) level. Local level performance can be measured using material-level stress or strain values that can be matched with damage states (e.g. see the discussion and proposals by Priestley (1997), Calvi (1999) and Crowley et al. (2004), among others). Alternatively, and currently a more common approach, local level performance can be defined using member response parameters such as chord rotation limit values and shear strength (e.g. see FIB, 2003a, b; EC8-3, 2005; and the more recent proposals by Grammatikou et al., 2015, 2016, 2017a, b). When using a global level approach, structural damage, and consequently performance levels, can usually be correlated with limit values of interstorey drift ratios (e.g. see Ramirez and Miranda, 2009; FEMA, 2012; D'Ayala et al., 2015 and references cited therein). More recently, performance-based assessment methodologies have started to account also for residual deformations when computing the probability that a building may have to be demolished after an earthquake due to excessive damage. As such, performance levels defined in terms of maximum admissible residual interstorey drifts are also available (e.g. see FEMA, 2012). With respect to non-structural damage, the common approach, as referred in Section 4.3.1, is to use peak interstorey drifts and peak floor accelerations to measure damage in non-structural elements. These are categorized as drift-sensitive or acceleration-sensitive components, depending on which of the parameters induces damage. As such, limit values of these parameters defining performance levels commonly considered in existing earthquake loss assessment models are also available (e.g. see FEMA, 2012; Porter et al., 2014; D'Ayala et al., 2015 and references cited therein).

When trying to account for damage induced by liquefaction in the definition of performance levels, it can be seen that available research and collected data on this matter are relatively scarce. In fact, building failure as a result of tilting, settlement or differential settlements is not common since excessive foundation settlement is often regarded as a serviceability problem and large values of tilt and rigid body rotation may not lead to building collapse. In cases where there is no or only minor structural damage, non-structural damage may be relevant in terms of losses and future use of the building. According to Negulescu and Foerster (2010), usual consequences of differential settlements are cracking of structural or architectural elements, uneven floors, or inoperable windows and doors, which are relevant damages for earthquake loss assessment. Furthermore, in extreme cases of tilting, the building may have to be considered fully damaged since it may only be suitable for demolition. Structural and non-structural damage resulting from differential settlements and tilting must therefore be correlated with (local or global) response parameters commonly considered when measuring earthquake demand to create new or integrate existing

LIQUEFACT
Deliverable D3.1
State of the art review of numerical modelling strategies to simulate liquefaction-induced
structural damage and of uncertain/random factors on the behaviour of liquefiable soils
v. 1.0

performance levels that will be used in a loss assessment framework. Existing proposals of performance levels accounting for soil failure that follow this line of reasoning are briefly reviewed in the following.

Bird et al. (2006) proposes a set of performance levels connecting commonly used structural damage states with limit values of rigid body settlement and rotation due to earthquake-induced ground deformations beneath RC buildings (**Table 6.1** and **Table 6.2**). Recently, Yasuda (2014) presented a set of performance levels in terms of maximum admissible levels of tilt and settlement to analyse the level of damage in buildings that occurred as a result of liquefaction during the 2011 earthquake in Japan (**Table 6.3**). Even though these limits were not defined for applications in earthquake loss assessment frameworks, it might be possible to establish them in a more suitable performance level format if more detailed descriptions of the global damage to the buildings where liquefaction damage was found can be obtained from that event. Interestingly, Tani et al. (2015) also presented a set of performance levels from the 2011 Japan earthquake that are connected to the likelihood of building occupants to develop health problems. These performance levels are presented in **Table 6.4** and correlate the tilt angle of houses with different health problems. Ways to integrate this information in existing earthquake loss assessment frameworks should also be pursued.

Table 6.1: Performance levels for rigid body settlement and rotation due to earthquake-induced ground deformations beneath RC frame buildings

Damage state	Structural damage	Additional description (rigid body deformation)	Settlement (S) only	Rotation (θ) only
Slight	Hairline cracks only	Repairs may be necessary for aesthetic reasons	$S \leq 0.1$m	$\theta \leq 0.6°$ 1/100
Moderate	Some cracks in load-bearing	Repairable damage, serviceability and/or functionality affected	0.1m $< S < 0.3$m	$0.6° < \theta \leq 2.3°$ 1/100-1/25
Extensive	Wide cracks and buckling of longitudinal reinforcement	Uninhabitable, but repairable	0.3m $< S \leq 1.0$ m	$2.3° < \theta \leq 4.6°$ 1/25 – 1/12.5
Complete	Repair not feasible, shear failures or excessive displacement	Demolition cheaper than repair. Structural integrity affected, possible instability	$S \geq 1.0$m	$\theta \geq 4.6°$ $\geq 1/12.5$

Table 6.2: Structural damage states associated to the performance levels of Table 6.1 based the proposal by Crowley et al. (2004)

Structural damage band	Description
None to slight	Linear elastic response, flexural or shear type hairline cracks (<1.0 mm) in some members, no yielding in any critical section
Moderate	Member flexural strengths achieved, limited ductility developed, crack widths reach 1.0 mm, initiation of concrete spalling
Extensive	Significant repair required to building, wide flexural or shear cracks, buckling of longitudinal reinforcement may occur
Complete	Repair of building not feasible either physically or economically, demolition after earthquake required, could be due to shear failure of vertical elements or excessive displacement

Table 6.3: Performance levels in terms of maximum admissible levels of tilt and settlement considered to analyse the level of liquefaction-induced damage to buildings that occurred during the 2011 earthquake in Japan

Global damage to the building	Type of liquefaction-induced damage	
	Tilt	Settlement
Completely destroyed	More than 1/20	More than 1.0m
Large-scale partially destroyed	1/60 to 1/20	Between 0.25 to 1.0 m
Partially destroyed	1/100 to 1/60	Up to 0.25 m

Table 6.4: Performance levels relating the tilt angle of houses and health problems

Tilt angles of houses	Health problems
5/1000	Feeling of tilting
6/1000	Feeling of differential settlement
8/1000	Strong feeling of tilting, Frequent complaints
10/1000	Need to level a floor
16.7/1000	Feeling of heaviness in head and loss of balance
33.3–50/1000	Serious disorder of dizziness, headache, nausea and anorexia
66.7–100/1000	Serious disorder of fatigue and sleep

Several studies have also proposed performance levels that were not specifically developed for liquefaction-induced damage but address some of the types of damage that occur due to liquefaction. For example, Negulescu and Foerster (2010) proposed a set of performance levels connecting expected limit values of differential settlements to limit values of strain in the concrete and steel elements of RC structures that are defined for different structural damage states. The differential settlement performance levels were defined based on the numerical analysis of simple one-bay-one-storey RC frames subjected to differential settlements, using 2D parametric nonlinear static analyses. Their analyses include the uncertainty about the type of foundation of the structure, the type of structural properties of the structural elements, the inclination angle of the settlement and the magnitude of the settlement displacement. This research was limited to low rise structures given it assumes that building height is not a critical parameter to assess building response due to ground failure, as proposed by Koutsourelakis et al. (2002). The analyses also assumed that differential settlements are transmitted directly to the building, without any interaction between the soil and the structure, using a displacement imposed at the base of the building column. According to the authors, this methodology is commonly used in practice to assess the response of a flexible structure with respect to ground movements (e.g. see (Deck et al., 2003)). The damage states considered by Negulescu and Foerster (2010) are defined in **Table 6.5** as a function of the limit values of material strains (concrete and steel). The performance levels connected to these damage states that were obtained in terms of admissible differential settlements are presented in **Table 6.6**. These performance levels are defined for each damage state by a median value α_k and by a standard deviation of the log of the data β_k.

Table 6.5: Limit strain states proposed for the reinforcement and the concrete by Negulescu and Foerster (2010).

Limit state	Damage definition	Limit strains	
		Steel	Concrete
LS1	Slight	0.002	0.002
LS2	Moderate	0.015	0.004
LS3	Extensive	0.040	>0.006
LS4	Complete	0.060	-

Table 6.6: Median and standard deviation of the performance levels associated to the four limit states proposed by Negulescu and Foerster (2010).

Limit State	Damage definition	Mean α_k (cm)	Standard deviation β_k
LS1	Slight	5	0.5
LS2	Moderate	12	0.5
LS3	Extensive	27	0.5
LS4	Complete	40	0.5

Research on the role of horizontal and vertical ground displacements in structural damage has also been analysed in other contexts (e.g. when analysing the effects of opencutting and tunnelling on constructions nearby). This type of research has also led to the development of performance levels but their outputs are usually defined in terms of horizontal strains in the soil which are then correlated with global deformation measures of the building such as angular distortion and qualitative descriptions of structural damage in the building. The outputs of a few relevant studies are presented herein nonetheless for completeness. A relevant example of this type of study was presented by Boscardin and Cording (1989) where simplified numerical models of buildings were used to develop a method estimating building response when subjected to horizontal ground strains. This research defined damage categories as a function of the relation between the horizontal strain ε_h and the angular distortion β. **Table 6.7** shows the proposal made by Boscardin and Cording (1989) which was later updated by Son and Cording (2005) using a relation between limiting tensile strain ε_{lim} and the damage categories. Boscardin and Cording (1989) also developed a chart relating angular distortion and horizontal strains to levels of damage for buildings with equal length to height ratio. An alternative chart that relates lateral strain and deflection ratio (instead of angular distortion) to the levels of damage was later proposed by Burland (1995). Finally, a more recent study proposed by Zhang and Ng (2007) developed performance levels for foundation design in the form of probability distributions of limiting tolerable displacements using data from 380 buildings. The buildings were divided according to four criteria (soil type, foundation type, structural type and building usage) and their observed performance led to the development of statistics for the limiting tolerable settlement and angular distortion.

LIQUEFACT
Deliverable D3.1
State of the art review of numerical modelling strategies to simulate liquefaction-induced
structural damage and of uncertain/random factors on the behaviour of liquefiable soils
v. 1.0

Table 6.7: Performance levels relating horizontal strains in the soil to qualitative descriptions of structural damage in the buildings as proposed by different methods.

Category of damage	Boscardin and Cording (1989)		Burland (1995)	Son and Cording (2005)a
	β (×10−3)	ε_h (%)	ε_{lim} (%)	ε_{crt} (%)
Negligible	0–1.1	0–0.05	0–0.05	0–0.05
Very slight	1.1–1.6	0.05–0.075	0.05–0.075	0.05–0.075
Slight	1.6–3.3	0.075–0.15	0.075–0.15	0.075–0.167
Moderate to severe	3.3–6.7	0.15–0.3	0.15–0.3	0.167–0.333
Severe to very severe	>6.7	>0.3	>0.3	>0.333

6.2   LOSS MODELS

Earthquake loss models for single assets involve two major components: seismic hazard (the probability of levels of ground shaking resulting from earthquakes, within a given time span) and vulnerability (defined as the probability of loss given a level of ground shaking for the case of physical vulnerability). Physical vulnerability functions are then functions that describe the probability distribution of loss (or loss ratio) due to structural or non-structural damage for increasing levels of the selected earthquake intensity measure. Loss might refer to repair costs or loss of life while a loss ratio might refer to the ratio of repair cost to replacement cost, or the ratio of number of fatalities to the number of occupants of the construction. Vulnerability functions can be derived directly, usually using empirical methods where losses from past events at given locations are related to the levels of ground motion intensity observed at those locations, directly using analytical methods or they can be derived indirectly by combining fragility functions and consequence (or damage to loss) functions. The last two approaches are the methods focussed herein given the scope of the report and the fact that empirical vulnerability functions explicitly accounting for liquefaction-induced damage have not been found in the available literature. Given that liquefaction-induced loss of life has not been frequent observed (Daniell et al., 2017), the following review is focussed on losses defined as repair costs or loss ratios.

A fragility function describes the probability of exceeding a given limit state (or performance level) for increasing levels of the selected earthquake intensity measure. A limit state (or performance level) defines the threshold value of a certain structural demand parameter (at the member-level or at the global level) that corresponds to a certain damage or injury level. Fragility functions can be derived by expert-opinion, empirically (using observed data), or analytically by performing numerical simulations of the behaviour of a given construction when subjected to increasing levels of ground motions. Recent research on this subject includes the work of Maurer et al. (2017) who developed empirical fragility functions for general infrastructures after analysing nearly 10000 liquefaction case histories from 23 global earthquakes. The proposed fragility functions express the probability of exceeding severities of liquefaction surface manifestation as a function of three different liquefaction damage measures. Given that damage is

LIQUEFACT
Deliverable D3.1
State of the art review of numerical modelling strategies to simulate liquefaction-induced
structural damage and of uncertain/random factors on the behaviour of liquefiable soils
v. 1.0

established in a format connected to ground damage (namely the extent and the severity of liquefaction ejecta), these fragility functions are difficult to use in frameworks that are designed to accommodate limit states connected to structural behaviour. The outcomes of the SYNER-G research project also analyse the development of fragility functions for different types of structures and infrastructures but, for most of these assets, liquefaction-induced damage is not explicitly accounted for (Pitilakis et al 2014). Exception is made for the case of bridges by reporting the studies of:

- Zhang et al. (2008) that developed fragility curves for typical bridges in California considering liquefaction by performing equivalent static analysis. In these analyses, lateral spreading of the soil was simulated by imposing displacements on the free edges of springs connected to the foundation elements of the model. The variability of the soil properties and the soil layer depth was also included in the analyses.

- Kwon et al. (2009) that studied a two-span bridge with monolithic deck-pier connection. The effect of liquefaction was accounted for by reducing the seismic forces on the bridge and consequently the fragility, particularly for higher damage levels. The probability of damage was further reduced when liquefaction was considered at all supports instead of only at the base of the central column.

- Aygun et al. (2011) performed time-history analyses of bridge-soil systems, where a 3D model of a continuous bridge with the deck connected to the piers through fixed bearings was combined with 2D soil elements and 1D springs for the soil-pile interaction. By accounting for the variability of the geometry, materials and soil properties, component fragility curves were produced for a suite of synthetic accelerograms. Liquefaction resulted in higher dispersion of the seismic demand. It affected mostly the fragility of piers and piles and to a lesser extent that of bearings and abutments. Because of larger displacements, bearings showed higher probability of damage due to liquefaction. On the other hand, the effect on piers and piles depended on the local soil conditions.

And for the case of quay walls from harbours by reporting the studies of:

- Ichii (2003, 2004) that developed fragility curves using simplified dynamic finite element analysis that considered the occurrence of liquefaction.

- Na et al. (2009) that developed fragility curves using effective stress analysis and nonlinear time history analysis that considered liquefaction and lateral spreading in the backfill and sand layers, as well as uncertainty in the soil parameters.

- Na and Shinozuka (2009) and Na et al. (2008) that developed fragility curves using nonlinear time history analysis and an effective stress analysis to consider the occurrence of liquefaction phenomena.

For the case of buildings, Bird et al. (2006) proposed a framework to develop fragility functions that include the influence of liquefaction-induced damage. The proposed framework accounts for the two following scenarios:

LIQUEFACT
Deliverable D3.1
State of the art review of numerical modelling strategies to simulate liquefaction-induced
structural damage and of uncertain/random factors on the behaviour of liquefiable soils
v. 1.0

- Liquefaction and ground-shaking hazard are independent: in this case a building has a probability $P(X)$ of being affected by liquefaction and a probability of $1 - P(X)$ of being damaged by ground shaking. The final damage distribution can therefore be estimated as in **Equation (22)**, where DS stands for the damage state (e.g. slight, moderate, extensive or complete) and L stands for liquefaction.

$$P(\text{DS}) = P(\text{L})P(\text{DS}|\text{Liquefaction}) + (1 - P(\text{L}))P(\text{DS}|\text{Shaking}) \tag{22}$$

- Liquefaction and ground-shaking hazard do not interact: in this case a building has a final damage state that is a function of both the initial damage caused by ground shaking and any subsequent damage caused by liquefaction. In this case the final damage distribution is determined as in **Equation (23)**:

$$P(\text{DS}) = P(\text{L})P(\text{DS}|\text{Shaking plus Liquefaction}) + (1 - P(\text{L}))P(\text{DS}|\text{Shaking only}) \tag{23}$$

In this scenario, the strong ground shaking causes an initial state of damage (assumed to be less than collapse) and the subsequent deformation caused by liquefaction induces further damage, either by increasing the deformation of the columns or by causing the damaged building to settle and rotate. The final damage state is thus a function of the damage state reached at the onset of liquefaction. This scenario assumes that, irrespective of the damage of the building induced by the ground shaking only, if liquefaction occurs, the final damage of the building is the result of adding the damage due to the ground motion and the damage induced by liquefaction. Therefore, this scenario assumes the damage due to ground shaking is independent of the damage due to liquefaction.

It should be noted that, according to results by Borozan (2017), this assumption of damage independence is expected to be inadequate in most cases. Still, it is also noted that the HAZUS methodology for multi-hazard loss assessment (NIBS, 2015) also assumes that, when developing earthquake fragility functions, the damage due to ground shaking is independent of the damage due to liquefaction.

A final reference is made to the research by Negulescu and Foerster (2010) who developed fragility curves for simple one-bay-one-storey RC frames subjected to differential settlements, using 2D parametric nonlinear static analyses. Even though their work is not exactly focussed on liquefaction-induced damage, they address one of the damage sources due to liquefaction. Their analyses include the uncertainty about the type of foundation of the structure, the type of structural properties of the structural elements, the inclination angle of the settlement and the magnitude of the settlement displacement. The fragility curves that are proposed are assumed to be defined by a lognormal distribution whose parameters were fitted using the data from the analyses for four different limit states. These limit states were defined in terms of expected values of the differential settlements that are connected to limit values of strain in the concrete

LIQUEFACT
Deliverable D3.1
State of the art review of numerical modelling strategies to simulate liquefaction-induced
structural damage and of uncertain/random factors on the behaviour of liquefiable soils
v. 1.0

and steel elements of the structure. In the overall, it can be seen that available fragility functions addressing ground failure are limited and aspects such as liquefaction-induced damage should be further investigated.

A final note is added regarding scenarios that do not account for liquefaction-induced damage. For this type of case, the capacity to develop analytical fragility functions (i.e. those that involve numerical simulations) is currently well developed. The level of detail and accuracy that is required for a given fragility function can be directly related to the type of analysis that is performed and to the level of detail/completeness of the numerical model representing the construction (e.g. see details in Sections 4.3.2 and 4.3.3 and in D'Ayala et al., 2015). In most cases, the fragility function is obtained fitting a parametric distribution model to the simulated fragility data (i.e. the data that define the probability of the response parameter exceeding the limit state value for each earthquake intensity level when using a stripe-based approach or the ground motion intensity values that correspond to the occurrence of the limit state when using an IM-based approach). The lognormal distribution is normally the selected distribution model even though, in some cases, the fitting could be improved by selecting alternative distributions. Additionally, for the use of empirical fragility functions, reference is made to the work by Rossetto et al. (2013) which provides an extensive review of existing empirical fragility (and vulnerability) functions worldwide in terms of their characteristics, data, sources and statistical modelling techniques. The report also provides a qualitative rating system that is described and applied to all the reviewed functions to aid users to choose between existing functions for use in seismic risk assessments.

With respect to consequence functions, these are used to derive the probability distribution of loss for a given performance level, and they are generally derived empirically or through expert opinion. Even though extensive liquefaction-induced damage data has been collected form recent earthquakes (e.g. Christchurch in 2010 and 2011 and from Japan in 2011) no consequence model explicitly accounting for liquefaction-induced damage have not been found in the available literature. An ongoing effort that is expected to account for liquefaction-induced losses is the GEM Global Earthquake Consequences Database (GEMECD) by the GEM Foundation. This initiative has the purpose of informing researchers on consequences from past earthquakes, providing a benchmarking tool for analytical loss models and to support the development of tools to create vulnerability data appropriate to specific countries, structures, or building classes. A detailed review of this initiative can be found in (So, 2014). For scenarios that do not account for liquefaction-induced damage, consequence functions are provided in (D'Ayala et al., 2015) for different types of buildings. To transform fragility functions into vulnerability functions in terms of repair cost, the so-called damage factors (ratios of cost of repair to cost of replacement) are needed for the considered building typology for each damage state considered in the fragility function. A number of studies have proposed damage factors for different damage states (generally based on damage cost data from previous earthquakes, though this is often mixed with expert opinion). Construction practices and costs, in particular those applied in the repair and reconstruction phase, vary significantly from one country to another, and thus damage factors should vary accordingly. Assigning repair types and associated costs to damage states depends on a number of factors from the failure mechanism, to the size and geometry of the building, to the engineering practice of the country. Some examples of attempts to calculate damage factors according to these factors are found in Hill and Rossetto (2008a, b).

LIQUEFACT
Deliverable D3.1
State of the art review of numerical modelling strategies to simulate liquefaction-induced
structural damage and of uncertain/random factors on the behaviour of liquefiable soils
v. 1.0

Alternatively to the approach that combines fragility functions with consequence functions, vulnerability functions at the building level can also be established by the procedure presented in (Porter et al., 2014) (see also (FEMA, 2012) for a similar approach or (Ramirez and Miranda 2009) for additional background). The proposed procedure simulates structural response, damage and repair cost for the structural and non-structural components that contribute most to the construction cost, and then scales up the results to account for the components that were not simulated. The procedure derives storey-level vulnerability functions, without considering collapse (collapse is addressed in a separate step). The vulnerability functions express the repair cost of components on the storey as a function of storey-level demand (interstorey drift, peak floor acceleration, or other measures of storey-level structural response). The methodology is based on the response results obtained by performing structural analyses for each level the selected earthquake intensity measure with the objective of estimating storey-level demand and collapse probability as a function of the ground motion intensity. The building-level vulnerability function is obtained by summing the storey-level losses over all the storeys, factoring up to account for the fact that only the top six to eight structural and non-structural component categories are considered, and applying the theorem of total probability to consider the probability of collapse. The vulnerability function is normalized by the replacement cost to represent a damage factor as a function of the ground motion intensity.

Finally, some additional comments are presented to address uncertainty-related factors that may affect the development of fragility and vulnerability functions. In the context of loss analysis, uncertainty is a term generally used to describe the variability in determining a response parameter, a cost or a loss value. Typical sources of uncertainty are the ground motion variability (also known as the record-to-record variability), the damage (or limit state) capacity and the associated variability of costs, material variability, and the errors due to modelling assumptions or imperfect analysis methods. Focussing on the aspects related to the numerical modelling and simulation, the ground motion variability is usually seen as the more important source of uncertainty and the variability of material properties is often neglected. However, when incorporating force-controlled limit states in the development of fragility functions (e.g. such as shear-deficient members), a larger contribution of the variability of material properties is expected. With respect to the influence of the structural modelling assumptions and the damage (or limit state) capacities, it is known that neglecting the effects of modelling uncertainties is usually unconservative since incorporating the modelling uncertainties increases the dispersion in the response fragility, and also shifts the prediction of its median value - the median of the fragility function typically decreases (Dolšek 2009; Liel et al., 2009). In particular, structural modelling uncertainties (as well as damage capacities) are essential for accurate collapse and collapse probability predictions (Goulet et al, 2007). Modelling uncertainties have also been seen to have greater impact when the relation between the model parameters and the structural response is highly nonlinear and when the key modelling parameters are more uncertain (Liel et al., 2009). This latter aspect is particularly relevant for the case of modelling the soil properties of a soil-structure interacting system to simulate liquefaction-induced damage. For the case of bridges for example, Padgett et al. (2013) concluded that, for damage due to liquefaction, the fragility functions were influenced by a different set of parameters, mainly those related to the soil properties.

A final remark is made regarding uncertainty propagation between the results of the response analyses and the subsequent fragility, vulnerability and loss analyses. Given that such steps often involve multiple convolution integrals, approximations are sometimes considered based on First Order Second Moment (FOSM) approaches. The use of these approximations is based on a significant reduction in computational time by not requiring direct numerical integration, and by the fact that only the first two moments of the distribution are normally needed. On this topic, reference is made to the work of Bradley and Lee (2010) that shows that great care should be taken in the use of such approximations, particularly considering the large uncertainties that must be propagated in a seismic loss assessment. The work analyses a complete loss assessment of a structure to determine the location where significant approximation errors may be involved, where caution must be taken in the interpretation of the results, and the computational demand of the various alternatives.

7. CONCLUSIONS

The performance of buildings subject to liquefaction has been a subject of engineering research for over 50 years. Until recently this research has focused on field studies and the development of empirical relationships. The development of more advanced soil constitutive models for numerical modelling and more sophisticated techniques for centrifuge modelling has resulted in major advances in our understanding of the important phenomena. The current state-of-the-art has been synthesised within this report to highlight key research findings that can form the basis of future research and to highlight potential future research objectives. This report has focused on the numerical approaches to assessing building performance but it is recognised throughout the report that performance assessment requires a multidisciplinary approach covering numerical, laboratory and field studies, from geotechnical and structural engineering, geology, seismology, economics and social science.

This report discussed the importance of understanding liquefaction damage in relation to previous earthquake events. The phenomena involved with soil liquefaction and methods to estimate its occurrence and impacts were presented. Numerous procedures to estimate liquefaction induced permanent deformations and the response of buildings and other infrastructure were reviewed and several areas requiring future research were identified. Current procedures for quantifying loss were discussed, especially in relation to the propagation of uncertainty and limitations of modelling techniques for assessment liquefaction induced damage.

The main limitations of current modelling techniques is that they are either focused on the geotechnical aspects or the structural aspects, whereas this problem requires a true multidisciplinary approach. The approaches for fragility analysis of buildings, which include a nonlinear model of the structure, focus only on the simulation of damage related to permanent ground deformations. These approaches do not involve coupled soil-structure interaction analysis, and as such are not capable of simulating the damage related to ground shaking. On the other hand there are numerous loss models for structures that do not account for liquefaction or any soil-structure interaction. The suitable combination of these two different disciplines to account for both ground deformation damage and shaking damage would represent an enhanced treatment of the problem, which is beyond the current state-of-the-art.

LIQUEFACT
Deliverable D3.1
State of the art review of numerical modelling strategies to simulate liquefaction-induced
structural damage and of uncertain/random factors on the behaviour of liquefiable soils
v. 1.0

REFERENCES

Acacio, A., Kobayashi, Y., Towhata, I., Bautista, R.T. and Ishihara, K. (2001). Subsidence of building foundation resting upon liquefied subsoil: case studies and assessment. Soils and Foundations, 41(6):111–128

Adachi, T., Iwai, S., Yasui, M. and Sato, Y. (1992). Settlement and inclination of reinforced concrete buildings in Dagupan City due to liquefaction during the 1990 Philippine earthquake. Earthquake Engineering, Tenth World Conference, Rotterdam, Holland. Pp. 147-152.

Adalier, K., Elgamal, A., Meneses J. and Baez, J.I. (2003). Stone columns as liquefaction countermeasure in non-plastic silty soils. Soil Dynamics and Earthquake Engineering, 23:571–584. DOI:10.1016/S0267-7261(03)00070-8.

Ahmed, A. and Soubra, A.H. (2014). Probabilistic analysis at the serviceability limit state of two neighboring strip footings resting on a spatially random soil. Structural Safety, 49:2-9.

Akbas, S.O. and Kulhawy, F.H. (2009). Reliability-based design approach for differential settlement of footings on cohesionless soils. Journal of Geotechnical and Geoenvironmental Engineering, 135(12):1779-1788.

Alarcon-Guzman, A., Leonards, G. A. and Chameau, J. L. (1988). Undrained Monotonic and Cyclic Strength of Sands. Journal of Geotechnical Engineering, 114(10): 1089–1109. https://doi.org/10.1061/(ASCE)0733-9410(1988)114:10(1089).

Alath, S. and Kunnath, S. (1995) Modeling inelastic shear deformations in rc beam-column joints. Engineering Mechanics Proceedings of 10th Conference, University of Colorado at Boulder, Boulder, Colorado.

American Lifeline Alliance - ALA (2001). Seismic fragility formulations for water systems. ASCE, Washington, DC.

Anderson, I., Hargy, J., Alba, P. de and Dewoolkar, M. (2012). Measurement of Residual Strength of Liquefied Soil in Centrifuge Models. In GeoCongress 2012 (pp. 1740–1749). Reston, VA: American Society of Civil Engineers. https://doi.org/10.1061/9780784412121.179

Andrade, J. E. (2009). A predictive framework for liquefaction instability. Géotechnique, 59(8), 673–682. https://doi.org/10.1680/geot.7.00087.

Andrianopoulos, K.I., Papadimitriou, A.G. and Bouckovalas, G.D. (2010). Bounding surface plasticity model for the seismic liquefaction analysis of geostructures. Soil Dynamics and Earthquake Engineering, 30(10):895–911, DOI: 10.1016/j.soildyn.2010.04.001.

Anić, F., Penava, D. and Sarhosis, V. (2017) Development of a three-dimensional computational model for the in-plane and out-of-plane analysis of masonry-infilled reinforced concrete frames. COMPDYN 2017, 6th International Conference on Computational Methods in Structural Dynamics and Earthquake Engineering, Rodos, Greece.

Arulmoli K, Project V, Corporation ET, Foundation NS. VELACS (1992). Verification of liquefaction analyses by centrifuge studies laboratory testing program: soil data report. Earth Technology Corporation.

Asteris, P. G., Antoniou, S. T., Sophianopoulos, D. S. and Chrysostomou, C. Z. (2011) Mathematical Macromodeling of Infilled Frames: State of the Art. Journal of Structural Engineering 137(12), 1508-1517.

Asteris, P. G., Cavaleri, L., Di Trapani, F. and Tsaris, A. K. (2017). Numerical modelling of out-of-plane response of infilled frames: State of the art and future challenges for the equivalent strut macromodels. Engineering Structures, 13: 110-122.

Aygün, B., Dueñas-Osorio, L., Padgett, J.E. and DesRoches, R. (2011). Efficient longitudianl seismic fragility assessment of a multispan continuous Steel bridge on liquefiable soils. Journal of bridge engineering, 16(1): 93-107. DOI: 10.1061/ASCEBE.1943-5592.0000131.

Ayoubi P. and Pak A. (2017). Liquefaction-induced settlement of shallow foundations on two-layered subsoil strata. Soil Dynamics and Earthquake Engineering, 94: 35-46.

LIQUEFACT
Deliverable D3.1
State of the art review of numerical modelling strategies to simulate liquefaction-induced
structural damage and of uncertain/random factors on the behaviour of liquefiable soils
v. 1.0

This project has received funding from the European Union's Horizon 2020 research and innovation programme under grant agreement No. 700748

Bakir, B.S., Sucuoğlu, H. and Yilmaz, T. (2002). An overview of local site effects and the associated building damage in Adapazari during the 17 August 1999 Izmit earthquake. Bulletin of the Seismological Society of America, 92(1):509-526.

Ballantyne D. (1995). Minimising earthquake damage. World Water and Environmental Engineering, September, 30-31.

Bán, Z., Mahler, A., Katona, T.J. and Győri, E. (2017). Assessment of liquefaction potential based on combined CPT and shear wave velocity measurements using energy concept. Proceedings of the 19th Int. Conf. on Soil Mechanics and Geotechnical Engineering. Seoul.

Barbato, M., Gu, Q., Conte, J.P. (2010). Probabilistic Push-Over Analysis of Structural and Soil-Structure System. Journal of Structural Engineering, 136(11), 1330-1341.

Barrios G., Larkin T. and Chouw N. (2017). Numerical analyses of interaction between adjacent structures on liquefied soil. 16th World Conference on Earthquake Engineering, Santiago, Chile, 9-13 January. Paper No. 3862.

Been, K. and Jefferies, M. (1985). A state parameter for sands. Géotechnique, 35(2): 99-112. https://doi.org/10.1680/geot.1985.35.2.99

Beaty, M. and Byrne, P.M. (1998). An effective stress model for predicting liquefaction behaviour of sand. In Geotechnical earthquake engineering and soil dynamics III. Edited by P. Dakoulas, M. Yegian, and R. Holtz. American Society of Civil Engineers, Geotechnical Special Publication 75(1), pp. 766-777.

Beaty, M.H. and Byrne, P.M. (2011). UBCSAND constitutive model, Version 904aR. Document report: UBCSAND Constitutive Model on Itasca UDM Web site: http://www.itasca-udm.com/pages/continuum.html

Bertalot, D. (2013). Seismic behaviour of shallow foundations on layered liqueable soils. PhD Thesis, University of Dundee, Scotland, UK

Bertalot, D. and Brennan, A.J. (2015). Influence of initial stress distribution on liquefaction-induced settlement of shallow foundations. Geotechnique, 65(5):418–428. DOI: 10.1680/geot.SIP.15.P.002.

Bertalot, D., Brennan, A.J. and Villalobos, F.A. (2013). Influence of bearing pressure on liquefaction-induced settlement of shallow foundations. Géotechnique 63(5):391-399.

Bhatnagar S., Kumari S., Sawant V.A. 2016. Numerical Analysis of Earth Embankment Resting on Liquefiable Soil and Remedial Measures. International Journal of Geomechanics, 16 (1).

Biddah, A. and Ghobarah, A. (1999). Modelling of shear deformation and bond slip in reinforced concrete joints. Structural Engineering and Mechanics, 7(4): 413-432.

Bird, J. and Bommer, J. (2004). Evaluating earthquake losses due to the ground failure and identifying their relative contribution. 13th World Conference on Earthquake Engineering, Canada. Paper 3156.

Bird, J.F., Bommer, J.J., Crowley, H. and Pinho, R. (2006). Modelling liquefaction-induced building damage in earthquake loss estimation. Soil Dynamics and Earthquake Engineering 26(1):15–30, DOI: 10.1016/j.soildyn.2005.10.002.

Bird, J.F., Crowley, H., Pinho, R. and Bommer, J.J. (2005). Assessment of building response to liquefaction-induced differential ground deformation. Bulletin of the New Zealand Society for Earthquake Engineering, 38(4):215–234.

Bjerrum, L. (1963). Allowable Settlement of Structures. Proceedings of the 3rd European Conf. on Soil Mech. and Found. Engng, Wiesbaden, 2, Brighton, England, 135–137.

Borozan, J. (2017). Numerical modelling of liquefaction effects on built structures. MSc thesis. Istituto Universitario di Studi Superiori di Pavia, Italy.

Boscardin M.D. and Cording E.J. (1989). Building response to excavation-induced settlement. J Geotech Eng; 115(1):1-21. https://doi.org/10.1061/(ASCE)0733-9410(1989)115:1(1)

LIQUEFACT
Deliverable D3.1
State of the art review of numerical modelling strategies to simulate liquefaction-induced
structural damage and of uncertain/random factors on the behaviour of liquefiable soils
v. 1.0

Bouckovalas, G. D., Tsiapas, Y. Z., Theocharis, A. I. and Chaloulos, Y. K. (2016). Ground response at liquefied sites: seismic isolation or amplification? Soil Dynamics and Earthquake Engineering, pages 1–0, DOI: 10.1016/j.soildyn.2016.09.028.

Boulanger, R.W. and Seed, R.B. (1995). Liquefaction of sand under bidirectional monotonic and cyclic loading. Journal of Geotechnical Engineering, 121(12): 870-878. https://doi.org/10.1061/(ASCE)0733-9410(1995)121:12(870).

Boulanger, R.W. and Ziotopoulou, K. (2013). Formulation of a sand plasticity plane-strain model for Earthquake engineering applications. Soil dynamicas and Earthquake engineering, 53 (2013) 254–267. http://dx.doi.org/10.1016/j.soildyn.2013.07.006

Boulanger, R.W. and Idriss, I.M. (2014). CPT and SPT based liquefaction triggering procedures. Technical report.

Boulanger, R.W. and Ziotopoulou, K. (2015). PM4SAND (Version 3): A sand plasticity model for earthquake engineering applications. Technical report.

Boulanger, R. W., Kamai, R. and Ziotopoulou, K. (2013). Liquefaction induced strength loss and deformation: simulation and design. Bulletin of Earthquake Engineering, 12(3):1107–1128, DOI: 10.1007/s10518-013-9549-x.

Bouziou, D. and O'Rourke, T.D. (2017). Response of the Christchurch water distribution system to the 22 February 2011 earthquake. Soil Dynamics and Earthquake Engineering 97, 14–24.

Bradley, B.A. and Lee, D.S. (2010). Accuracy of approximate methods of uncertainty propagation in seismic loss estimation. Structural Safety 32(1):13–24. DOI: 10.1016/j.strusafe.2009.04.001.

Bray, J. D. and Luque, R. (2017). Seismic performance of a building affected by moderate liquefaction during the Christchurch earthquake. Soil Dynamics and Earthquake Engineering, 102:99–111, DOI: 10.1016/j.soildyn.2017.08.011.

Bray, J.D. and Macedo, J. (2017). 6th Ishihara lecture: Simplified procedure for estimating liquefaction induced building settlement. Soil Dynamics and Earthquake Engineering, 102: 215–231. http://dx.doi.org/10.1016/j.soildyn.2017.08.026.

Bray, J.D., Markham, C.S. and Cubrinovski, M. (2017a). Liquefaction assessments at shallow foundation building sites in the Central Business District of Christchurch, New Zealand. Soil Dynamics and Earthquake Engineering 92(C):153-164, DOI: 10.1016/j.soildyn.2016.09.049.

Bray, J.D., Macedo, J. and Luque, R. (2017b). Key trends in assessing liquefaction-induced building settlement. In 3rd International Conference on Performance-based Design in Earthquake Geotechnical Engineering, Vancouver. Paper n0. 520

Bray, J.D., Sancio, R.B., Durgunoglu, T., Onalp, A., Seed, R.B., Stewart, J.P., Youd, T.L., Baturay, M.B., Cetin, K.O., Christensen, C., Karadayilar, T., and Emrem, C. (2001). Ground Failure in Adapazari, Turkey. pp 1–10.

Buch, S.H. and Bhat, D.M. (2015). Comparative Modelling of Infilled Frames: A Descriptive Review and Analysis. In Advances in Structural Engineering: Materials, Matsagar, V. (Ed). Springer, New Delhi, India.

Burland, J. B. (1995). Assessment of risk of damage to buildings due to tunnelling and excavation. Proceedings of the 1st International Conference on Earthquake Geo-technical Engineering, Vol. 3, Balkema, Rotterdam,Netherlands, 1189-1201.

Byrne P.M. (1991). A Cyclic Shear-Volume Coupling and Pore Pressure Model for Sand. Second International Conference on Recent Advances in Geotechnical Earthquake Engineering and Soil Dynamics, St. Louis, Missouri. Paper No. 1.24: 11-15.

Byrne, P. M., Park, S.-S., Beaty, M., Sharp, M., Gonzalez, L. and Abdoun, T. (2004). Numerical modeling of liquefaction and comparison with centrifuge tests. Canadian Geotechnical Journal, 41(2):193–211. DOI: 10.1139/t03-088.

Calvi, G.M. (1999). A displacement-based approach for vulnerability evaluation of classes of buildings. Journal of Earthquake Engineering3(3), 411–438.

LIQUEFACT
Deliverable D3.1
State of the art review of numerical modelling strategies to simulate liquefaction-induced
structural damage and of uncertain/random factors on the behaviour of liquefiable soils
v. 1.0

This project has received funding from the European Union's Horizon 2020 research and innovation programme under grant agreement No. 700748

Campbell, K.W. and Bozorgnia, Y.(2012) A Comparison of Ground Motion Prediction Equations for Arias Intensity and Cumulative Absolute Velocity Developed Using a Consistent Database and Functional Form. Earthquake Spectra, Vol. 28, No. 3, pp. 931-941. https://doi.org/10.1193/1.4000067.

Cascone, E. and Bouckovalas, G. (1998). Seismic bearing capacity of footings on saturated sand with a clay cap. Proc.

Castro, G., and Poulos, S. J. (1977). Factors Affecting Liquefaction and Cyclic Mobility. Journal of the Geotechnical Engineering Division, 103(6): 501–506.

Catherin, J. M., Jayalekshmi, B. R. and Katta, V. (2013) Modeling of Masonry infills-A review. American Journal of Engineering Research, 2: 59-63.

Celik, O. and Ellingwood, B. (2008). Modeling beam-column joints in fragility assessment of gravity load designed reinforced concrete frames. Journal of Earthquake Engineering, 12(3): 357-381.

CEN (2004). Eurocode 8: Design of structures for earthquake resistance - Part 1: General rules, seismic actions and rules for buildings, EN 1998–1. European Committee for Standardisation: Brussels.

CERA (2012). Geotechnical database for Canterbury Earthquake Sequence, NZ. Canterbury Earthquake Recovery Authority (CERA). August 2012. (https://canterburygeotechnicaldatabase.projectorbit.com).

Cetin, K.O., Seed, R.B., Der Kiureghian, A.K., Tokimatsu, K., Harder, L.F., Kayen, R.E. and Moss, R.E.S. (2004). Standard penetration test-based probabilistic and deterministic assessment of seismic soil liquefaction potential. Journal of Geotechnical and Geoenvironmental Engineering, 130(12):1314–1340.

Cetin, K. O., Unutmaz, B. and Jeremic, B. (2012). Assessment of seismic soil liquefaction triggering beneath building foundation systems. Soil Dynamics and Earthquake Engineering 43(C): 160–173. DOI: 10.1016/j.soildyn.2012.07.021.

CGF (2012). Liquefaction interpreted from aerial photography, map layer CGD0200–11 Feb 2013. Canterbury Geotechnical Database. August 2012. (https://canterburygeotechnicaldatabase.projectorbit.com/)

Chatzigogos, C.T., Figini, R., Pecker, A. and Salençon, J. (2011). A macro-element formulation for shallow foundations on cohesive and frictional soils. International Journal for Numerical and Analytical Methods in Geomechanics, 35(8):902–931. DOI: 10.1002/nag.934.

Chiaradonna A., Flora A., dOnofrio A., Bilotta E. and Silvestri F. (2017). una procedura semplificata per la stima del cedimento di consolidazione post-sismico. Incontro Annuale dei Ricercatori di Geotecnica, IARG 2017, Matera.

Chopra, A. K. and McKenna, F. (2016) Modeling viscous damping in nonlinear response history analysis of buildings for earthquake excitation. Earthquake Engineering and Structural Dynamics, 45(2): 193-211.

Cinicioglu, S. F., Bozbey, I. and Oztoprak, S. (2006). Discussion of "Subsurface Characterization at Ground Failure Sites in Adapazari, Turkey" by Jonathan D. Bray, Rodolfo B. Sancio, Turan Durgunoglu, Akin Onalp, T. Leslie Youd, Jonathan P. Stewart, Raymond B. Seed, Onder K. Cetin, Ertan Bol, MB Baturay, C. Christensen, and T. Karadayilar. Journal of Geotechnical and Geoenvironmental Engineering, 132(4):539-541.

Christopoulos, C. and Pampanin, S. (2004). Towards performance-based design of MDOF structures with explicit consideration of residual deformations. ISET Journal of Earthquake Technology 41(1):53–73, ISSN: 0972-0405.

Coduto, D.P. (1994). Foundation design: Principles and practices, Prentice-Hall, Englewood Cliffs, New Jersey.

Coduto, D.P. (2001). Foundation design principles and practices, Prentice Hall, Upper Saddle River, NJ.

Coelho, P.A.L.F. (2007). In Situ densification as a liquefaction resistance measure for bridge foundations. PhD Thesis. University of Cambridge, Cambridge.

Coelho, P. A. L. F., Haigh, S. K. and Madabhushi, S. P. G. (2004). Centrifuge modelling of the effects of earthquake-induced liquefaction on bridge foundations. Proc., 11th Int. Conference on Soil Dynamics and Earthquake Engineering (ICSDEE), Univ. of California, Berkeley, CA.

Crowley, H., Pinho, R. and Bommer, J. J. (2004). A probabilistic displacement-based vulnerability assessment procedure for earthquake loss estimation. Bulletin of Earthquake Engineering, 2(2), 173-219.

Cubrinovski, M. and Ishihara, K. (1998a). Modelling of sand behaviour based on state concept. Soils and foundations 38(3):115–127.

Cubrinovski, M. and Ishihara, K. (1998b). State concept and modified elastoplasticity for sand modelling. Soil and Foundations. pp 1–13.

Cubrinovski, M. Hughes, M., Bradley, B., McCahon, I., McDonald, Y., Simpson, H., Cameron, R., Christison, M., Henderson, B., Orense, R. and O'Rourke, T. (2011). Liquefaction impacts on pipe networks. University of Canterbury, Civil and Natural Resources Engineering, Research Report 2011-04.

Cubrinovski, M., Rees, S. and Bowman, E. (2010). Effects of Non-plastic Fines on Liquefaction Resistance of Sandy Soils. Geotechnical, Geological and Earthquake Engineering. 17. 125-144. 10.1007/978-90-481-9544-2_6.

Cubrinovski, M., Rhodes, A., Ntritsos, N. and Van Ballegooy, S. (2017a) System response of liquefiable deposits. In 3rd International Conference on Performance-based Design in Earthquake Geotechnical Engineering, Vancouver. Paper, n. 540.

Cubrinovski, M., Bray, J.D., Torre, C. de la, Olsen, M.J., Bradley, B.A., Chiaro, G., Stocks, E. and Wotherspoon, L. (2017b). Liquefaction effects and associated damages observed at the Wellington centreport from the 2016 Kaikoura Earthquake. Bulletin of the New Zealand Society for Earthquake Engineering, 50(2):152-173.

D'Appolonia, D.J., D'Appolonia, E.E. and Brissette, R.F. (1968). Settlement of spread footings on sand. J. Soil Mech. and Found. Div., ASCE, 94(3), 735–760.

D'Ayala, D., Meslem, A., Vamvatsikos, D., Porter, K. and Rossetto, T. (2015). Guidelines for Analytical Vulnerability Assessment of low/mid-rise Buildings. GEM Technical Report 2015-08 v1.0.0. Vulnerability Global Component Project. Global Earthquake Model.

Dafalias Y.F. and Manzari M.T. (2004). Simple Plasticity Sand Model Accounting for Fabric Change Effects. Journal of Engineering Mechanics, 130 (6).

Daftari, A. and Kudla, W. (2014). Prediction of soil liquefaction by using UBC3D-PLM model in Plaxis. International Scholarly and Scientific Research and Innovation 8(2):106-111.

Daniell, J. E., Schaefer, A. M. and Wenzel, F. (2017). Losses Associated with Secondary Effects in Earthquakes. Frontiers in Built Environment, 3, 30.

Das, S. (2014) Three Dimensional Formulation for the Stress-Strain-Dilatancy Elasto-Plastic Constitutive Model for Sand Under Cyclic Behaviour, Master's Thesis, University of Canterbury.

Dashti S. and Bray J.D. (2013). Numerical Simulation of Building Response on Liquefiable Sand. Journal of Geotechnical and Geoenvironmental Engineering, 139 (8): 1235-1249.

Dashti, S., Bray, J. D., Pestana, J. M., Riemer, M. and Wilson, D. (2010a). Mechanisms of Seismically Induced Settlement of Buildings with Shallow Foundations on Liquefiable Soil. Journal of Geotechnical and Geoenvironmental Engineering, 136(1):151–164. DOI: 10.1061/ ASCE GT.1943-5606.0000179.

Dashti, S., Bray, J. D., Pestana, J. M., Riemer, M. and Wilson, D. (2010b). Centrifuge testing to evaluate and mitigate liquefaction-induced building settlement mechanisms. Journal of Geotechnical and Geoenvironmental Engineering 136(7):918–929

Deck, O., Al Heib, M., and Homand, F. (2003). Taking the soil-structure interaction into account in assessing the loading of a structure in a mining subsidence area, Eng. Struct. 25, 435–448.

Deierlein, G., Reinhorn, A. and Willford, M. (2010). Nonlinear structural analysis for seismic design. NEHRP seismic design technical brief, 4, National Earthquake Hazards Reduction Program.

LIQUEFACT
Deliverable D3.1
State of the art review of numerical modelling strategies to simulate liquefaction-induced
structural damage and of uncertain/random factors on the behaviour of liquefiable soils
v. 1.0

This project has received funding from the European Union's Horizon 2020 research and innovation programme under grant agreement No. 700748

Deng, L. and Kutter, B. L. (2012). Characterization of rocking shallow foundations using centrifuge model tests. Earthquake Engineering and Structural Dynamics, 41(5):1043– 1060. DOI: 10.1002/eqe.1181.

Deng, L., Kutter, B. L. and Kunnath, S. K. (2012). Centrifuge Modeling of Bridge Systems Designed for Rocking Foundations. Journal of Geotechnical and Geoenvironmental Engineering, 138(3):335–344, DOI: 10.1061/(ASCE)GT.1943-5606.0000605.

Deng, L., Kutter, B. L. and Kunnath, S. K. (2014). Seismic Design of Rocking Shallow Foundations: Displacement-Based Methodology. Journal of Bridge Engineering, 19(11):04014043–11. DOI: 10.1061/(ASCE)BE.1943-5592.0000616.

Diaz, D (2016). Vulnerabilidad de construcciones debido a licuación inducida por sismo. MSc Thesis, National Autonomous University of Mexico. Mexico City.

Dimitriadi, V.E., Bouckovalas, G.D. and Papadimitriou, A.G. (2017). Seismic performance of strip foundations on liquefiable soils with a permeable crust. Soil Dynamics and Earthquake Engineering 100:396-409

Dobry, R. and Liu, L. (1994). Centrifuge modeling of soil liquefaction. In 10th World Conference of Earthquake Engineering.

Dolšek, M. (2009). Incremental dynamic analysis with consideration of modeling uncertainties. Earthquake engineering & structural dynamics, 38(6): 805-825.

Dolšek, M. (2012). Simplified method for seismic risk assessment of buildings with consideration of aleatory and epistemic uncertainty. Structure and Infrastructure Engineering, 8(10):939–953.

Dolšek, M. (2016). Analytic Fragility and Limit States [P(EDP|IM)]: Nonlinear Static Procedures. In: Beer, M. (ed.), Kougioumtzoglou, I.A. (ed.), Patelli, E. (ed.), Au, I.S.-K. (ed.), Encyclopedia of Earthquake Engineering, Springer: 3200 p.

Douglas, J., Seyedi, D.M., Ulrich, T., Modaressi, H., Foerster, E., Pitilakis, K., Pitilakis, D., Karatzetzou, A., Gazetas, G., Garini, E. and Loli, M. (2014). Evaluation of seismic hazard for the assessment of historical elements at risk: description of input and selection of intensity measures. Bull Earthquake Eng. doi:10.1007/s10518-014-9606-0.

Drucker, D. C. and Prager, W. (1952). Soil mechanics and plastic analysis or limit design. Quarterly of applied mathematics.

Dutta, S.C. and Roy, R. (2002). A critical review on idealization and modeling for interaction among soil-foundation-structure system. Computer and Structures, 80:1579-1594.

EC8-3 (2005). ENV 1998-3. Eurocode 8: Design of structures for earthquake resistance - Part 3: Assessment and retrofitting of buildings. European Committee for Standardization, Brussels, Belgium.

EERI (1986). Reducing earthquake hazards: lessons learned from earthquakes. Earthquake Engineering Research Institute, El Cerrito, Publication n_86-02

Eguchi RT (1987) Seismic risk to natural gas and oil systems. FEMA 139. Earthq Hazard Reduct Ser 30:15–33

Elgamal, A., Lu, J. and Yang, Z. (2005). Liquefaction-induced settlement of shallow foundations and remediation: 3D numerical simulation. J. Earthquake Eng., 9(1): 17–45.

Elgamal, A., Yang, Z., Parra, E. and Ragheb, A. (2003). Modelling of Cyclic Mobility in Saturated Cohessionless Soils. International Journal of Plasticity, 19: 883-905.

El Ganainy, H. and El Naggar, M. H. (2009). Efficient 3D nonlinear Winkler model for shallow foundations. Soil Dynamics and Earthquake Engineering, 29(8):1236–1248. DOI: 10.1016/j.soildyn.2009.02.002.

Fajfar, P. (2000). A nonlinear analysis method for performance-based seismic design. Earthquake Spectra, 16(3), 573–592.

FEMA (2003) Multi hazard loss estimation methodology: earthquake model – HAZUS-MH MR3 technical manual. FEMA Federal Emergency Management Agency, Washington, DC

FEMA (2012) FEMA P-58: Seismic Performance Assessment of Buildings. Applied Technology Council. Federal Emergency Management Agency.

Fenton, G.A. and Griffiths, D.V. (2002). Probabilistic foundation settlement on spatially random soil. Journal of Geotechnical and Geoenvironmental Engineering, ASCE 128 (5), 381–390.

FIB (2003a) Seismic assessment and retrofit of reinforced concrete buildings. Bulletin nº24, Fédération Internationale du Béton. Lausanne, Switzerland.

FIB (2003b) Displacement-based seismic design of reinforced concrete buildings. Bulletin nº25, Fédération Internationale du Béton. Lausanne, Switzerland.

Figini, R., Paolucci, R. and Chatzigogos, C. T. (2012). A macro-element model for non- linear soil-shallow foundation-structure interaction under seismic loads: theoretical development and experimental validation on large scale tests. Earthquake Engineering and Structural Dynamics, 41(3):475–493. DOI: 10.1002/eqe.1140.

Fragiadakis, M., Vamvatsikos, D. (2010). Fast performance uncertainty estimation via pushover and approximate IDA. Earthquake Engineering and Structural Dynamics, 39, 683–703.

Gajan, S., Kutter, B. L., Phalen, J. D., Hutchinson, T. C., and Martin, G. R. (2005). Centrifuge modeling of load-deformation behavior of rocking shallow foundations. Soil Dynamics and Earthquake Engineering, 25(7-10):773–783. DOI: 10.1016/j.soildyn.2004.11.019.

Gazetas, G. (1991). Foundation Vibrations. In Fang, H.-Y., editor, Foundation Engi- neering Handbook, pages 553–593. Springer.

Gazetas, G. and Mylonakis, G. (1998). Seismic soil-structure interaction: new evidence and emerging issues. Geotechnical earthquake engineering and soil dynamics III, pp 1119–1174.

Gelagoti, F., Kourkoulis, R., Anastasopoulos, I. and Gazetas, G. (2011). Rocking isolation of low-rise frame structures founded on isolated footings. Earthquake Engineering and Structural Dynamics, 41(7):1177–1197. DOI: 10.1002/eqe.1182.

Geo-engineering Extreme Events Reconnaissance Association (2010). Geo-engineering reconnaissance of the 2010 Maule, Chile earthquake. Report No. GEER-022.

Geo-engineering Extreme Events Reconnaissance Association (2011). Geotechnical reconnaissance of the 2011 Christchurch, New Zealand earthquake, Report No. GEER-027.

Gingery, J.R. (2014). Effects of Liquefaction on Earthquake Ground Motions. PhD dissertation, University of California, San Diego.

Gingery, J.R., Elgamal, A. and Bray J.D. (2015). Liquefaction Model Calibration: Element-Level Versus 1-D Site Response. 6th International Conference on Earthquake Geotechnical Engineering, Christchurch, New Zealand, 1-4 November; Paper No. 682.

Goulet, C. A., Haselton, C. B., Mitrani-Reiser, J., Beck, J. L., Deierlein, G. G., Porter, K. A. and Stewart, J. P. (2007). Evaluation of the seismic performance of a code-conforming reinforced-concrete frame building—from seismic hazard to collapse safety and economic losses. Earthquake Engineering and Structural Dynamics, 36(13), 1973-1997.

Grammatikou, S., Biskinis, D. and Fardis, M. N. (2015). Strength, deformation capacity and failure modes of RC walls under cyclic loading. Bulletin of Earthquake Engineering, 13(11), 3277-3300.

Grammatikou, S., Biskinis, D. and Fardis, M. N. (2016). Ultimate strain criteria for RC members in monotonic or cyclic flexure. Journal of Structural Engineering, 142(9), 04016046.

Grammatikou, S., Biskinis, D. and Fardis, M. N. (2017a). Flexural rotation capacity models fitted to test results using different statistical approaches. Structural Concrete. DOI: 10.1002/suco.201600238.

Grammatikou, S., Fardis, M.N. and Biskinis, D. (2017b). Bulletin of Earthquake Engineering. DOI: 10.1007/s10518-017-0202-y.

Hall, W.J. (1987). Earthquake engineering research needs concerning gas and liquid fuel lifelines. FEMA 139. Earthq Hazard Reduct Ser, 30:35–49

Hamburger, R., Deierlein, G., Lehman, D., Lowes, L., Shing, B., Van de Lindt, J., Lignos, D. and Hortacsu, A. (2016). ATC-114 Next-Generation Hysteretic Relationships for Performance-based Modeling and Analysis. In Proceedings of the SEAOC Convention (No. EPFL-CONF-223937). Structural Engineers Association of California.

Harden, C.W. and Hutchinson, T.C. (2009). Beam-on-nonlinear-Winkler-foundation modelling of shallow, rocking-dominated footings. Earthquake Spectra, 25(2):277– 300. DOI: 10.1193/1.3110482.

Haselton, C. B., Liel, A. B., Taylor Lange, S. and Deierlein, G. G. (2008). Beam-Column Element Model Calibrated for Predicting Flexural Response Leading to Global Collapse of RC Frame Buildings. Pacific Earthquake Engineering Research Center, Berkeley, CA.

Hashash, Y.M.A., Hook, J.J., Schmidt, B. and Yao, J.I-C. (2001). "Seismic design and analysis of underground structures," Tunneling and Underground Space Technology, 16, 247-293.

Hausler, E.A. (2002). Influence of ground improvement on settlement and liquefaction: A study based on field case history evidence and dynamic geotechnical centrifuge tests. Ph.D Thesis, University of Califormia, Berkeley.

Hayden C.P., Zupan J.D., Bray J.D., Allmond J.D. and Kutter B.L. (2014). Centrifuge Tests of Adjacent Mat-Supported Buildings Affected by Liquefaction. Journal of Geotechnical and Geoenvironmental Engineering, 141 (3).

Huang, X. and Kwon, O. (2015). Numerical models of RC elements and their impacts on seismic performance assessment. Earthquake Engineering and Structural Dynamics, 44(2): 283-298.

Hill, M. and Rossetto, T. (2008a). Improving seismic loss estimation for Europe through enhanced relationships between building damage and repair costs. Proceedings of 14th World Conference on Earthquake Engineering, Beijing, China.

Hill, M. and Rossetto, T. (2008b). Development of parameters for use in seismic recovery estimation of residential buildings in Lima, Peru. Proceedings of 14th World Conference on Earthquake Engineering, Beijing, China.

Hong Y., Lu Y. and Orense R.P. (2017). Effective stress simulation of liquefaction-induced building settlements. 16th World Conference on Earthquake Engineering, Santiago, Chile, 9-13 January 2017; Paper No. 283.

Hynes, M. E. and Olsen, R. S. (1999). Influence of confining stress on liquefaction resistance. Physics and mechanics of soil liquefaction, P. Lade and J. Yamamuro, eds., Balkema, Rotterdam, The Netherlands, 145–151.

Iai, Tobita, Ozutsumi, Ueda. (2011). Dilatancy of Granular Materials in Strain Space Multiple Mechanism Model. Int. J. Numel. Meth. Geomech. 35: 360-392.

Ichii K (2003) Application of performance-based seismic design concept for caisson-type quay walls. Ph.D. thesis, Kyoto University.

Ichii K (2004) Fragility curves for gravity-type quay walls based on effective stress analyses. Proceedings of the 13th World Conference on Earthquake Engineering Vancouver, Canada.

IDNDR- DHA (1992) International Decade for Natural Disaster Reduction — Department of Humanitarian Affairs: Glossary: Internationally Agreed Glossary of Basic Terms Related to Disaster Management, United Nations, Geneva, 83 pp.

Ishihara, K. (1985). Stability of natural deposits during earthquakes. In 11th international conference on soil mechanics and foundation engineering (pp. 321–376). San Fransisco: Balkema.

Ishihara, K. (1993). Liquefaction and flow failure during earthquakes. Géotechnique, 43(3): 351–451. https://doi.org/10.1680/geot.1993.43.3.351

Ishihara, K. and Cubrinovski, M. (2005). Characteristics of ground motion in liquefied deposits during earthquakes. Journal of Earthquake Engineering, 9(S1):1–15.

Ishihara, K. and Yoshimine, M. (1992). Evaluation of settlements in sand deposits following liquefaction during earthquakes. Soils Foundations; 32(1): 173–88.

Ishihara, K., Acacio, A.A. and Towhata, I. (1993). Liquefaction induced ground damage in Dagupan city in the July 16, 1990 Luzon earthquake. Soils and Foundations 33(1):133-154

Itasca (2017). FLAC, Fast Lagrangian Analysis of Continua, Itasca Consulting Group, Inc. Additional information available on: www.itascacg.com\flac.

Iwasaki, T., Tatsuoka, F., Tokida, K. and Yasuda, S.A. (1978). Practical method for assessing soil liquefaction potential based on case studies at various sites in Japan. In Proceedings of the 2nd international conference on microzonation. SanFrancisco, CA,USA; p.885–96.

Jalayer, F., Elefante, L., Iervolino, I., Manfredi, G. (2013). Knowledge-Based Performance Assessment of Existing RC Buildings. Journal of Earthquake Engineering, 15(3), 362-389.

Jefferies, M. and Been, K. (2015). Soil Liquefaction: A Critical State Approach (2nd ed.). Milton Park, Abingdon: CRC Press.

Juang, C.H., Ching, J., Wang, L., Khoshnevisan, S. and Ku, C.-S. (2013). Simplified procedure for estimation of liquefaction-induced settlement and site-specific probabilistic settlement exceedance curve using cone penetration test (CPT). Canadian Geotechnical Journal, 50: 1055–1066 dx.doi.org/10.1139/cgj-2012-0410

Kachadoorian, R. (1976). "Earthquake: correlation between pipeline damage and geologic environment." Journal of American Waterworks Association, 68, 165-167.

Kaklamanos, J., Bradley, B. A., Thompson, E. M. and Baise, L. G. (2013). Critical Parameters Affecting Bias and Variability in Site-Response Analyses Using KiK-net Downhole Array Data. Bulletin of the Seismological Society of America, 103(3):1733– 1749, DOI: 10.1785/0120120166.

Karamitros, D.K., Bouckovalas, G.D., Chaloulos and Y.K. (2013a). Insight into the seismic liquefaction performance of shallow foundations. Journal of Geotechnical and Geoenvironmental Engineering, 139(4):599-607.

Karamitros, D.K., Bouckovalas, G.D. and Chaloulos, Y.K. (2013b). Numerical analysis of liquefaction-induced bearing capacity degradation of shallow foundations on a two-layered soil profile. Soil Dynamics and Earthquake Engineering, 44:90-101

Karamitros, D.K., Bouckovalas, G.D. and Chaloulos, Y.K. (2013c). Seismic settlements of shallow foundations on liquefiable soil with a clay crust. Soil Dynamics and Earthquake Engineering, 46:64-76

Karimi, Z. and Dashti, S. (2016). Seismic performance of shallow founded structures on liquefiable ground: validation of numerical simulations using centrifuge experiments. Journal of Geotechnical Geoenvironment Engineering 142(6): 13 pp.

Karimi, Z. and Dashti, S. (2017). Ground motion intensity measures to evaluate II: the performance of shallow-founded structures on liquefiable ground. Earthquake Spectra 33(1):277-298

Kawasaki, K., Sakai, T., Yasuda, S., and Satoh, M. (1998). Earthquake induced settlement of an isolated footing for power transmission tower. Proc., Centrifuge 1998, Tokyo, 271–276.

Kayser, M. and Gajan, S. (2014). Application of probabilistic methods to characterize soil variability and their effects on bearing capacity and settlement of shallow foundations: state of the art. International Journal of Geotechnical Engineering, 8(4):352-364.

Kiyota, T., Tani, K., Matsushita, K., Hashimoto, T., Yamamoto, A., Takeuchi, H., Ohbayashi, J., Noda, T. and Kiku, H. (2014) Mitigation of liquefaction-induced damage to residential houses by shallow ground improvement. Soil Liquefaction during recent large-scale earthquakes - Orense, Towhata and Chouw (Eds). pp. 157-166

LIQUEFACT
Deliverable D3.1
State of the art review of numerical modelling strategies to simulate liquefaction-induced
structural damage and of uncertain/random factors on the behaviour of liquefiable soils
v. 1.0

Kolymbas, D. and Wu, W. (1993). Introduction to Hypoplasticity. In Modern Approaches to Plasticity, pages 213–223. Elsevier, ISBN: 9780444899705, DOI: 10.1016/B978-0-444-89970-5.50015-7.

Kosič, M., Fajfar, P., Dolšek, M. (2014). Approximate seismic risk assessment of building structures with explicit consideration of uncertainties. Earthquake Engineering and Structural Dynamics, 43(10):1483–1502.

Kosič, M., Dolšek, M., Fajfar, P. (2016). Dispersions for pushover-based risk assessment of reinforced concrete frames and cantilever walls. Earthquake Engineering and Structural Dynamics, 45(13), 2163-2183.

Koutsourelakis, S., Pŕevost, J.H. and Deodatis, G. (2002). Risk analysis of an interacting structure-soil system due to liquefaction, Earthq. Eng. Struct. D., 31, 851–879.

Kramer, S. L. (1996). Geotechnical Earthquake Engineering. Prentice Hall, 1 edition, ISBN: 0133749436.

Kramer, S. L. and Elgamal, A. W. (2001). Modeling soil liquefaction hazards for performance-based earthquake engineering, PEER Report 2001/13.

Kramer, S. L. and Holtz, R. D. (1991). Soil Improvement and Foundation Remediation with Emphasis on Seismic Hazards. National Science Foundation, Washington, DC, 113 p.

Kramer, S. L. and Wang, C.-H. (2015). Empirical Model for Estimation of the Residual Strength of Liquefied Soil. Journal of Geotechnical and Geoenvironmental Engineering, 141(9):04015038–15, DOI: 10.1061/(ASCE)GT.1943-5606.0001317.

Kramer, S. L., Hartvigsen, A. J., Sideras, S. S. and Ozener, P. T. (2011). Site response modeling in liquefiable soil deposits. 4th IASPEI/IAEE international

Ku, C.-S., Juang, C.H., Chang, C.-W., and Ching, J. (2012). Probabilistic version of the Robertson and Wride method for liquefaction evaluation: Development and application. Canadian Geotechnical Journal, 49(1): 27–44. Doi:10.1139/t11-085

Kwon, O. S., Sextos, A., Elnashai, A. (2009) Seismic fragility of a bridge on liquefaction susceptible soil. Proceedings of the 10th international conference on seismic safety and reliability, Osaka, Japan.

LeBorgne, M. R., and Ghannoum, W. M. (2009) Local deformation measures for RC column shear failures leading to collapse. Proceedings of the 2009 ATC and SEI Conference on Improving the Seismic Performance of Existing Buildings and Other Structures, American Society of Civil Engineers, 500-511.

Liel, A., Haselton, C., Deierlein, G. and Baker, J. (2009). Incorporating modeling uncertainties in the assessment of seismic collapse risk of buildings. Structural Safety 31(2), 197-211.

Lin, Y.-Y. and Miranda, E. (2007). Kinematic soil-structure interaction effects on maximum inelastic displacement demands of SDOF systems. Bulletin of Earthquake Engineering, 6(2):241–259, DOI: 10.1007/s10518-007-9049-y.

Liu, L. (1992). Centrifuge earthquake modelling of liquefaction and its effect on shallow foundations. PhD thesis, Rensselaer Polytechnic Institute, Troy, N.Y.

Liu, H. (1995). An empirical formula for evaluation of buildings settlement due to earthquake liquefaction. Proceedings of 3rd international conference on recent advances in geotechnical earthquake engineering and soil dynamics, St. Louis, Missouri, 1:289–93

Liu, L. and Dobry, R. (1997). Seismic Response of Shallow Foundation on Liquefiable Sand. Journal of Geotechnical and Geoenvironmental Engineering, 123(6):557–567. DOI: 10.1061/(ASCE)1090-0241(1997)123:6(557).

Liu, H., and Qiao, T. (1984). Liquefaction potential of saturated sand deposits underlying Foundation of structure. Proceedings, Eighth World Conference on Earthquake Engineering, Vol. III. San Francisco, California.

Liu, W., Hutchinson, T. C., Kutter, B. L., Hakhamaneshi, M., Aschheim, M. A., and Kunnath, S. K. (2013). Demonstration of Compatible Yielding between Soil-Foundation and Superstructure Components. Journal of Structural Engineering, 139(8):1408–1420. DOI: 10.1061/(ASCE)ST.1943-541X.0000637.

LIQUEFACT
Deliverable D3.1
State of the art review of numerical modelling strategies to simulate liquefaction-induced
structural damage and of uncertain/random factors on the behaviour of liquefiable soils
v. 1.0

Lopez-Caballero F. and Farahmand-Razavi A.M. (2008). Numerical simulation of liquefaction effects on seismic SSI. Soil Dynamics and Earthquake Engineering, 28: 85-98.

Lowes, L. and Altoontash, A. (2003). Modeling Reinforced Concrete Beam-Column Joints Subjected to Cyclic Loading. Journal of Structural Engineering, 129(12): 1686-1697.

Lu, C.W. (2017). A simplified calculation method for liquefaction-induced settlement of shallow foundation. Journal of Earthquake Engineering, DOI:10.1080/13632469.2016.1264327

Luco, J. E. and Lanzi, A. (2017). A new inherent damping model for inelastic time-history analyses. Earthquake Engineering and Structural Dynamics, 46(12): 1919-1939.

Luque R. and Bray J.D. (2015). Dynamic Analysis of a Shallow-Founded Building in Christchurch during the Canterbury Earthquake Sequence. 6th International Conference on Earthquake Geotechnical Engineering, Christchurch, New Zealand, 1-4 November; Paper No. 632.

Luque, R. and Bray, J. D. (2017). Dynamic analyses of two buildings founded on liquefiable soils during the Canterbury Earthquake sequence, 143(9):04017067–04017014, DOI: 10.1061/(ASCE)GT.1943-5606.0001736.

Mackie, K., and B. Stojadinovic (2003). Seismic Demands for Performance-Based Design of Bridges. PEER Report No. 2003/16, Pacific Earthquake Engineering Research Center, University of California Berkeley

Markham, C. S., Bray, J. D., Macedo, J. and Luque, R. (2016). Evaluating nonlinear effective stress site response analyses using records from the Canterbury earthquake sequence. Soil Dynamics and Earthquake Engineering, 82(C):84–98, DOI: 10.1016/j.soildyn.2015.12.007.

Martin, G. R., Finn W.D.L. and Seed H. B. (1975). Fundamentals of liquefaction under cyclic loading. Journal of Geotechnical Division, 101 (5): 423-438.

Matasovic, N. and Vucetic, M. (1993). Cyclic characterization of liquefiable sands. Journal of Geotechnical Engineering 119(11): 1805–1822.

Maurer, B.W., Green, R.A., Cubrinovski, M. and Bradley, B.A. (2014). Evaluation of the liquefaction potential index for assessing liquefaction hazard in Christchurch, New Zealand. J Geotech Geoenviron Eng, 140(7):04014032.

Maurer, B.W., Green, R.A., Taylor, O.S. (2015). Moving towards an improved index for assessing liquefaction hazard: lessons from historical data. Soils and Foundations 55(4): 778–787

MBIE (2017). Module 5: Ground improvement of soils prone to liquefaction: 1–62.

McGann, C.R. and Arduino, P. (2015). Numerical assessment of the influence of foundation pinning, deck resistance, and 3D site geometry on the response of bridge foundations to demands of liquefaction-induced lateral soil deformation. Soil Dynamics and Earthquake Engineering 79 (2015) 379–390.

McLachlan, R., Morris, J., Kathirgamanathan, P. and Callosa-Tarr, J. (2013). Seismic response of underground utilities following the Canterbury earthquakes. Proc. 19th NZGS Geotechnical Symposium. Ed. CY Chin, Queenstown

Mehrzad B., Haddad A. and Jafarian Y. (2016). Centrifuge and Numerical Models to Investigate Liquefaction-Induced Response of Shallow Foundations with Different Contact Pressures. International Journal of Civil Engineering, 14: 177-131.

Metelli, G., Messali, F., Beschi, C. and Riva, P. (2015). A model for beam-column corner joints of existing RC frame subjected to cyclic loading. Engineering Structures, 89: 79-92.

Meyerhof, G.G. and Hanna, A.M. (1978). Ultimate bearing capacity of foundations on layered soils under inclined load. Canadian Geotechnical Journal, 15(4): 565-572

Millen, M. D. L. (2016). Integrated Performance-based Design of Building-foundation Systems. PhD thesis.

Millen, M. D. L., Cubrinovski, M., Pampanin, S. and Carr, A. J. (2015). Consideration of Soil-Foundation Induced Deformations in Building Design. In 6th International Conference on Earthquake Geotechnical Engineering. pp 1–9.

Millen, M. D. L., Pampanin, S., Cubrinovski, M. and Carr, A. J. (2016). A performance assessment procedure for existing buildings considering foundation deformations. In 2016 NZSEE Conference: pp 1–8.

Moghaddasi, M., Cubrinovski, M., Chase, J. G., Pampanin, S. and Carr, A. J. (2011). Probabilistic evaluation of soil-foundation-structure interaction effects on seismic structural response. Earthquake Engineering and Structural Dynamics, 40(2):135–154. DOI: 10.1002/eqe.1011.

Mohamed, H. (2017). Seismic risk assessment of reinforced concrete frames with masonry infill. PhD thesis. Faculty of Engineering of the University of Porto.

Molina-Gómez, F. A., Camacho-Tauta, J. F. and Reyes-Ortiz, O. J. (2016). Stiffness of a granular base under optimum and saturated water contents. Revista Tecnura, 20(49): 75–85. https://doi.org/dx.doi.org/10.14483/udistrital.jour.tecnura.2016.3.a05

Montgomery, J. and Boulanger, R.W. (2016). Effects of spatial variability on liquefaction induced settlement and lateral spreading. Journal of Geotechnical and Geoenvironmental Engineering, 143 (1).

Moss, R. E. S., Seed, R. B., Kayen R., Stewart, J. P. and Der Kiureghian, A. (2005). CPT-Based Probabilistic Assessment of Seismic Soil Liquefaction Initiation, PEER report.

Moss, R. E. S., Seed, R. B., Kayen, R. E., Stewart, J. P., Der Kiureghian, A., and Cetin, K. O. (2006). CPT-based probabilistic and deterministic assessment of in situ seismic soil liquefaction potential, J. Geotechnical and Geoenvironmental Eng., ASCE 132(8), 1032–051.

Mousavi, S. A., Bastami, M. and Zahrai, S. M. (2016). Large-scale seismic isolation through regulated liquefaction: a feasibility study. Earthquake Engineering and Engineering Vibration, 15(4):579–595. DOI: 10.1007/s11803-016-0350-0.

Mylonakis, G. and Gazetas, G. (2000). Seismic soil-structure interaction: beneficial or detrimental?. Journal of Earthquake Engineering, 4(3):277–301. DOI: 10.1080/13632460009350372.

Na, U. J. and Shinozuka, M. (2009). Simulation-based seismic loss estimation of seaport transportation system. Reliability Engineering and System Safety, 94(3), 722-731.

Na, U. J., Chaudhuri, S. R., Shinozuka, M. (2008) Probabilistic assessment for seismic performance of port structures. Soil Dynamics and Earthquake Engineering, 28(2), 147-158.

Na, U. J., Chaudhuri, S. R., Shinozuka, M. (2009) Performance evaluation of pile-supported wharf under seismic loading. Proceedings of the 2009 TCLEE conference: Lifeline Earthquake Engineering in a Multihazard Environment, Oakland, USA.

National Academies of Sciences, Engineering, and Medicine – NASEM (2016). State of the art and practice in the assessment of earthquake-induced soil liquefaction and its consequences. Washington, DC: The National Academies Press. DOI: 1017226/23474.

Negulescu, C. and Foerster, E. (2010). Parametric studies and quantitative assessment of the vulnerability of a RC frame building exposed to differential settlements. Natural Hazards and Earth System Sciences, 10:1781-1792.

Newmark, N.M. (1967). Problems in wave propagation in soil and rocks. Proceedings of the International Symposium on Wave Propagation and Dynamic Properties of Earth Materials, University of New Mexico Press, 7-26.

Newmark, N. and Hall, W. (1982). Earthquake Spectra and Design. Earthquake Engineering Research Institute, Berkeley.

Newmark, N. and Rosenbleuth, E. (1971). Fundamentals of Earthquake Engineering, Prentice-Hall, Inc.

NIBS (2004). Earthquake loss estimation methodology HAZUS. National Institute of Building Sciences, FEMA, Washington, DC.

NIBS (2015) Hazus®-MH 2.1 Multi-hazard Loss Estimation Methodology Technical and User Manuals. Federal Emergency Management Agency (FEMA), Washington, DC

LIQUEFACT
Deliverable D3.1
State of the art review of numerical modelling strategies to simulate liquefaction-induced structural damage and of uncertain/random factors on the behaviour of liquefiable soils
v. 1.0

This project has received funding from the European Union's Horizon 2020 research and innovation programme under grant agreement No. 700748

Noh, N., Liberatore, L., Mollaioli, F. and Tesfamariam, S. (2017). Modelling of masonry infilled RC frames subjected to cyclic loads: State of the art review and modelling with OpenSees. Engineering Structures, 150: 599-621.

Ohsaki, Y. (1966). Niigata earthquakes, 1964 building damage and soil condition. Soils and Foundations, 6(2): 14-37.

Olarte J., Paramasivam B. , Dashti S., Liel A. and Zannin J. (2017). Centrifuge modeling of mitigation-soil-foundation-structure interaction on liquefiable ground. Soil Dynamics and Earthquake Engineering, 97: 304-323.

Olson, S. M. and Stark, T. D. (2002). Liquefied strength ratio from liquefaction flow failure case histories. Canadian Geotechnical Journal, 39(3):629–647, DOI: 10.1139/t02-001.

Open system for earthquake engineering simulation (OpenSees) (2017). Pacific Earthquake Engineering Research Center, University of California, Berkeley, CA. Available from: http://opensees.berkeley.edu.

O'Rourke, M.J. and Ayala G. (1990). Seismic damage to pipeline: case study. Journal of transportation engineering. 116(2): 123-134.

O'Rourke, M.J. and Liu, X. (1999). Response of Buried Pipelines Subject to Earthquake Effects. MCEER Monograph No. 3.

O'Rourke, M, J. and Nordberg, C. (1990). Analysis procedures for buried pipelines subject to longitudinal and transverse permanent ground deformation. Proc., 3rd Japan-US. Workshop on Earthquake Resistant Design of Lifeline Facilities and Counter-measures for Soil Liquefaction; Tech. Rep, NCEER-9l-000l, Nat. Ctr. for Earthquake Engrg. Res., Buffalo, N.Y

O'Rourke TD, Jeon S-S, Toprak S, Cubrinovski M. and Jung JK. (2012). Underground lifeline system performance during the Canterbury Earthquake Sequence. In: Proc. of the 15th world conference on earthquake engineering, Lisbon, Portugal. p. 24.

O'Rourke TD, Jeon S-S, Toprak S, Cubrinovski M, Hughes M, van Ballegooy M. and Bouziou D. (2014). Earthquake response of underground pipeline networks in Christchurch, NZ. Earthq Spectra; 30 (1):183–204. http://dx.doi.org/10.1193/030413EQS062M.

Padgett, J. E., Ghosh, J. and Dueñas-Osorio, L. (2013) Effects of liquefiable soil and bridge modelling parameters on the seismic reliability of critical structural components. Structure and Infrastructure Engineering, 9(1), 59-77.

Paolucci, R., Figini, R. and Petrini, L. (2013). Introducing Dynamic Nonlinear Soil-Foundation-Structure Interaction Effects in Displacement-Based Seismic Design. Earthquake Spectra, 29(2):475–496. DOI: 10.1193/1.4000135.

Pecker, A. (2007). Soil Structure Interaction. In Advanced Earthquake Engineering Analysis, pages 1–10. Springer.

Pecker, A. and Pender, M. J. (2000). Earthquake Resistant Design of Foundations- New Construction. In GeoEng2000 conference, pages 1–22.

PEER/ATC-72-1 (2010) PACIFIC EARTHQUAKE ENGINEERING RESEARCH CENTER - APPLIED TECHNOLOGY COUNCIL. Modeling and Acceptance Criteria for Seismic Design and Analysis of Tall Buildings .

Petalas A. and Galavi V. (2013). PLAXIS liquefaction model UBC3D-PLM. PLAXIS model documentation, 40 pp.

Phan, V. T.-A., Hsiaob, D.-H. and Thuc-LanNguyen, P. (2016). Critical State Line and State Parameter of Sand-Fines Mixtures. Procedia Engineering, 142, 299–306. https://doi.org/10.1016/J.PROENG.2016.02.045

Pietruszczak, S. and Oulapour, M. (1999). Assessment of dynamic stability of foundations on saturated sandy soils. J. Geotech. Geoenviron. Eng., 125(7): 576–582.

Pitilakis, K. and Argyroudis, S. (2014). Seismic Vulnerability Assessment: Lifelines. Encyclopedia of Earthquake Engineering DOI 10.1007/978-3-642-36197-5_255-1 # Springer-Verlag Berlin Heidelberg 2014

Pitilakis, K., Crowley, E. and Kaynia, A. (eds) (2014a) SYNER-G: typology definition and fragility functions for physical elements at seismic risk, vol 27, Geotechnical, Geological and Earthquake engineering. Springer, Heidelberg. ISBN 978-94-007-7872-6

Pitilakis, K., Franchin, P., Khazai, B. and Wenzel, H. (eds) (2014b) SYNER-G: systemic seismic vulnerability and risk assessment of complex urban, utility, lifeline systems and critical facilities. Methodology and applications, Geotechnical, geological and earthquake engineering. Springer, Heidelberg. ISBN 978-94-017-8834-2

PLAXIS (2017). Information available on https://www.plaxis.com/

Popescu, R. and Prevost, J.H. (1993). Centrifuge Validation of a numerical model for dynamic soil liquefaction. Soil dynamics and earthquake engineering. 12(2): 73-90. https://doi.org/10.1016/0267-7261(93)90047-U

Popescu, R., Prevost, J. H., Deodatis, G. and Chakrabortty, P. (2006). Dynamics of nonlinear porous media with applications to soil liquefaction. Soil. Dyn. Earthquake Eng., 26(6–7): 648–665.

Porter, K., Cho, I. and Farokhnia, K. (2012). Contents seismic vulnerability estimation guidelines. Global Vulnerability Consortium.

Porter, K., Farokhnia, K., Vamvatsikos, D. C. I., Cho, I. (2014) Guidelines for component-based analytical vulnerability assessment of buildings and nonstructural elements. GEM Technical Report 2014--13 V1.0.0. Global Earthquake Model.

Priestley, M.J.N. (1997). Displacement-based seismic assessment of reinforced concrete buildings. Journal of Earthquake Engineering, 1(1): 157–192.

Priestley M.J.N., Calvi G.M. and Kowalsky M.J. (2007). Displacement-Based Seismic Design of Structures. IUSS PRESS.

Prisco, C. and Maugeri, M. (2013). Seismic Response of Shallow Footings: A promising application for the macro-element approach. Earthquake Geotechnical Engineering Design pp 195-222. Geotechnical, Geological and Earthquake Engineering (Springer book series: GGEE, volume 28).

Puebla H., Byrne M. and Phillips P. (1997). Analysis of CANLEX liquefaction embankments prototype and centrifuge models. Canadian Geotehnical Journal, 34: 641-657.

Pyke, R. M. (1980). Nonlinear soil models for irregular cyclic loadings. Journal of Geotechnical and Geoenvironmental.

Ramberg, W. and Osgood, W. R. (1943). Description of stress-strain curves by three parameters. ISBN: 19930081614.

Ramirez, C. and Miranda, E. (2009). Building-specific loss estimation methods and tools for simplified performance-based earthquake engineering. Report № 171. John A. Blume earthquake engineering research center. Stanford University. Stanford, California, USA.

Ramirez, C. and Miranda, E. (2012) Significance of residual drifts in building earthquake loss estimation. Earthquake Engineering and Structural Dynamics, 41(11), 1477-1493.

Ramos, A. (2011). Instabilities in Sands. *University of Los Andes*, *PhD Thesis*, 224.

Riemer, M. F., Roman, O. and Paihua, S. (2017). Effects of stress state on the cyclic response of mine tailings and its impact on expanding a tailings impoundment. In 3rd International Conference on Performance-based Design in Earthquake Geotechnical Engineering, pages 1–15, Vancouver.

Robertson, P. K. (2009a). Evaluation of flow liquefaction and liquefied strength using the cone penetration test. Journal of Geotechnical and Geoenvironmental. http://doi.org/10.1061/(ASCE)GT.1943-5606.0000286;

Robertson, P.K. 2009b. Performance based earthquake design using the CPT. In Proceedings of the IS Tokyo Conference. CRC Press/Balkema, Taylor and Francis Group. pp. 3–20.

Robertson, P.K. 2009c. Interpretation of cone penetration tests — a unified approach. Canadian Geotechnical Journal, 46(11): 1337–1355. doi:10.1139/T09-065.

Robertson, P.K. (2015). Comparing CPT and Vs Liquefaction Triggering Methods. Canadian Geotechnical Journal, 141(9): 04015037-1, DOI: 10.1061/(ASCE)GT.1943-5606.0001338.

Robertson, S. (2017). Evaluation of Flow Liquefaction: influence of high stresses. In 3rd International Conference on Performance-based Design in Earthquake Geotechnical Engineering, Vancouver. Paper, n. 509.

LIQUEFACT
Deliverable D3.1
State of the art review of numerical modelling strategies to simulate liquefaction-induced structural damage and of uncertain/random factors on the behaviour of liquefiable soils
v. 1.0

This project has received funding from the European Union's Horizon 2020 research and innovation programme under grant agreement No. 700748

Rollins, K.M. and Seed, H.B. (1990) Influence of buildings on potential liquefaction damage. Journal of geotechnical engineering, 116(2): 165-185.

Roten, D., Fah, D. and Bonill, L. F. (2013). High-frequency ground motion amplification during the 2011 Tohoku earthquake explained by soil dilatancy. Geophys. J. Int. (2013) 193, 898–904 doi: 10.1093/gji/ggt001

Rossetto, T., Ioannou, I. and Grant, D. N. (2013) Existing empirical vulnerability and fragility functions: compendium and guide for selection. GEM Technical Report 2013-X. Global Earthquake Model.

Sancio, R. B., Bray, J. D., Stewart, J. P., Youd, T. L., Durgunoˇglu, H. T., Oˊnalp, A., Seed, R. B., Christensen, C., Baturay, M. B., and Karadayılar, T. (2002). Correlation between ground failure and soil conditions in Adapazari, Turkey. Soil Dynamics and Earthquake Engineering, 22(9-12):1093–1102, DOI: 10.1016/S0267-7261(02)00135-5.

Scheneider, H.R., Romer, B. and Weishaupt, R. (2015). Probabilistic assessment of total and differential settlements due to spatial soil variability. International Journal of Geotechnical Engineering, 9(1): 61-66.

Seed, H.B. and Idriss, I.M. (1971). Simplified procedure for evaluating soil liquefaction potential. Journal of Geotechnical Engineering Division 97(9):1249–1273.

Seed, H. B., Tokimatsu, K., Harder, L. F. Jr. and Chung, R. (1984). The influence of SPT procedures in soil liquefaction resistance evaluations. Earthquake Engineering Research Center, University of California, Berkeley, Report No. UCB/EERC-84/15, 50 pp.

Seed, R. B., Cetin, K.O., Moss, R.E.S., Kammerer, A.M., Wu, J., Pestana, J.M., Riemer, M.F., Sancio, R.B., Bray, J.D., Kayen, R.E., Faris, A. (2003). "Recent advances in soil liquefaction engineering: A unified and consistent framework." Rep. EERC 2003–06, Earthquake Engineering Research Center http://eerc.berkeley.edu/ reports/.

Seyedi, D.M., Gehl, P., Douglas, J., Davenne, L., Mezher, N. and Ghavamian, S. (2010). Development of seismic fragility surfaces for reinforced concrete buildings by means of nonlinear time-history analysis. Earthq Eng Struct 39:91–108.

Shafaei, J., Zareian, M., Hosseini, A. and Marefat, M. (2014). Effects of joint flexibility on lateral response of reinforced concrete frames. Engineering Structures, 81: 412-431.

Shahir, H. and Pak, A. (2009). Variation of permeability during liquefaction and its effects on seismic response of saturated sand deposits. In: 8th International Congress on Civil Engineering, Shiraz, Iran.

Shahir, H. and Pak, A. (2010). Estimating liquefaction-induced settlement of shallow foundations by numerical approach. Computers and Geotechnics, 37(3):267–279, DOI: 10.1016/j.compgeo.2009.10.001.

Shahir, H., Pak, A., Taiebat, M. and Jeremić, B. (2012). Evaluation of variation of permeability in liquefiable soil under earthquake loading. Computers and Geotechnics 40:74-88.

Shahir, H., Mohammadi-Haji, B., Ghassemi, A. (2014). Employing a variable permeability model in numerical simulation of saturated sand behaviour under earthquake loading. Computers and Geotechnics, 55:211-223. https://doi.org/10.1016/j.compgeo.2013.09.007

Sharma, A., Eligehausen, R. and Reddy, G. (2011). A new model to simulate joint shear behavior of poorly detailed beam-column connections in RC structures under seismic loads, Part I: Exterior joints. Engineering Structures, 33(3): 1034-1051.

Shoraka, M. (2013).Collapse assessment of concrete buildings: an application to non-ductile reinforced concrete moment frames. PhD thesis. University of British Columbia.

So, E. (2014) Introduction to the GEM Earthquake Consequences Database GEMECD. GEM Technical Report 2014--14 V1.0.0. Global Earthquake Model.

Son, M. and Cording, E. J. (2005). Estimation of building damage due to excavation-induced ground movements. Journal of Geotechnical and Geoenvironmental Engineering, 131(2), 162-177.

LIQUEFACT
Deliverable D3.1
State of the art review of numerical modelling strategies to simulate liquefaction-induced
structural damage and of uncertain/random factors on the behaviour of liquefiable soils
v. 1.0

Souliotis, C. and Gerolymos, N. (2016). Seismic effective stress analysis of quay wall in liquefiable soil: the case history of Kobe. International journal of Geomate, 10 (2): 1770-1775.

St. John, C.M. and Zahrah, T.F. (1987). "Aseismic design of underground structures", Tunneling and Underground Space Technology, 2 (2), 165-197.

Stuedlein, A. and Bong, T. (2017). Effect of spatial variability on static and liquefaction-induced differential settlements. Geo-Risk, June, Denver, Colorado.

Tani, K., Kiyota, T., Matsushita, K., Hashimoto, T., Yamamoto, A., Takeuchi, H., Noda, T., Kiku, H. and Obayashi, J. (2015). Liquefaction countermeasures by shallow ground improvement for houses and their cost analysis. Soil Dynamics and Earthquake Engineering, 79, 401-414.

Task Force Report (2007). Geotechnical Design Guidelines for Buildings on Liquefiable Sites in Accordance with NBC 2005 for Greater Vancouver Region. pages 1–75.

Tarque, N., Candido, L., Camata, G. and Spacone, E. (2015). Masonry infilled frame structures: state-of-the-art review of numerical modelling. Earthquakes and Structures, 8(1): 225-251.

Terzaghi, K., Peck, R. B. and Mesri, G. (1996). Soil Mechanics in Engineering Practice, 3rd edn., John Wiley and Sons, New York, pp. 549.

Tokimatsu, K., Hino, K., Kyoko, O., Tamura, S., Suzuki, H. and Suzuki, Y. (2017). Liquefaction-induced settlement and tilting of buildings with spread foundation based on field observation and laboratory experiments. 3rd International Conference on Performance-based Design in Earthquake Geotechnical Engineering, Vancouver, 13 pp.

Toprak S. (1998). Earthquake Effects on Buried Lifeline Systems. Ph.D. Thesis, Cornell University, Ithaca, NY.

Toprak, S. and Taskin, F. (2007). Estimation of earthquake damage to buried pipelines caused by ground shaking. Natural hazards, 40(1), 1-24, DOI 10.1007/s11069-006-0002-1.

Toprak, S., Nacaroğlu, E. and Koç, A.C. (2015). Seismic Response of Underground Lifeline Systems. In Perspectives on European Earthquake Engineering and Seismology (pp. 245-263). Springer International Publishing.

Tromans I. (2004). Behavior of buried water supply pipelines in earthquake zones. PhD thesis. Imperial College of Science, Technology and Medicine, University of London.

Tsai, C-C., Lu, C-C., Hwang, Y-W. and Hsu, S-Y. (2017). ASSESSMENT OF LIQUEFACTION IN RESIDENTIAL AREAS DURING THE 2016 MW 6.4 MEINONG EARTHQUAKE IN TAIWAN s. In 3rd International Conference on Performance-based Design in Earthquake Geotechnical Engineering, Vancouver. Paper, n. 171.

United Nations Office for Disaster Risk Reduction (UNISDR), (2009), Terminology on Disaster Risk Reduction

Unutmaz, B. and Cetin, K.O. (2012). Post-cyclic settlement and tilting potential of mat foundations. Soil Dynamics and Earthquake Engineering, 43:271-286.

Uma, S. R., Pampanin, S. and Christopoulos, C. (2010). Development of probabilistic framework for performance-based seismic assessment of structures considering residual deformations. Journal of Earthquake Engineering, 14(7), 1092-1111.

Vaid, Y.P. and Finn, W.D.L. (1979). Static shear and liquefaction potential. Journal of Geotechnical and Geoenvironmental Engineering. Vol. 105

Vaid, Y.P. and Sivathayalan, S. (1996). Static and cyclic liquefaction potential of Fraser Delta sand in simple shear and triaxial tests. Canadian Geotechnical Journal. Vol 33.

Vamvatsikos D. and Cornell C.A. (2002). Incremental dynamic analysis. Earthquake Engineering and Structural Dynamics, 31 (3), 491-514.

LIQUEFACT
Deliverable D3.1
State of the art review of numerical modelling strategies to simulate liquefaction-induced
structural damage and of uncertain/random factors on the behaviour of liquefiable soils
v. 1.0

Van Ballegooy, S., Malan P.J., Jacka M.E., Lacrosse V.I.M.F., Leeves J.R., Lyth J.E. and Cowan H. (2012). Methods for characterising effects of liquefaction in terms of damage severity. 15th World Conference on Earthquake Engineering, Lisboa.

Van Ballegooy, S., Malan, P., Lacrosse, V., Jacka, M.E., Cubrinovski, M. and Bray, J.D. (2014) Assessment of liquefaction-induced land damage for residential Christchurch. Earthq Spectra EERI; 30(1): 31–55.

Verdugo, R. (1992). Characterization of Sandy Soil Behavior under Large Deformation. Department of Civil Engineering, University of Tokyo, Tokyo, Japan

Verdugo, R. and Ishihara, K. (1996). The Steady State of Sandy Soils. soils and foundations, 36(2): 81-91. https://doi.org/10.3208/sandf.36.2_81

Verdugo, R. and Gonzalez, J. 2015. Liquefaction- induced ground damages during the 2010 Chile Earthquake. Soil Dynamics and Earthquake Engineering, 79, 280–295. DOI: 10.1016/j.soildyn.2015.04.0160267-726.

Viana da Fonseca, A., Coop, M.R., Fahey, M., Consoli, N.C. (2011). The interpretation of conventional and non-conventional laboratory tests for challenging geotechnical problems. International Symposium on Deformation Characteristics of Geomaterials, Seoul, Korea.

Viana da Fonseca, A., Ramos, C. and Cubrinovski, M. (2016). Report on the Sessions on Liquefaction. Geotechnical and Geophysical Site Characterization, ISC'5. Australian Geomechanics Society, Sydney, Vol. 1, № 217-232. http://australiangeomechanics.org/public-resources/

Viana Da Fonseca, A., Soares, M. and Fourie, A. B. (2015). Cyclic DSS tests for the evaluation of stress densification effects in liquefaction assessment. *Soil Dynamics and Earthquake Engineering, 75*, 98-111. doi:10.1016/j.soildyn.2015.03.016

Viggiani, C. (1993) Fondazioni. Editore: Hevelius. 568 pp.

Wang, R., Zhang, J.M. and Wang. G. (2014). A unified plasticity model for large post-liquefaction shear deformation of sand. Computers and Geotechnics, 59: 54-66.

Wang R., Liu X. and Zhang J.M. (2015). Analysis of seismic pile response in liquefiable ground using a constitutive model for large post-liquefaction deformation. 6th International Conference on Earthquake Geotechnical Engineering, Christchurch, New Zealand, 1-4 November 2015; Paper No. 670.

Weatherill, G., Esposito, S., Iervolino, I., Franchin, P. and Cavalieri, F. (2014). Framework for seismic hazard analysis of spatially distributed systems. In: Pitilakis K et al (eds) SYNER-G: systemic seismic vulnerability and risk assessment of complex urban, utility, lifeline systems and critical facilities. Methodology and applications. Springer, Dordrecht. ISBN 978-94-017-8834-2

Wengstrom, T.R. (1993). "Comparative analysis of pipe break rates: a literature review." Chalmers Univ of Technology, Publication 2:93, 95pp.

Whitman, R. V. and Lambe, P. C. (1982). Liquefaction: consequences for a structure. Proc., Conference Soil Dynamics and Earthquake Engineering, Southampton Univ., A. A. Balkema, Rotterdam, Netherlands, 941-949.

World Meteorological Organization (2006). Comprehensive_Risk_Assessment_for_Natural WMO/TD No. 955

Wotherspoon, L. M., Orense, R. P., Green, R. A., Bradley, B. A., Cox, B. R. and Wood, C. M. (2015). Assessment of liquefaction evaluation procedures and severity index frameworks at Christchurch strong motion stations. Soil Dynamics and Earthquake Engineering, 79(Part B):335–346, DOI: 10.1016/j.soildyn.2015.03.022.

Yang, Z., Elgamal, A. and Parra, E. (2003). Computational Model for Cyclic Mobility and Associated Shear Deformations. Journal of Geotechnical and Geoenvironmental Engineering, 129 (12): 1119-1127.

Yang, Z., Lu, J. and Elgamal A. (2008). OpenSees Soil Models and Solid-Fluid Coupled Elements, User's Manual, Version 1.0, UCSD Dept. of Structural Engr.

Yasuda, S. (2014). New liquefaction countermeasures for wooden houses. Soil liquefaction during recent large-scale earthquake – Orense, Towhata and Chouw.

Yoshida, N., Tokimatsu, K., Yasuda, S., Kokusho, T., and Okimura, T. (2001). Geotechnical aspects of damage in Adapazari city during 1999 Kocaeli, Turkey earthquake. Soils and foundations, 41(4), 25-45.

Yoshimi, Y. (1980). Liquefaction of Sands. Gihodo (ed.), Tokyo, Japan (in Japanese)

Yoshimi, Y. and Kuwabara, F. (1973). Effect of subsurface liquefaction on the strength of surface soil. Soils and Foundations, 13(2) 67-81.

Yoshimi, Y., and Tokimatsu, K. (1977). Settlement of buildings on saturated sand during earthquakes. Soils and Foundations, 17(1):23–28.

Yoshimine, M. and Ishihara, K. (1998). Flow potential of sand during liquefaction. Soils and foundations, 38(3): 189-198. https://doi.org/10.3208/sandf.38.3_189

Youd, T. L., Idriss, I. M., Andrus, R. D., Arango, I., Castro, G., Christian, J. T., Dobry, R., Finn, L., Harder, L. F. J., Hynes, M. E., Ishihara, K., Mitchell, J. K., Moriwaki, Y., Power, M. S., Robertson, P. K., Seed, R. B. and Stokoe, K. H. (2001). LIQUEFACTION RESISTANCE OF SOILS: SUMMARY REPORT FROM THE 1996 NCEER AND 1998 NCEER/NSF WORKSHOPS ON EVALUATION OF LIQUEFACTION RESISTANCE OF SOILS. Journal of Geotechnical and Geoenvironmental Engineering, pages 1–17.

Youssef, M. and Ghobarah, A. (2001). Modelling of RC beam-column joints and structural walls. Journal of Earthquake Engineering, 5(1): 93-111.

Zhai, C. H., Kong, J. C., Wang, X. M. and Wang, X. H. (2017) Finite-element analysis of out-of-plane behaviour of masonry infill walls. Proceedings of the Institution of Civil Engineers - Structures and Buildings, DOI: 10.1680/jstbu.15.00093 2017.

Zhang, L. and Ng, A. M. (2007). Limiting tolerable settlement and angular distortion for building foundations. Probabilistic Applications in Geotechnical Engineering, ASCE.

Zhang J.M. and Wang G. (2012). Large post-liquefaction deformation of sand, part I: physical mechanism, constitutive description and numerical algorithm. Acta Geotechnica, 7: 69-113.

Zhang G., Robertson P.K. and Brachman R.W.I. (2002). Estimating liquefaction-induced ground settlements from CPT for level ground. Canadian Geotechnical Journal, 39: 1168-1180.

Zhang, G., Robertson, P.K. and Brachaman, R.W.I. (2004). Estimating liquefaction-induced lateral displacements using the standard penetration test or cone penetration test. Journal of feotechnical and geoenvironmental engineering, 130(8): 861-871

Zhang, J., Huo, Y., Brandenberg, S. J., Kashighandi, P. (2008) Effects of structural characterizations on fragility functions of bridges subject to seismic shaking and lateral spreading. Earthquake Engineering and Engineering Vibration, 7(4), 369-382.

Ziotopoulou, K. and Boulanger, R. W. (2013). Numerical modeling issues in predicting post-liquefaction reconsolidation strains and settlements. In Proceedings of the 10th International Conference on Urban Earthquake Engineering.

Ziotopoulou, K. and Boulanger, W. (2015). Validation protocols for constitutive modeling of liquefaction. 6 th International Conference on Earthquake Geotechnical Engineering, 1-4 November, Christchurch, New Zealand.

Ziotopoulou K. and Montgomery J. (2017). Numerical modeling of earthquake-induced liquefaction effects on shallow foundations. 16th World Conference on Earthquake Engineering, Santiago, Chile, 9-13 January; Paper No. 2979.

Ziotopoulou, K., Maharjan, M., Boulanger, R.W., Beaty, M.H., Armstrong, R.J. and Takahashi, A. (2014). Constitutive modeling of liquefaction effects in sloping ground. Proceedings of the 10th National Conference in Earthquake Engineering, Earthquake Engineering Research Institute, July 21-25, Anchorage, Alaska